



12-2015

EXTENDING THE LEAN LIMIT OF METHANE-AIR MIXTURES BY OXYGEN, NITROGEN AND CARBON DIOXIDE INJECTION IN THE GAP OF THE SPARK PLUG'S ELECTRODES

Artem Alexandrov Temerev

University of Tennessee - Knoxville, atemerev@vols.utk.edu

Recommended Citation

Temerev, Artem Alexandrov, "EXTENDING THE LEAN LIMIT OF METHANE-AIR MIXTURES BY OXYGEN, NITROGEN AND CARBON DIOXIDE INJECTION IN THE GAP OF THE SPARK PLUG'S ELECTRODES." Master's Thesis, University of Tennessee, 2015.

https://trace.tennessee.edu/utk_gradthes/3611

This Thesis is brought to you for free and open access by the Graduate School at Trace: Tennessee Research and Creative Exchange. It has been accepted for inclusion in Masters Theses by an authorized administrator of Trace: Tennessee Research and Creative Exchange. For more information, please contact trace@utk.edu.

To the Graduate Council:

I am submitting herewith a thesis written by Artem Alexandrov Temerev entitled "EXTENDING THE LEAN LIMIT OF METHANE-AIR MIXTURES BY OXYGEN, NITROGEN AND CARBON DIOXIDE INJECTION IN THE GAP OF THE SPARK PLUG'S ELECTRODES." I have examined the final electronic copy of this thesis for form and content and recommend that it be accepted in partial fulfillment of the requirements for the degree of Master of Science, with a major in Mechanical Engineering.

Ke Nguyen, Major Professor

We have read this thesis and recommend its acceptance:

David Irick, Madhu S. Madhukar, Michael D. Kass, Stuart C. Daw

Accepted for the Council:

Carolyn R. Hodges

Vice Provost and Dean of the Graduate School

(Original signatures are on file with official student records.)

**EXTENDING THE LEAN LIMIT OF METHANE-AIR MIXTURES BY OXYGEN,
NITROGEN AND CARBON DIOXIDE INJECTION IN THE GAP OF THE SPARK
PLUG'S ELECTRODES**

A Thesis Presented for the
Master of Science
Degree
The University of Tennessee, Knoxville

Artem Alexandrovich Temerev
December 2015

ACKNOWLEDGMENT

Many individuals provided irreplaceable support and encouragement to me in completion of this research work. I would like to thank my major professor, Prof. Ke. Nguyen, who provided guidance and help that made it possible to complete this research, and for his suggestions in my graduate course work. I would also like to thank my other thesis committee members, Dr. Irick Butch, Dr. Madhu Madhukar, Dr. Mike Kass and Dr. Stuart Daw, for their valuable suggestions and comments on my thesis.

I greatly appreciate Dr. Todd Toops of National Transportation Research Center (NTRC) for allowing me setting up the experimental apparatus of this research in his lab. And last but not least Dr. Brian Kahl who helped me with the LabView acquisition system and the heat released analysis calculations.

I would like to thank the Laboratory Directed Research and Development Program of Oak Ridge National Laboratory for sponsorship of this project under Contract No. DE-AC05-00OR22725 with the U.S. Department of Energy

ABSTRACT

An experimental investigation is carried out to investigate the feasibility of extending the lean limit for methane–air mixtures by injecting oxygen and other gases such as nitrogen and carbon dioxide in the area between spark plug electrodes. Additionally, the effect of oxygen injection on exhaust gas recirculation (EGR) is investigated. The pressure in the chamber and the equivalence ratio of the mixture are varied from 0.35 MPa to 1.03 MPa and 0.46 to 1.0, respectively. Delco 12620540 spark plug is used as the ignition source and the gas injection into spark plug gap is accomplished through a 0.159-cm OD stainless steel injection nozzle. With oxygen injection the lean limit is extended from an equivalence ratio of 0.54 to 0.46 at all pressures investigated in the present study.

Similar trend is observed with nitrogen and carbon dioxide injection in the area between the spark plug's electrodes. This indicates that the extension of the lean limit of methane-air mixtures is mainly due to induced charge motion. From high-speed video camera the flame kernel between the electrodes in the case of oxygen, nitrogen and carbon dioxide injections is observed to be much larger than the flame kernel in the case of without injection. Thus, it appears that one of the effects of injection is to enlarge the initial flame kernel to a radius exceeding the critical radius. As a result the flame front grows and propagates, resulting in more energy transferred to the unburned mixture, enhancing the burning and reaction rates.

The effect of the oxygen injection on percent EGR represented by carbon dioxide dilution in a stoichiometric methane-air mixture is also investigated. Without oxygen injection combustion of a stoichiometric methane-air mixture is impossible to obtain with 18 % EGR, however with oxygen injection combustion is achieved even at 22 % EGR. As a result of oxygen injection the peak pressure at 22 % EGR is the same as at 15 % EGR. In contrast it is impossible to ignite the methane-air mixture with nitrogen and carbon dioxide injection, even at 10 % EGR.

TABLE OF CONTENTS

1 INTRODUCTION	1
2 LITERATURE SURVEY	7
2.1 Overview of Lean Air-Fuel Mixture	7
2.2 Hydrogen Addition to Improve Lean Burn Capacity	8
2.3 Direct Injection Techniques to Extend Lean Limit.....	10
2.4 Use of High Energy Ignition System to Extend Lean Limit.....	17
3 EXPERIMENTAL APPARATUS AND PROCEDURE	25
3.1 Combustion Chamber Assembly.....	25
3.2 Oxygen Injection System	33
3.3 High-Speed Video Camera	33
3.4 Data Acquisition System.....	35
3.5 Description Of Experimental Conditions and Procedure.....	35
3.6 Injection Solenoid Valve Time Response	41
3.7 Mass of Injected Gases.....	43
4 RESULTS AND DISCUSSION	44
4.1 Combustion Analysis.....	44
4.1.1 Effects of Elapsed Time Between end of Charging and Energizing Spark Plug..	45
4.1.2 Determining Lean Limit for Air-Methane Mixture at Different Pressures.....	50
4.1.3 Solenoid Valve Injection Analysis	53
4.2 Effects of O ₂ , N ₂ and CO ₂ Injection on Ignition, Combustion and Lean Limit of Methane-Air Mixture	55
4.2.1 Determining Lean Limit for Range of Chamber Pressures with O ₂ Injection	56

4.2.2	Extending Lean Limit at Chamber Pressure of 1.03 MPa with N ₂ Injection	66
4.2.3	Determining Lean Limit at Initial Chamber Pressure of 1.03 MPa with Carbon Dioxide Injection	72
4.2.4	Effects of O ₂ , N ₂ and CO ₂ Injections on Combustion of Fuel/Air Mixture with Images from High-Speed Video Camera.....	75
4.3	Effects of O ₂ , N ₂ and CO ₂ Injection on Flammability Limit of Air–Methane–Carbon Dioxide Mixture at 0.69 MPa Pressure and Near Stoichiometric Equivalence Ratio.	90
4.3.1	Determination of Flammability Limit of Methane-Air Mixture with Exhaust Gas Recirculation (EGR)	90
4.3.2	Determination of Highest Percent EGR with O ₂ , N ₂ and CO ₂ Injection	96
5 CONCLUSIONS.....		100
REFERENCES.....		102
APPENDIX.....		106
VITA.....		109

LIST OF TABLES

4.1 Effects of chamber pressure and equivalence ratio on average peak pressure of methane-air mixture without injection	51
4.2 Effects of chamber pressure and equivalence ratio on average peak pressure with oxygen injection	57
4.3 Oxygen injection pressure performed to obtain average peak pressure for each chamber pressure and equivalence ratio.	58
4.4 Average peak pressure with O ₂ injection at chamber pressure of 1.03 MPa and equivalence ratios of 0.5, 0.48 and 0.46	71
4.5 Average peak pressure with N ₂ injection at chamber pressure of 1.03 MPa and equivalence ratios of 0.5, 0.48 and 0.46	73
4.6 Average peak pressures with CO ₂ injection at chamber pressure of 1.03 MPa and equivalence ratios 0.5, 0.48 and 0.46	76
4.7 Effects of O ₂ , N ₂ and CO ₂ injection on pressure and temperature traces of methane-air mixture at $\phi = 0.6$ and chamber pressure of 0.69 MPa.....	80
4.8 Effects of O ₂ , N ₂ and CO ₂ injection on pressure and temperature traces of methane-air mixture at $\phi = 0.54$ and chamber pressure of 0.69 MPa.....	88
4.9 Effects of percent EGR on average peak pressure.....	92
4.10 Effects of percent EGR on average peak pressure with O ₂ injection	97

LIST OF FIGURES

2.1 Research engine: a – single cylinder research engine, b – quiescent chamber local injection design, c – swirl chamber local injection design	11
2.2 UBC 1C squish – jet combustion chamber.....	15
2.3 Experimental setup on the influence of electronically excited oxygen molecule on combustion of H ₂ -O ₂ mixture (Smirnov 2008).....	16
2.4 PCJ injector and detail of its cavity.....	20
2.5 Engine stability increases with the addition of microwave energy.....	24
3.1 Photograph of combustion chamber used in present investigation.	26
3.2 Top flange with capillary injection nozzle, high-speed camera observation window and type-K thermocouple.....	28
3.3 Sketch of control panel used to vary equivalence ratio and pressure of methane-air mixtures. (CC) combustion chamber; (LPCH ₄ G) low-pressure gage for methane, (HPCH ₄ G) high-pressure gage for methane, (PAG) and (PCO ₂ G) pressure gage for air and carbon dioxide; (NCH ₄), (NA) and (NCO ₂) needle valves for methane, air and carbon dioxide; (KCH ₄), (KA) and (KCO ₂) control valves for methane, air and carbon dioxide; (TCH ₄), (TA) and (TCO ₂) toggle switch for methane, air and carbon dioxide; (KH-LPG) control valve between low and high pressure gages for methane; (TH-LPG) toggle switch between low and high pressure gages for methane.	31
3.4 Photograph of control panel used in present investigation.....	32

3.5 Photograph of injection system used in present investigation.	34
3.6 Photograph of high-speed camera used for experiments.....	36
3.7 Lab View virtual interface.....	37
3.8 Schematic of experimental apparatus.	39
3.9 The set up for determining response time of solenoid valve.	42
4.1 Effects of time delay between chamber charging and energizing spark plug on pressure rise of methane-air mixture at chamber pressure of 0.34 MPa and $\phi =$ 0.6.....	47
4.2 Effects of time delay between chamber charging and energizing spark plug on temperature rise near the center of chamber.....	48
4.3 Effects of time delay between chamber charging and energizing spark plug on temperature rise near spark plug	49
4.4 Effects of equivalence ratio and chamber pressure on average peak pressure for methane-air mixture.....	52
4.5 Effects of temperature at center and at top on chamber pressure at $\phi=0.6$	54
4.6 Effects of O ₂ injection on pressure of methane-air mixture at $\phi = 0.6$ and chamber pressure of 0.34 MPa (--- without O ₂ injection, --- with O ₂ injection)	60
4.7 Effects of O ₂ injection on temperature at center of combustion chamber of methane-air mixture at $\phi = 0.6$ and chamber pressure of 0.34 MPa (--- without O ₂ injection, --- with O ₂ injection)	61

4.8 Effect of O ₂ injection on temperature near the spark plug of methane-air mixture at $\phi = 0.6$ and chamber pressure of 0.34 MPa (--- without O ₂ injection, --- with O ₂ injection).....	62
4.9 Effect of O ₂ injection on pressure of methane-air mixture at $\phi = 0.6$ and chamber pressure of 0.69 MPa (--- without O ₂ injection, --- with O ₂ injection).....	63
4.10 Effect of O ₂ injection on temperature at center of combustion chamber of methane-air mixture at $\phi = 0.6$ and chamber pressure of 0.69 MPa (---without O ₂ injection, --- with O ₂ injection)	64
4.11 Effect of O ₂ injection on temperature near the spark plug of methane-air mixture at $\phi = 0.6$ and a chamber pressure of 0.69 MPa (--- without O ₂ injection, --- with O ₂ injection)	65
4.12 Effect of equivalence ratio on peak pressure of methane-air mixture at a chamber pressure of 0.34 MPa with O ₂ injection.....	67
4.13 Effect of equivalence ratio on peak pressure of methane-air mixture at a chamber pressure of 0.48 MPa with O ₂ injection.....	68
4.14 Effect of equivalence ratio on peak pressure of methane-air mixture at a chamber pressure of 0.69 MPa with O ₂ injection.....	69
4.15 Effect of equivalence ratio on pressure of methane-air mixture at chamber pressure of 1.03 MPa with O ₂ injection	70
4.16 Effects of O ₂ and N ₂ injection on pressure and temperature at center of a methane-air mixture at $\phi = 0.5$ and a chamber pressure of 1.03 MPa (--- with N ₂ injection, --- with O ₂ injection)	74

4.17 Effects of CO ₂ and N ₂ injection on pressure and temperature at center of a methane-air mixture at $\phi = 0.5$ and chamber pressure of 1.03 MPa (--- with N ₂ injection, --- with CO ₂ injection)	77
4.18 Effects of O ₂ , N ₂ and CO ₂ injection on pressure and temperature traces of methane-air mixture at $\phi = 0.6$ and chamber pressure of 0.69 MPa (--- with N ₂ injection, --- with CO ₂ injection, --- with O ₂ injection, --- with no injection)	81
4.19 Images taken via high-speed video camera with no injection and duration of each event. Initial pressure in chamber is 0.69 MPa and $\phi = 0.6$	82
4.20 Images taken via high-speed video camera with O ₂ injection and duration of each event. Initial pressure in chamber is 0.69 MPa, $\phi = 0.6$	83
4.21 Images taken via high-speed video camera with N ₂ injection and duration of each event. Initial pressure in chamber is 0.69 MPa, $\phi = 0.6$	85
4.22 Images taken via high-speed video camera with CO ₂ injection and duration of each event. Initial pressure in chamber is 0.69 MPa, $\phi = 0.6$	86
4.23 Effects of O ₂ , N ₂ and CO ₂ injection on pressure and temperature traces of methane-air mixture at $\phi = 0.54$ and chamber pressure of 0.69 MPa (--- with N ₂ injection, --- with CO ₂ injection, --- with O ₂ injection).....	89
4.24 Pressure and temperature at chamber center in case of 10% EGR and chamber pressure of 0.69 MPa as function of time for five different experiments	93
4.25 Pressure and temperature at chamber center in case of 15% EGR and chamber pressure of 0.69 MPa as function of time for five different experiments	94

4.26 Pressure and temperature at chamber center in the case of 18% EGR and chamber pressure of 0.69 MPa as function of time for five different experiments 95

4.27 Effects of O₂ injection on pressure and temperature traces of methane-air mixture diluted with 10% CO₂ and chamber pressure of 0.69 MPa (--- without injection, --- with O₂ injection) 98

CHAPTER 1

INTRODUCTION

There are numerous benefits that make Natural Gas Engines (NGEs) Vehicles so attractive. Vehicles powered by NGEs are much safer due to thicker and stronger storage tanks as compared to those of either diesel or gasoline engines. In addition, natural gas is much cheaper and burns cleaner. Compared with conventional gasoline vehicles, natural gas vehicles reduce smog-producing pollutants by 60-90 % (DOE and EPA 2010). EPA has rated the natural gas fueled Honda Civic as the cleanest internal combustion engine in the world. The CO and NO_x emissions are much lower from the NGEs, and thus they do not require as many catalysts as gasoline or diesel engines in order to meet stringent emissions standards (Rood 2010 of). Other advantages NGEs are their lower maintenance cost and the low price of natural gas. Known world reserves of conventional natural gas total about 6,000 TCF, and the expected lifetime of proven natural gas reserves is more than 60 years and the prediction of the total life time expectancy is kept on revising by discovering new reserves (Suplee 2008). The use of natural gas as fuel for vehicles is also encouraged by an initiative from the European Commission, which sets up a goal of replacing 20% of all fossil transport fuels with alternative fuels by the year 2020, and natural gas is expected to account for approximately half of this replacement (Tunestal 2002).

It is more beneficial to operate NGEs in the lean region of the methane-air mixture due to not only higher thermal efficiency and fuel economy, but more

importantly significantly lower NO_x and CO₂ emissions. However, running engines using the mixture near the lean limit creates several difficulties including slow flame propagation speed, increased cycle-by-cycle variations and incomplete combustion. These can lead to poor engine performance especially in the natural gas engines, since they have smaller laminar burning velocities and higher ignition energy.

Previous studies showed that in order for the engine to effectively operate at the lean region, some additional strategies have to be implemented if stable working conditions (especially at high loads) are to be achieved.

One way to increase the burning rates of the methane-air mixture and to extend the lean limit operation is the addition of hydrogen to the mixture (Tunestal 2002). It can enhance the efficiency with significant reduction of emissions. Another way is to use high-energy devices to extend the lean limit. For example, multiple spark ignition systems or microwave-assisted spark plugs, etc. All these devices supply the mixture with a higher energy that excites the electrons and enhance mixture activity through electron impact reactions that generate radical and metastable electronically-excited chemical species (Rapp 2012). Enhanced turbulent mixing inside the chamber is another possible way to extend the lean limit. It has been done by modifying the geometry of the chamber along with geometry of the piston (Evans 2009). Partially stratified charge is also one effective technique to extend the lean limit and to provide stability in gasoline engines (Gold 1997). In partially stratified charge engines, a fuel-rich region is created near the spark plug, with a leaner mixture at a greater distance from the spark plug. As a result, a stable ignitable mixture is formed around the spark plug. However, in order

for the partially-stratified charge method to work well, it is necessary to optimize the mixture stratification pattern (Wang 2007). It is very important to control the mixing method such that the optimum fuel concentration near the spark plug gap can be obtained.

Very few studies have been done on stratified charge for natural gas engines. Mezo investigated methane-rich fuel injection inside the combustion bomb that was filled with a pure air. He showed that it is crucial to define appropriate pressure of injection along with the spark plug ignition timing, where the spark plug timing is defined as the time elapse between triggering the fuel injector and the spark (Mezo 2009). Combustion of the resulting mixture near the spark plug is achieved under limited range of experimental conditions.

There are not much studies done, however, on injection of other gases besides fuel-rich mixtures to enhance the output parameters of the engine for lean equivalence ratio ϕ .

An understanding of the spark ignition process is important for improving fuel efficiency, especially in the lean limit region. The typical spark plug of an internal combustion engine creates a high-temperature plasma kernel between the electrodes. When a streamer from one electrode reaches another, it is referred to as the breakdown phase. This phase has a short duration (20-50 ns) and high temperature rise ($\sim 60,000$ K) between the spark plug gap. During this phase if voltage drop is high enough, the electrons gain enough energy to ionize molecules that lowers the impedance of the gap. The increasing concentration of electrons further reduces the gap impedance to the point where current flow begins and

breakdown is achieved. The faster a rising voltage is applied, the faster breakdown occurs. The transfer of electrical energy to spark plasma is the most efficient during this phase. The rapid increase in the gas temperature to about 60,000 K causes a fast rise in pressure, which produces the shock wave. A strong shockwave propagates outward the channel expending its energy, and as a result the temperature and pressure decrease. Some energy (about 30 %) is carried away by the shockwave, however most of it regains, and the spherical blast wave transfers most of its energy to the gas, and the breakdown plasma then soon expands. The kernel temperature then decreases to approximately 10,000 K on a microsecond time scale (Dale 1997).

Followed the breakdown phase is the arc phase, where the degree of dissociation and ionizations are not as high, but still are quite significant. The glow discharge lasts for about 1 ms and during this time the maximum temperature reaches 6000 K. Plasma energy is decreased by 50 % compared to breakdown phase, and consequently the radiative heat loss to the electrodes decreases by almost 50%. The glow phase follows after the arc phase, and it lasts for about 1ms. The plasma energy is decreased even further by 30 % of the breakdown phase plasma. The temperature during the glow phase still remains the same as during the arc phase. The heat losses are increased due to heat transferred to electrodes.

The highest temperature is achieved during the breakdown phase. The energies are such that the gases in the volume are fully dissociated and almost fully ionized. On the high-temperature side of the ignition zone, a large number of radicals transfer their energy to the mixture within a few milliseconds. In their study, Maly and Vogel determined that the most important phase of a spark

discharge is the breakdown phase, whereas other phases are less important, because the electrical energy is dissipated into the electrodes during glow and arc discharge (Keck 2010).

Maly and Zeigler's study on the formation of lean methane-air mixture also concluded that the temperature drops rapidly due to heat dissipation during glow and arc phases. Thus, the ignition system with the shortest duration and highest level of energy is the best to ignite lean methane-air mixture (Keck 2010).

Free radicals are atoms, molecules or ions that have one or more unpaired electrons. These unpaired electrons make free radicals highly reactive. A significant amount of energy is required to form free radicals, because the covalent bond must be broken. It requires about 0.98 eV to excite oxygen molecules to lower singlet state, where the singlet state of the oxygen is also characterized as an extremely reactive molecule. This can be accomplished by supplying the oxygen with temperatures as high as those during breakdown phase of the spark plug. In addition, the investigation of the stoichiometric methane-air mixture revealed that the energy of 1.2 eV is enough for combustion to take place (Smirnov 2008). Smirnov and his research team, for example, successfully showed great potential of the control of combustion process by using oxygen molecules O_2 ($a^1\Delta_g$) and O_2 ($b^1\Sigma_g^+$) at a singlet state on combustion of an H_2 - O_2 mixture. Adding electronically-excited oxygen molecules to the mixture that flowed through heated flow reactor provided earlier combustion and larger flame propagation along the reactor's axis. The self-ignition of the mixture was initiated even with a lower temperature of the flow reactor with excited oxygen molecules.

Using oxygen injection during a lean operation may be an effective technique to extend the lean limit operation. Injection of the oxygen molecules into the gap between the electrodes of the spark plug during breakdown phase dissociates the oxygen molecules into either oxygen or ionized oxygen atoms, creating highly reactive radicals due to high temperature achieved in this phase. In addition, the injection of oxygen can enlarge the initial flame kernel to a radius that exceeds the critical radius.

In the present study, the effects of the oxygen injection as well nitrogen and carbon dioxide injection on the extension of the lean-limit for a methane-air mixture are investigated. The experiments are carried out in a combustion chamber at a chamber pressures between 0.35 and 1.03 MPa. Oxygen is injected into the gap between the two electrodes of a spark plug prior to the spark discharge via an injection system. The injection pressure is varied until the peak pressure as a result of combustion of the mixture is at maximum. Experiments are also performed for the case of exhaust gas recirculation (EGR) where the methane-air mixture is diluted with pure CO₂. In addition to oxygen, nitrogen and carbon dioxide are injected into the spark plug gap in order to ascertain whether the ignition process in the lean limit is due to the formation of highly reactive oxygen radicals or due to induced charge motion in the region of the spark plug. The development of the flame kernel during the ignition process is recorded with a high-speed video camera, from which differences, if any, between the oxygen, nitrogen and carbon dioxide injections can be determined.

CHAPTER 2

LITERATURE SURVEY

The development of the first internal combustion engines (ICE) occurred about 400 years ago. Christian Huygens was the first person who experimented with them in 1680. The internal combustion engines have had numerous improvements since then in all aspects, from the type of gasoline, control, and management to simply shape and size. Presently, a number of companies are working on hybrid engines in which the power train consists of electric motors and small internal combustion engines. Even though electrical vehicles are extremely popular, the interest of the companies in the ICE still stays high, and there are a large number of studies on alternative fuels such as natural gas engines.

2.1 OVERVIEW OF A LEAN AIR-FUEL MIXTURE

The majority of the vehicles on the market as of now are powered by gasoline engines operating at stoichiometric air–fuel ratio. It guarantees that the engine is used with the highest percent of efficiency. The highest temperature and pressure rise can be achieved only under stoichiometric conditions; however it results in high emissions and a high number of unburned fuel molecules in the product. Most of these engines require the use of three-way catalytic converters in order to reduce the emissions of pollutants to allowable levels.

Another way to decrease greenhouse gases and increase thermal efficiency is to operate the engines in the lean region. Ideally, it is desired to decrease the emissions without sacrificing the engine efficiency. Historically, it has been achieved in a number of ways.

2.2 HYDROGEN ADDITION TO IMPROVE LEAN BURN CAPACITY

Previous research has shown that hydrogen enrichment of the natural gas can improve combustion characteristics of natural gas and extend the lean operation limit. Hydrogen has higher ignition energy and a higher laminar flame speed than natural gas. Thus, hydrogen addition to the air–fuel mixture improves flame propagation, especially close to a lean limit where laminar flame speed and turbulent flame speed are very low (Tunestal 2002). Natural gas is supplied to the engine with enrichment levels of 0%, 5%, 10% and 15% hydrogen by volume. The hydrogen is added for the lean limit cases and for two types of piston bowl geometries, which included turbine and quartette geometries. It creates two turbulence scenarios that are used to simulate slow-burn and the fast-burn combustions. The quarter piston head configuration proved to be very effective; however, the effect on a lean limit extension is more pronounced for the turbine geometry. This suggested that the benefits gained from hydrogen enrichment are truly realized in speeding up otherwise slow burning combustion. The addition of hydrogen to natural gas increases the burn rate and extends the lean limit. However from the emission point of view, it decreases hydrocarbon emission but increases

NO_x emission for constant air excess ratio and ignition timing. Ignition timing decreases the heat loss and NO_x emission and, thus, increases the thermal efficiency (Tunestal 2002).

Similar results were obtained at University of Alabama, where Bell's research group performed experiments on a 1987 GM four-cylinder spark-ignited natural gas engine. The lean limit was extended appreciably with hydrogen enrichment, increasing from a lean limit of $\phi=0.64$ down to $\phi=0.42$ with a 15 % hydrogen addition by volume. (Bell 1996).

Bauer's studies on the one-cylinder natural gas engine discovered that adding hydrogen to the mixture would extend the lean limit. The experiments were performed on an engine running at full (wide-open throttle operation) and partial (throttle operation) loads. The hydrogen was added to the air-fuel mixture with concentrations of 0, 20, 40 and 60 percent by volume. As expected, the lean limit was extended further with the highest percentage of hydrogen in the mixture. The equivalence ratio was decreased to $\phi=0.34$ compared to $\phi=0.58$ for pure air-fuel ratio. As expected, fuel consumption increased. However, power output and thermal efficiency decreased with increasing hydrogen addition, which is likely the result of a lower density of hydrogen fuel when compared to methane. From an emission standpoint, unburned hydrocarbon emissions decreased with the addition of hydrogen, and though NO_x emissions increased with an increase of hydrogen at similar equivalence ratios, the NO_x as well as CO emissions at the extended partial burn limits were lower than all other values. (Bauer 2001).

Ma and Wang used an in-line 6-cylinder, spark-ignition natural gas engine. They found that besides hydrogen injection, other factors such as engine load, engine speed and spark timing also play a significant role in lowering the lean limit. However, results from their experiments indicated that increasing engine load and speed at the same time affected the lean limit in the controversial manner. At a low load levels, turbulence intensity was relatively low and the residual gas fraction was high, and when the engine sped up it led to enhanced in-cylinder flow motion and improved gas exchange efficiency that contributed to higher combustion rate and greater lean burn capacity. On the other hand, at higher load levels, flow motion and gas exchange efficiency became much higher, and in turn, less dependent on the engine speed (Ma 2007).

2.3 DIRECT INJECTION TECHNIQUES TO EXTEND LEAN LIMIT

Gold and his team showed that the lean limit could be extended using direct injection of propane-air mixture between the spark plug gap (Gold 1997). A small single-cylinder engine running at two different speeds of 1000 RPM and 1500 RPM was used in the experiments. Two slightly different modifications of injection systems were used for the injection of the mixture between the spark plug gap. Figures 2.1b and 2.1c show direct injection without swirl and with swirl, respectively. As expected, the lean limit was extended to about $\phi=0.55$. The swirls and direct modifications showed no significant differences in the results. More importantly is the difference in equivalence ratio of injected methane-air mixture.

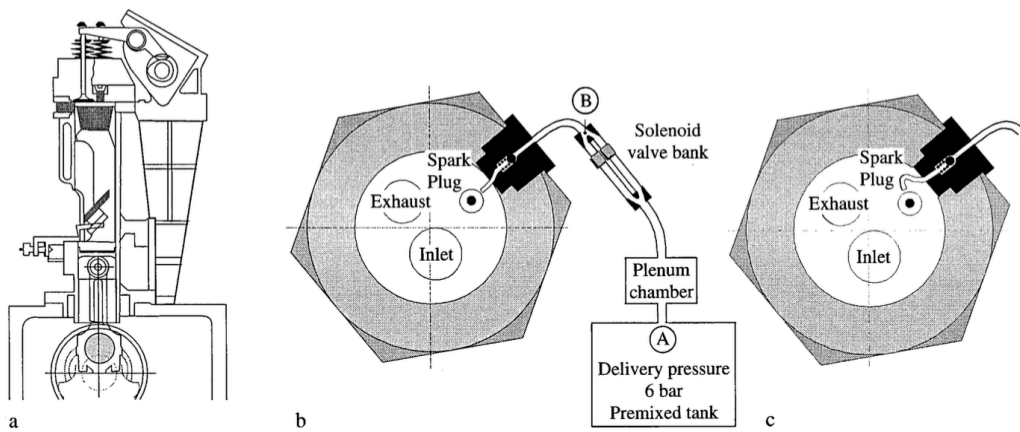


Figure 2.1 Research engine: a–single cylinder research engine, b–quiescent chamber local injection design, c–swirl chamber local injection design

Those experiments with a slightly rich injecting mixture ($\phi=1.1$) resulted in a faster flame growth, and more stable combustion. Another important benefit of a controlled locally rich mixture was its ability to extend the lean drivability limit to $\phi=0.61$.

Wang and his team at the University of Sussex, UK found that double-pulse injection in a gasoline engine had a lot more benefits compared to single injection. The double-pulse injection significantly reduced fuel consumption and exhaust emissions, including NO_x , for a wide range of engine loads (Wang 2006).

The work of Gold showed that injection of a rich mixture near the spark plug gap could extend the lean limit. The stratification techniques with propane and gasoline engines were successfully implemented in Mitsubishi, Ford Proco, Honda CVCC, and Porsche SKS engines.

Reynolds and his team used a similar idea in their study. Instead of injection, the rich region near the spark plug gap was achieved through a partial stratification technique. The methane-rich area near the spark plug was used to compensate for an extremely fuel-lean composition in other regions. The partial stratified charge (PSC) was achieved near the spark plug gap, in which a small amount of fuel was injected near the spark plug electrodes to ensure that a slightly rich region near stoichiometric air-fuel ratio was presented at the time of a spark discharge. With this strategy, the lean limit could be extended to $\phi=0.57$ for a stratification injection of 14g/h and at a speed of 2500 RPM. The extension resulted in lower brake mean effective pressure and power without losses due to throttling. In addition, Reynolds and his team were able to optimize the engine performance at 1500 RPM, an

equivalence ratio of 0.6, and an injection flow rate of 20 g/h. Based on their work, they found that injection timing was relatively unimportant as long as the spark introduced after the mixture became fuel rich near the gap. From the emission stand point, the increase in the injection flow rate decreased hydrocarbon and carbon oxide emissions. On the other hand, the NO_x emission was increased due to more complete combustion and higher temperatures; however it was still lower than at stoichiometric conditions (Reynolds 2003). Cheolwoong et al. obtained similar results when they experimented on a gasoline engine (Cheolwoong 2012). A fuel-rich region was generated via direct injection of a rich mixture into the spark plug region prior to ignition.

In order to study the mixing of methane and air during the partial stratification, Mezo conducted his experiments using a partial stratified charge injection system and a constant volume combustion bomb filled with pure air. A specially-designed spark plug was equipped with channels that were used to inject methane into a region near the spark plug gap. A Schlieren optical apparatus was used along with a high-speed video camera at a frame rate of 4700 frames/s. The pressure in the chamber was held constant at 6.9 bar, while the pressure of injection and the spark timing were varied. The “spark timing” was taken as the time elapsed between triggering the fuel injector and the spark plug. The injection was carried out at the pressures of 2, 3, and 4-times higher than the chamber pressure. Based on his experiments, the combustion of the resulting mixture near the spark plug was achieved under limited range of injection pressure and spark timing (Mezo 2009). The largest frequency of combustion success was achieved with a pressure ratio of

three. Results also indicated that minimum spark timing led to successful combustion increase with increasing pressure ratio.

In addition to a partially stratified combustion systems, the lean limit can be extended using geometry modification of the chamber and the piston. The piston is designed to generate some mixture motions or turbulence during the intake and the compression stroke to increase the mixture burning velocity. Most new engines use some combination of the “swirl” and “bowl” to force the mixture to move in the center of the piston. Evans used a piston with the channels on top; they enhanced squish effect to trap the fuel and generated a series of jets directed towards the center of the chamber. A technical drawing of the piston is shown in Figure 2.2. This modification is referred to as a squish/jet combustion chamber configuration (Evans 2009). He successfully showed that using this kind of design could extend the lean operation to $\phi = 0.63$. This modification reduced NO_x emission due to lower in-cylinder temperatures.

A number of studies have been carried out on the influence of electronically excited oxygen molecules on the combustion of hydrogen–oxygen mixtures. This approach is based on the fact that excited atoms and molecules are highly reactive. Smirnov and his team investigated the effects of excited oxygen molecules in a flow reactor with transparent sidewall as depicted schematically in Figure 2.3. Electronically-excited oxygen molecules $\text{O}_2 (a^1\Delta_g)$ and $\text{O}_2 (b^1\Sigma_g^+)$ at singlet state were generated in the water-cooled discharge cell. The discharge cell was connected to the main flow reactor. The hydrogen pressure tank was connected to the flow reactor through a separate line, and the mixing took place right before entering the

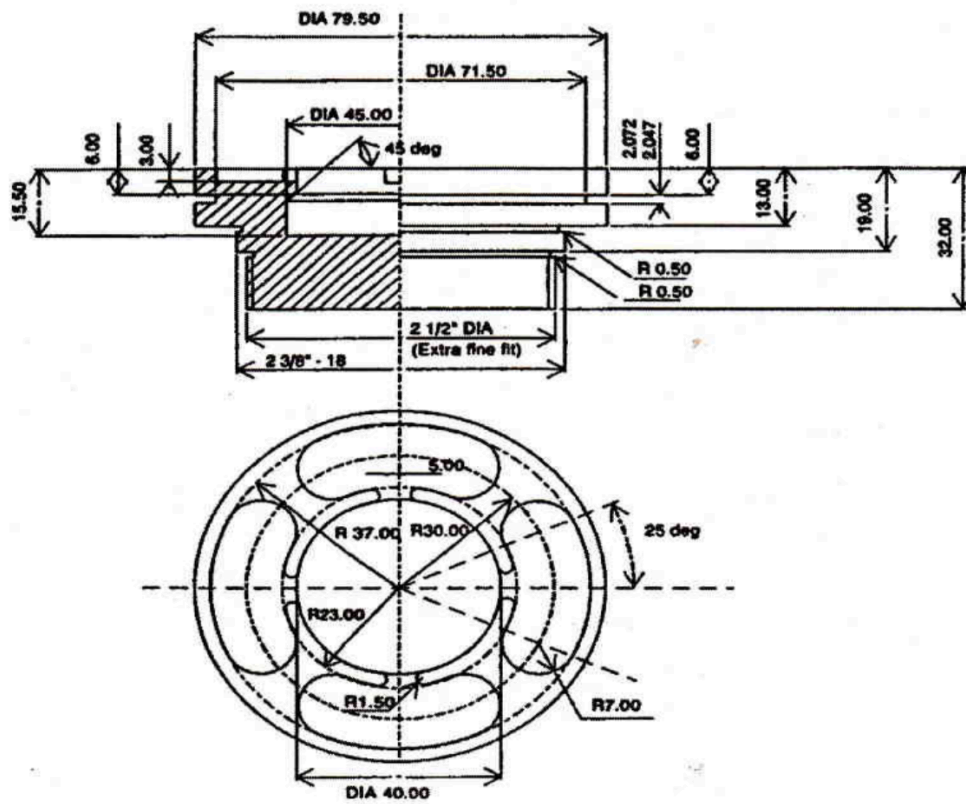


Figure 2.2 UBC 1C squish - jet combustion chamber.

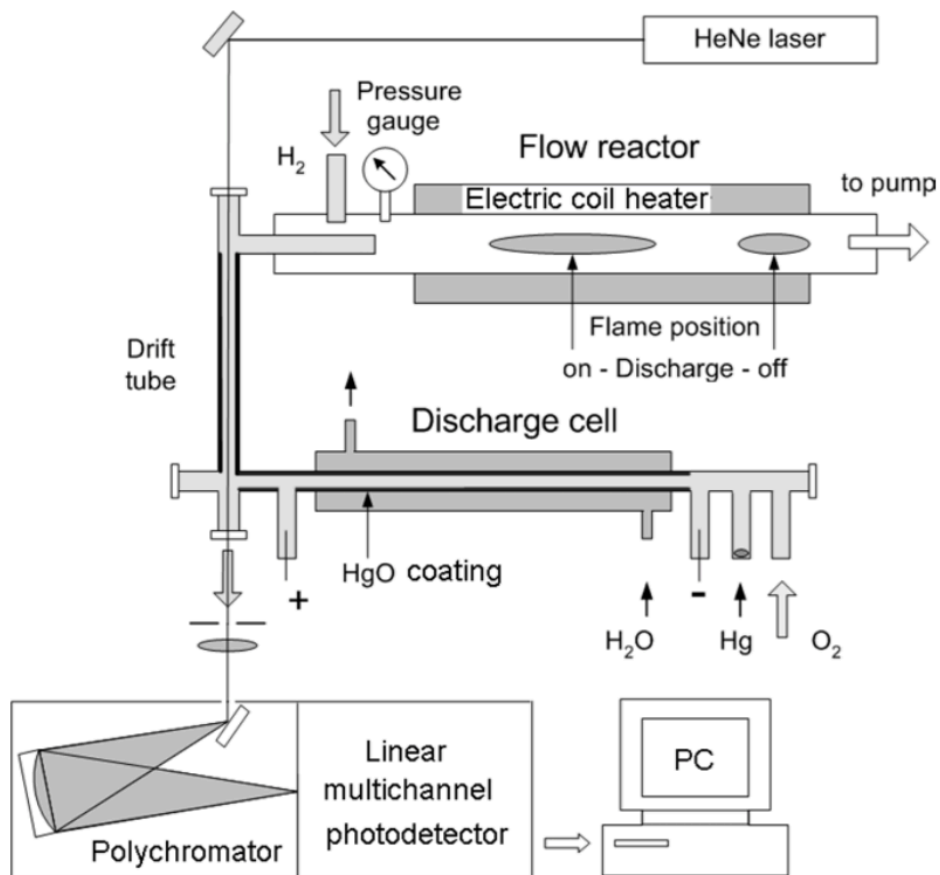


Figure 2.3 Experimental setup on the influence of electronically excited oxygen molecule on combustion of H₂-O₂ mixture (Smirnov 2008).

main flow reactor. To provide the ignition in the flow, the wall of the reactor was heated to temperatures between 700 and 1000 K. The flame position along the flow reactor axis was used as the criterion of successful enhancement in the flame zone by electronically-excited O₂ molecules. Without O₂ excited molecules, the beginning of an initial flame growth was observed much further along the tube than in the case of electronically-excited O₂ molecules (Smirnov 2008). In addition, self-ignition occurred at a much lower temperature of flow reactor walls with electronically-excited O₂ molecules. The results obtained from the experiments were confirmed with results obtained from an analytical CFD model.

2.4 USE OF HIGH ENERGY IGNITION SYSTEM TO EXTEND LEAN LIMIT

Repetitive spark discharges, multiple spark plug systems, laser ignition systems, corona spark plug systems, etc. have been studied for decades and proven their ability to extend the lean limit operations. Ignition of the lean fuel-air mixture using high-energy ignition systems stabilizes the lean-mixture combustion and reduces pollutant emissions considerably (Checkel 1997). Harrington proposed method that could be implemented to extend the lean limit operation is to enhance the applied energy from a spark plug or other similar device. The lean operation could be extended using a multiple spark capacitor discharge (MSCD) ignition system in a standard internal combustion engine. Harrington tailored the MSCD system to deliver a spark every 300 μ s for a period of about 15 ms for every cylinder firing (Harrington 1974). His results showed that for light load, the lean misfire limit

could be extended as well as EGR tolerance; furthermore, the engine performance also appeared not to be affected at high loads.

Rado and Durbin showed that multipoint spark ignition with several spark plug gaps was more effective in reducing the fuel consumption and extending the lean misfire limit. Energy of a multipoint gap could be delivered up to twice the energy from a single gap spark plug in a much shorter time using the same ignition system. The multiple-gap spark plug allows increasing overall flame kernel's size and reduces the combustion duration (Rado 1976, Durbin 1983).

Nakamura et al. investigated the effect of using 12 spark points on the performance of a 4-cylinder engine. The number of sparks used at any one time and the distance between the sparks were varied so that the most efficient combination could be determined. They concluded that using the highest number of the spark plugs resulted in the highest efficiency and the highest extension of the lean limit; however, spacing between the gaps did not affect the results as much as the numbers of the spark plugs did (Nakamura 1985).

Kupe and Wilhelm investigated the effect of the plasma jet ignition (PJI) on the extension of a lean limit for methane-air mixture in a constant volume chamber (Kupe & Wilhelm 1987). The high-energy plasma was created by charging a condenser and discharging the energy into a modified spark plug. Such a high energy would create highly charged and reactive free radicals and electrons that would play the role of catalyst in igniting the air-fuel mixture. An equivalence ratio of the mixture was varied from 1 to 0.66. Combustion of an air-methane mixture was observed through quartz windows using a high-speed video camera and a

Schlieren system. As expected, the plasma jet ignited a comparatively large mixture volume only 1 ms after the spark timing, as compared to conventional ignition (CI). The flame propagation turned out to be much faster for the PJI injection. The PJI system was then installed in a single cylinder engine and tested under different loads and engine speeds. The operational range was extended to a very high air-fuel ratio. The combustion of the mixture with PJI propagated at a much higher speed, and the NO_x emission was much lower compared to CI.

Another way to extend the lean limit is to use the pre-chamber where the ignition of a fuel-rich mixture occurs, after the products simply jet out into the lean mixture in the main chamber. One of these systems is the pulsed combustion jet (PCJ) system shown in Figure 2.4. It was designed by Hanada and his research group (Hanada 1994). A small amount of a fuel rich mixture ($\phi = 1.5$) entered the pre-chamber through two small channels of 1 mm in diameter and mixture was simultaneously ignited with a spark. The ignition was carried out with either a pulse plasma jet (PPJ) ignition system or a standard ignition system. In the case of PPJ ignition system, a high amount of energy first charged the capacitor, and then was discharged sending a high-energy plasma jet out into the main combustion chamber. Results indicated that PCJ ignition system had the most advantage in the combustion stability where the lean limit was extended to $\phi = 0.41$ as compared to PPJ and standard ignition system, where $\phi = 0.55$ and $\phi = 0.65$, respectively. Results indicated that PCJ ignition system had the most advantage in the combustion stability where the lean limit was extended to $\phi = 0.41$ as compared to PPJ and standard ignition system, where $\phi = 0.55$ and $\phi = 0.65$, respectively. Additional

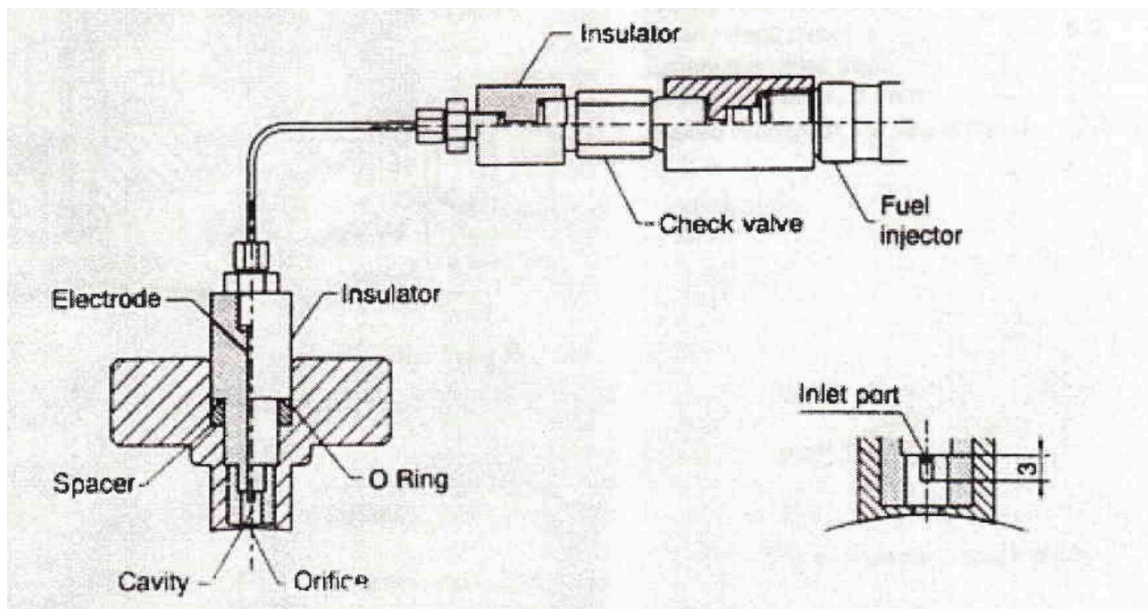


Figure 2.4 PCJ injector and detail of its cavity.

testing was conducted for an equivalence ratio of $\phi = 0.8$ with several different PCJ systems and the standard igniter system, to compare pressure recordings with respect to time. All geometries of the PCJ ignition system decrease the time in which the maximum pressure is reached, while an increase in pre chamber cavity volume shows a trend towards marginal decreases in maximum pressure time. Similar tests were run for PPJ systems, which showed similar decreases in time to reach maximum in-cylinder pressures.

Previously, Nakamura showed that the lean limit could be extended by using 12 spark points system. In contrast, Hotta et al. showed that the lean limit could be extended by use of a single spark plug connected to a small-sized inductive energy storage (IES) circuit with a semiconductor switch (Hotta 2010). The total discharge period for this type of system for 10 pulses was found to be about 400 μs . The experiments were divided into two parts. The first part consisted of experiments on the simple combustion chamber for different fuels such as C_3H_8 and C_8H_{18} . Results showed that combustion probability was increased for lean mixtures even with a single spark of short duration. Repetitive short-duration sparks further improved the extension of the lean limit. In fact, visual observation from the high-speed camera with Schlieren system showed that the flame kernel was much larger for short duration sparks as compared to a conventional spark. The second part of investigation was an engine performance test series and used a single-cylinder gasoline engine. The IES proved to noticeably extend the lean limit from $\text{AF}=20$ to $\text{AF}=23$. The dilution limit tests showed similar improvement, with EGR tolerances increasing from 17.5% EGR by volume out to 22.5% EGR. From an emission

standpoint, NO_x emission was reduced with IES system. On the other hand, CO emission was slightly increased, probably due to a lower amount of oxygen at a high EGR coupled with higher temperatures in cylinders.

Technically, plasma can be separated into two categories: thermal (PJI ignition systems) and non-thermal. The most common non-thermal plasma is microwave-assisted combustion. The electromagnetic wave passes through the fuel mixture causing excitation of the electrons and resulting in an increase in electron collisions. This process creates a large amount of free ions and highly reactive radicals that enhance chemical reactions. (DeFilippo 2011). Practically, this method is applied by creating non-thermal plasma using pulses of focused microwave introduced via specially adapted spark plug. DeFilippo et al. implemented this method using a single-cylinder Waukesha ASTM-Cooperative Fuel Research engine, with 91 Octane gasoline fuel. They investigated the effect of microwave power on the performance of the engine. Results indicated that the higher the energy input of the microwave, the lower the lean limit could be extended (DeFilippo 2011). The energies of the spark that have been used in the experiments were 130, 900, and 1600 mJ. With the highest energy input, the lean limit was extended to $\phi = 0.66$ compared to $\phi = 0.72$ for 900 mJ. They also observed that as the equivalence ratio of the mixture decreased, the power also decreased. This result was expected because the amount of fuel in the mixture was reduced considerably at low equivalence ratios. The specific fuel consumption also decreased with decreasing equivalence ratio; however, it sharply increased after the extension of the lean limit, due to a large amount of unburned fuel being produced when the engine misfired.

Flame development for different energy levels of microwave assistance was strongly dependent on the power of additional energy (the higher the energy, the faster the flame propagation). The NO_x emission, even though it decreased, was not sufficient enough to allow the removal of the after-treatment system.

The same microwave-assisted spark plug device was also used in a single-cylinder Waukesha ASTM-Cooperative Fuel Research engine but with methane as a fuel (Rapp 2012). The energy of the spark plug was varied the same way as in the previous experiments. The indicated mean effective pressure (IMEP) and indicated thermal efficiency were used to determine when the lean limit had been reached. The first parameter was the coefficient of variation (COV). The COV increased when the engine operation became unstable, leading to partial burn cycles and misfires. The second parameter was characterized by a modified pressure ratio (MPR). The MPR defines if a cycle has complete combustion, partially burned or misfired. Engine operation was considered to be stable when COV was no more than 10%, and the percentage of complete combustion 95%. Effect of the microwave energy on engine stability at different air-fuel ratio (λ) is shown in Figure 2.5. As can be seen in the figure engine stability increases with the addition of microwave energy. Rapp et al. showed that the lean limit could be extended using microwave-assisted spark plug to $\phi = 0.59$ ($\lambda = 1.68$) for both 900 and 1600 mJ of energy input. As the energy level of the microwave increased, the number of misfires and partial burns increased greatly. However, it is interesting to note that the lowest COV was obtained with a microwave input energy of 900 mJ instead of an input of 1600 mJ.

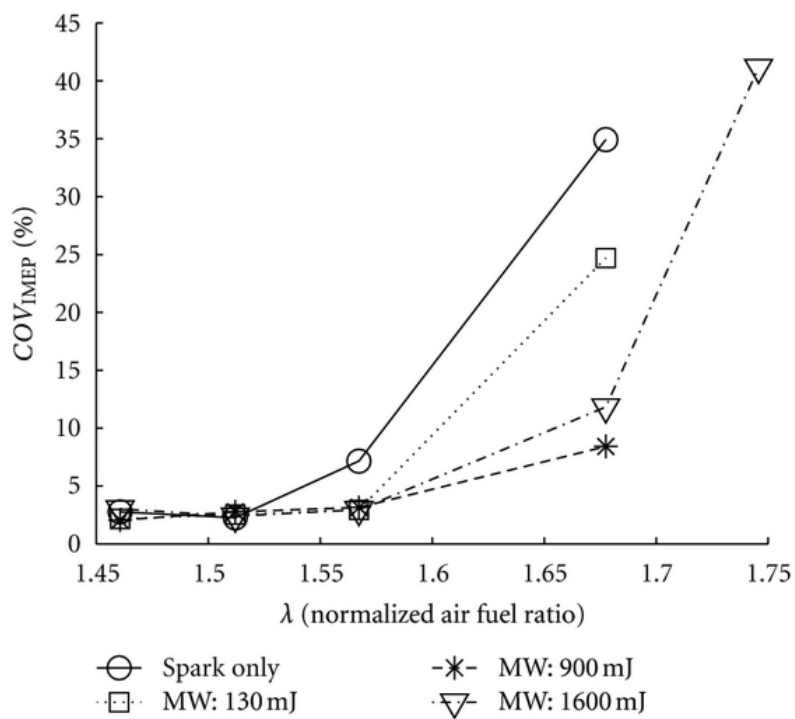


Figure 2.5 Engine stability increases with the addition of microwave energy as λ increases. Increasing microwave energy from 900 mJ to 1600 mJ did not further increase engine stability (Rapp 2012).

CHAPTER 3

EXPERIMENTAL APPARATUS AND PROCEDURE

This chapter describes the experimental apparatus and procedure used in the present investigation. The experiments are performed at the National Transportation Research Center (NTRC) of Oak Ridge National Laboratory (ORNL). The major components of the experimental apparatus consist of a high-pressure combustion chamber, a gas injection system, a high-speed video camera and data acquisition system. A detailed description of the experimental apparatus and procedure are given below.

3.1 COMBUSTION CHAMBER ASSEMBLY

The combustion chamber assembly consists of a gas control panel, a high-pressure combustion chamber, gas cylinders and a vacuum pump.

A high-pressure combustion chamber designed to withstand pressures up to 20 MPa is used in the present investigation. Figure 3.1 is a photograph of the combustion chamber. The outside surface of the chamber is of hexagonal design, whereas the inside surface is of cylindrical design of 6.5 cm in diameter and 12 cm high, resulting in an internal volume of approximately 400 cc. Both the chamber and the top flange are machined from 316 stainless steel. With this particular design each surface of the hexagon has a minimum wall thickness of 2.4 cm at the center of the surface and a maximum wall thickness of 2.8 cm at the edges of the surface.

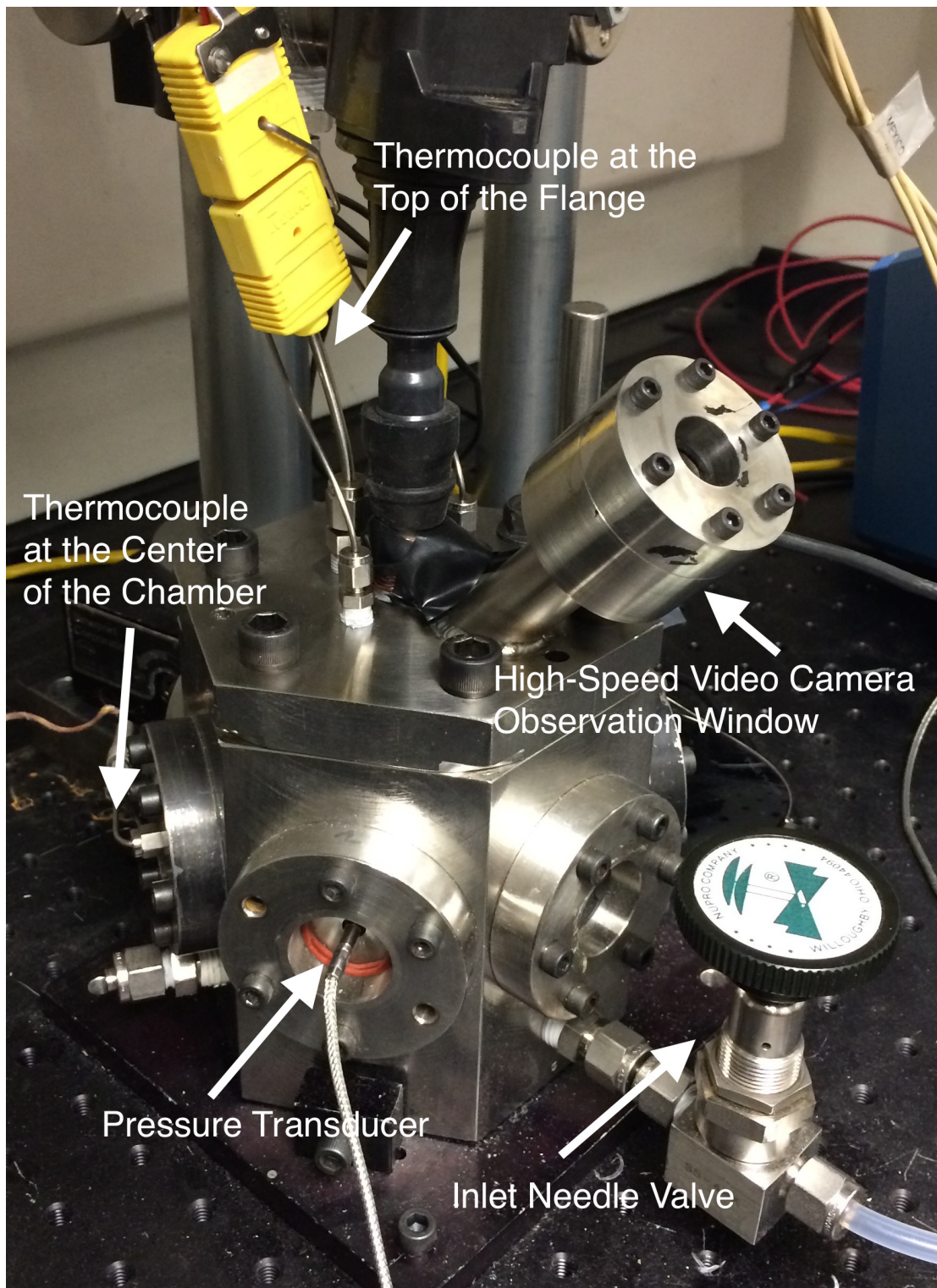


Figure 3.1 Photograph of combustion chamber used in present investigation.

The top flange as seen in Figure 3.2 is secured to the main chamber by six Allen head 3/8-16 Cr-alloy machine screws. An O-ring is used to seal between the flange and the main chamber. A Delco 12620540 spark plug is installed at the center of the top flange and is used to ignite the methane-air mixtures. Also located on the top flange is a 1/8 NPT fitting through which a 0.16-cm OD stainless steel capillary injection nozzle is inserted. The injection of either O₂ or other gases of interest such as N₂ and CO₂ through the nozzle into the spark plug gap is accomplished via an injection system, which will be described in details later. The temperature of the gases after ignition in the region of the spark plug is measured with a type-K thermocouple inserted through a 1/8 NPT fitting mounted on the top flange.

To provide the optical access for the high-speed camera, an observation window machined from 316 stainless steel is positioned on the top flange. The observation window consists of a thick-walled welded to the upper flange at an angle of 44° at one end and a quartz window housing at the other end. By placing the observation at an angle of 44° access to the six 3/8-16 Cr-alloy machine screws is easily facilitated. The cylindrical tube is of 1.9 cm in outside diameter with a wall thickness of 3 mm and a length of 5.2 cm. The optical window housing consists of upper and lower flanges of 4.45 cm in outside diameter and 1.9 cm in inside diameter. The optical window is a quartz window of 2.54 cm in diameter and 1.27 cm in thickness. The upper flange of the observation window is secured to the lower flange by six 3/16-32 Cr-alloy machine screws. Two O-rings are used to seal between the quartz and the upper and lower flanges of the optical window housing. This design of the observation window would permit the area around the spark plug

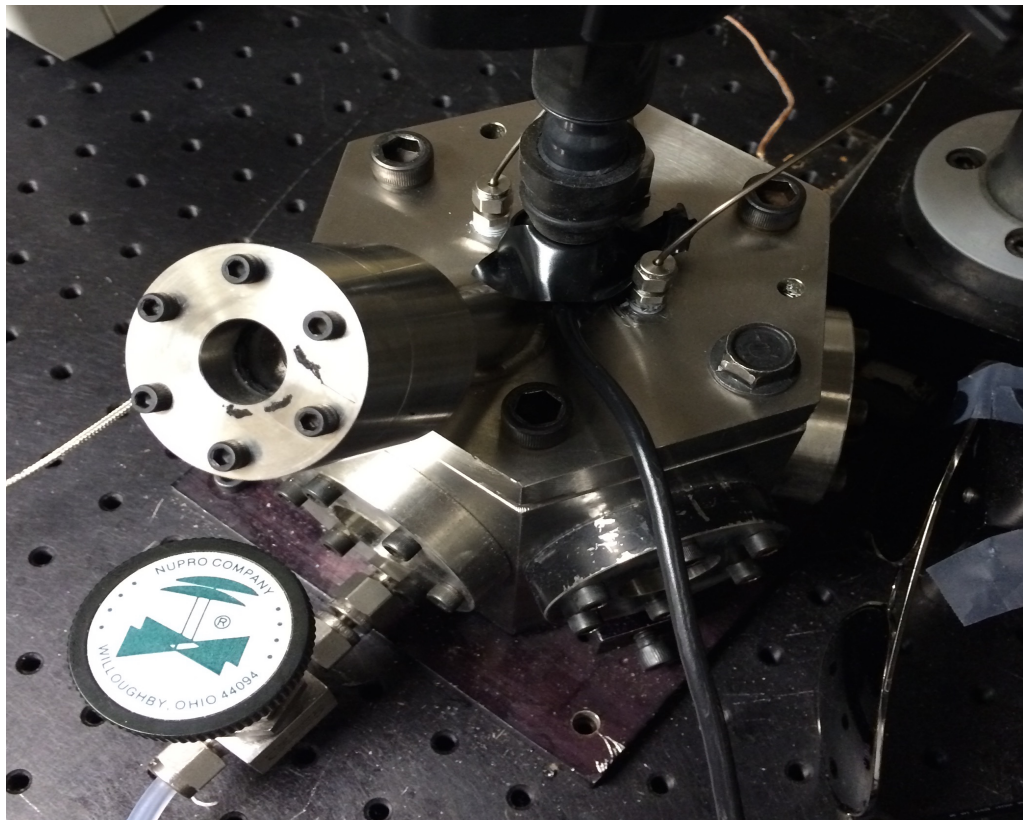
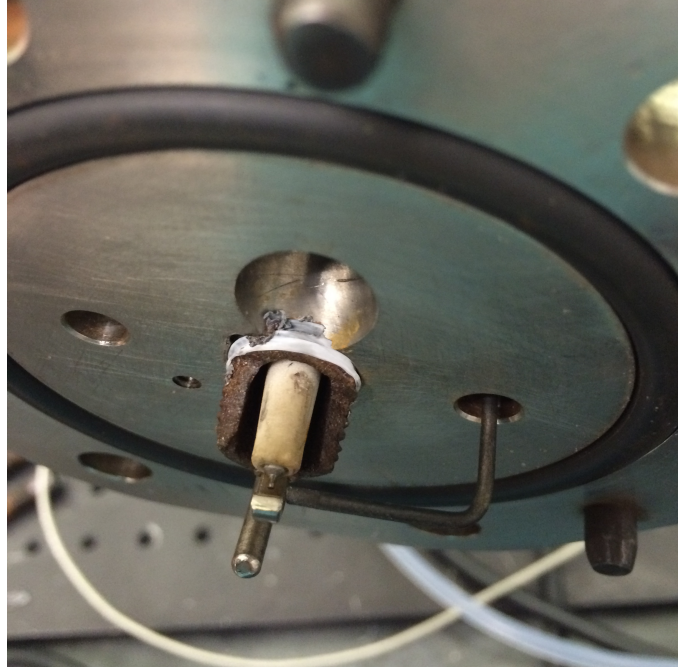


Figure 3.2 Top flange with capillary injection nozzle, high-speed camera observation window and type-K thermocouple.

gap to be recorded by the high-speed camera during the ignition and combustion of the methane-air mixtures.

Located halfway on each surface of the hexagonal combustion chamber is either a 2.54 cm diameter stainless steel disc of 3.05-cm thickness or 2.54 cm diameter fused silica window of 1.25 cm thickness. The stainless steel disc or the fused silica window is held in place by a circular stainless steel flange secured to the chamber with six 10-32 Cr-alloy Allen head machine screws.

Of the six windows on the surfaces of the combustion chamber, only three are being used in the current investigation. One is used to mount a type-K thermocouple, which measures the gas temperature at the center of the chamber, and the other on the opposite side is reserved for a Kistler-6054 AR pressure transducer; the output of the pressure transducer is connected to a dual mode Kistler type 5010 amplifier. The fused silica window is used to observe the ignition and combustion events inside the chamber.

The thermocouples and the pressure transducer are used to obtain the temperature and the pressure during the ignition and combustion of the methane-air mixture, respectively. Moreover, based on the strength of their signals, it is possible to ascertain whether ignition has taken place, especially at the lean limit of the mixture.

The ignition and combustion of methane-air mixtures is carried out at chamber pressures of 0.34, 0.48, 0.69 and 1.03 MPa. At a given pressure the methane-air mixture is varied from stoichiometric to the lean limit at which ignition is no longer possible. The equivalence ratio of the mixture is varied by varying the

partial pressures of methane and air. Once the lean limit at a given pressure is determined, oxygen is injected into the gap of the spark plug, and its effects on the lean limit are investigated. Based on calculations it is determined that the injection of oxygen into the gap of the spark plug in a short duration of 14 ms would alter the nominal equivalence ratio of the mixture to no more than 3%; and thus there is no need to make the correction for the partial pressure of the air.

The introduction of the gaseous mixture into the combustion chamber is regulated by a gas control panel shown schematically in Figure 3.3. Figure 3.4 is a photograph of the gas control panel. The two pressure gauges on the left-hand side of the panel are used to indicate the partial pressures of methane. The low-pressure gauge in the lower left of the panel has the range between -30 mm Hg and 0.21 MPa, whereas the range of the high-pressure gauge in the upper left is between -30 Hg and 0.31 MPa. Low-pressure gauge is used for low equivalence ratios less than 0.6 and pressures between 0.34 and 0.69 MPa. A high-pressure gauge is used for high equivalence ratios between 0.6 and 1 and a high pressure of 1.03 MPa. A toggle valve (TH-LPG) and a three-way valve (KH-LPG) are used to select the appropriate pressure gauge depending on the equivalence ratio and initial chamber pressure. A high precision needle valve (NCH₄) is used to meter the correct amount of methane introduced into the combustion chamber for a given equivalence ratio.

Located in the middle of the panel are the pressure gauge, a toggle valve, a three-way valve and a needle valve for the metering of air into the combustion chamber. The gauge for air has a range between -30 Hg and 2.17 MPa. Similarly, the introduction of carbon dioxide into the combustion chamber is controlled by the

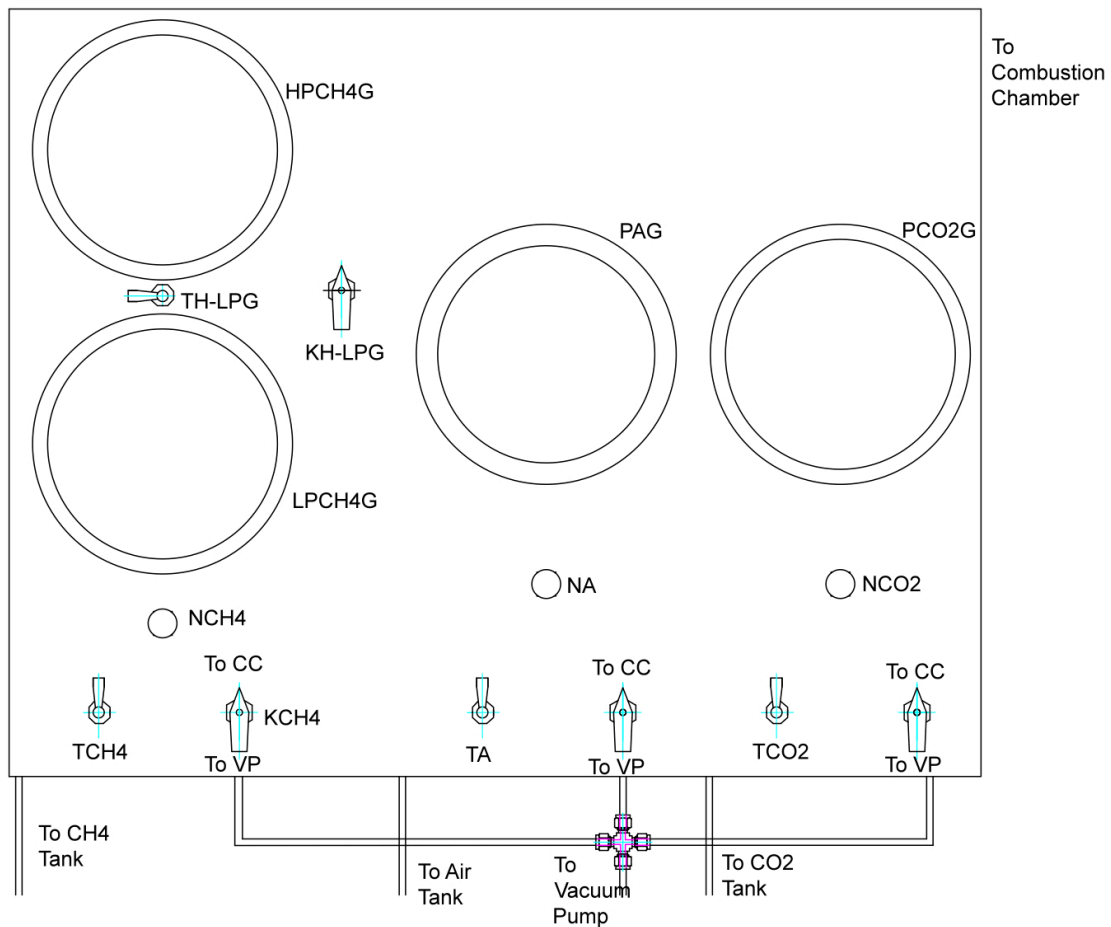


Figure 3.3 Sketch of control panel used to vary equivalence ratio and pressure of methane-air mixtures. (CC) combustion chamber; (LPCH4G) low-pressure gage for methane, (HPCH4G) high-pressure gage for methane, (PAG) and (PCO2G) pressure gage for air and carbon dioxide; (NCH4), (NA) and (NCO2) needle valves for methane, air and carbon dioxide; (KCH4), (KA) and (KCO2) control valves for methane, air and carbon dioxide; (TCH4), (TA) and (TCO2) toggle switch for methane, air and carbon dioxide; (KH-LPG) control valve between low and high pressure gages for methane; (TH-LPG) toggle switch between low and high pressure gages for methane.

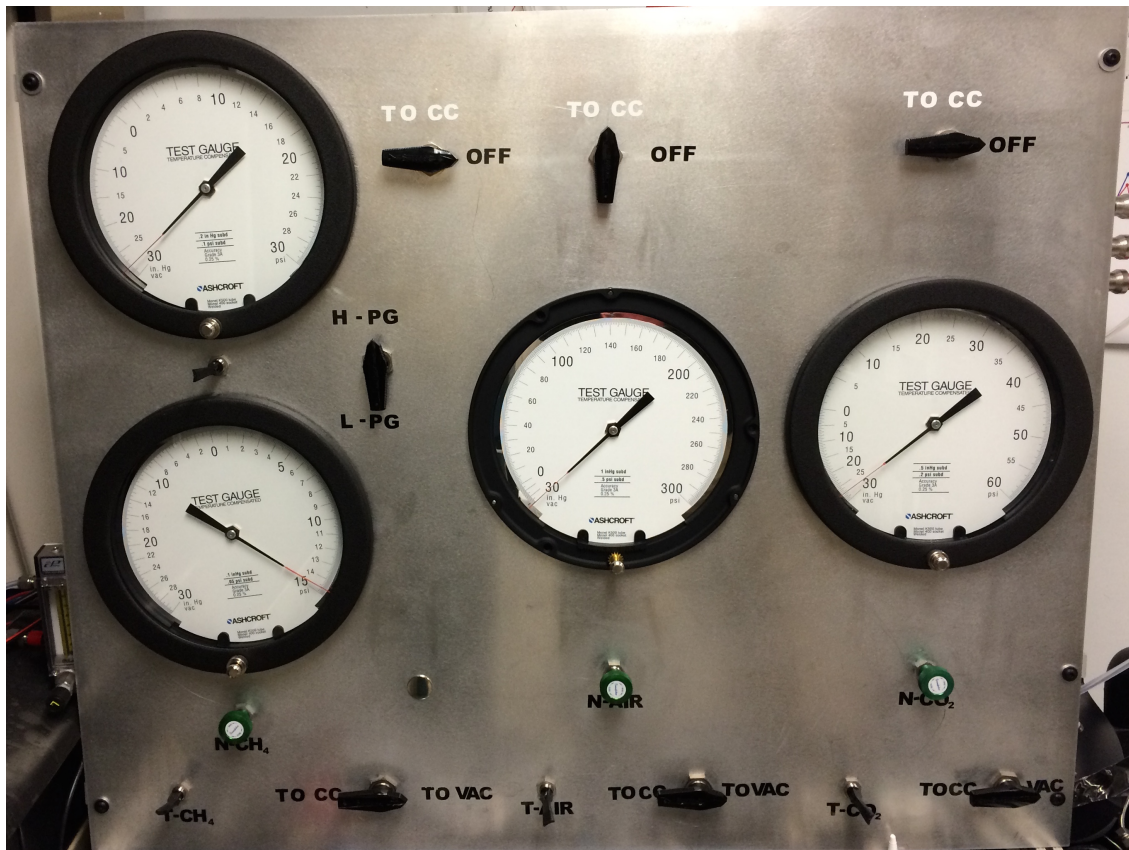


Figure 3.4 Photograph of control panel used in present investigation.

valves and the pressure gauge located on the right side of the panel. For CO₂ the pressure gauge has a range between -30 Hg and 0.52 MPa.

3.2 OXYGEN INJECTION SYSTEM

The oxygen injection system shown in Figure 3.5 consists of a solenoid valve, a pressure gage rated at a maximum pressure of 200 psig, a needle valve and a high-pressure oxygen cylinder. The PeterPaul DC-solenoid valve has a maximum pressure rating of 500 psi and a 0.15875-cm diameter orifice. It is connected to a 0.15875-cm OD stainless steel capillary injection nozzle installed on the upper flange of the chamber as described previously in Section 3.1. Typical response time of the solenoid valve is 13 ms. One of the needle valves is installed right after the oxygen cylinder to adjust the pressure in the line. Since pressuring the line to the prescribed pressure is not always achievable, a purge valve is used to relieve the pressure in the line in case of over-pressurizing. The injection of other gasses such as nitrogen and carbon dioxide is performed using the same injection system.

3.3 HIGH-SPEED VIDEO CAMERA

The high-speed video camera, PowerView HS-650, is used in the present investigation to capture the major events during the ignition and combustion of the methane-air mixtures. The high-speed video camera equipped with a Nikon Af-s DX 18-140mm F/3.5-5.6g focusing lens system is mounted on a tripod and faced towards an oblique observation window on the upper flange of the combustion

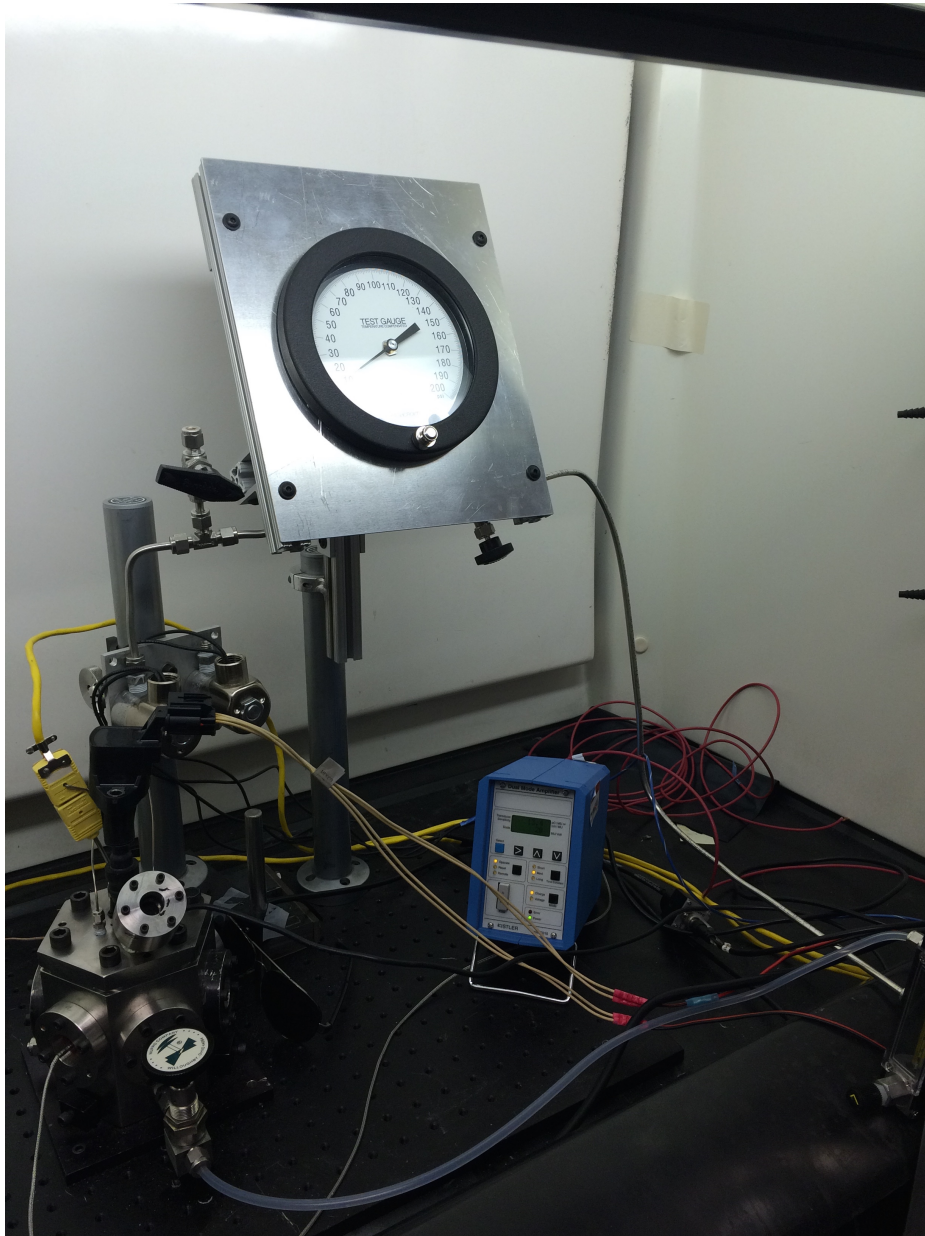


Figure 3.5 Photograph of injection system used in present investigation.

chamber as seen in Figure 3.6. The high-speed camera is connected to a laptop using CamView software Version 3.15 and triggered separately from the LabView acquisition system. The images are taken with a frequency of 3000 frames/s.

3.4 DATA ACQUISITION SYSTEM

The data acquisition hardware is connected to a laptop with NI LabView software. The high-speed data are recorded at a sampling rate of 100 kHz with a NI-cRIO-9076 data acquisition card. Connected to the data acquisition card are a NI-9401 card that is used to trigger the spark plug, a NI-9211 card for recording the temperature measurements from all type-K thermocouples, a NI-9201 card for the pressure transducer, and a DriveView PFI driver used to trigger the solenoid valve. Readings from all these devices are recorded and saved as CSV files in Lab View. The files are then converted to the excel files and analyzed with MatLab R2013b. A screen shot of the Lab View control interface is shown in Figure 3.7.

3.5 DESCRIPTION OF EXPERIMENTAL CONDITIONS AND PROCEDURE

Prior to the experiment the combustion chamber is evacuated using a vacuum pump. Since the vacuum pump is not powerful enough to create absolute vacuum inside the chamber (only -736.6 instead of -762.0 Torr) it was decided to pressurize and evacuate the system with only air three times prior to each experiment. Thus, it is assumed that air of 25.4 Torr is initially present in the system, and it is taken into account in the calculations of the equivalence ratio. At a

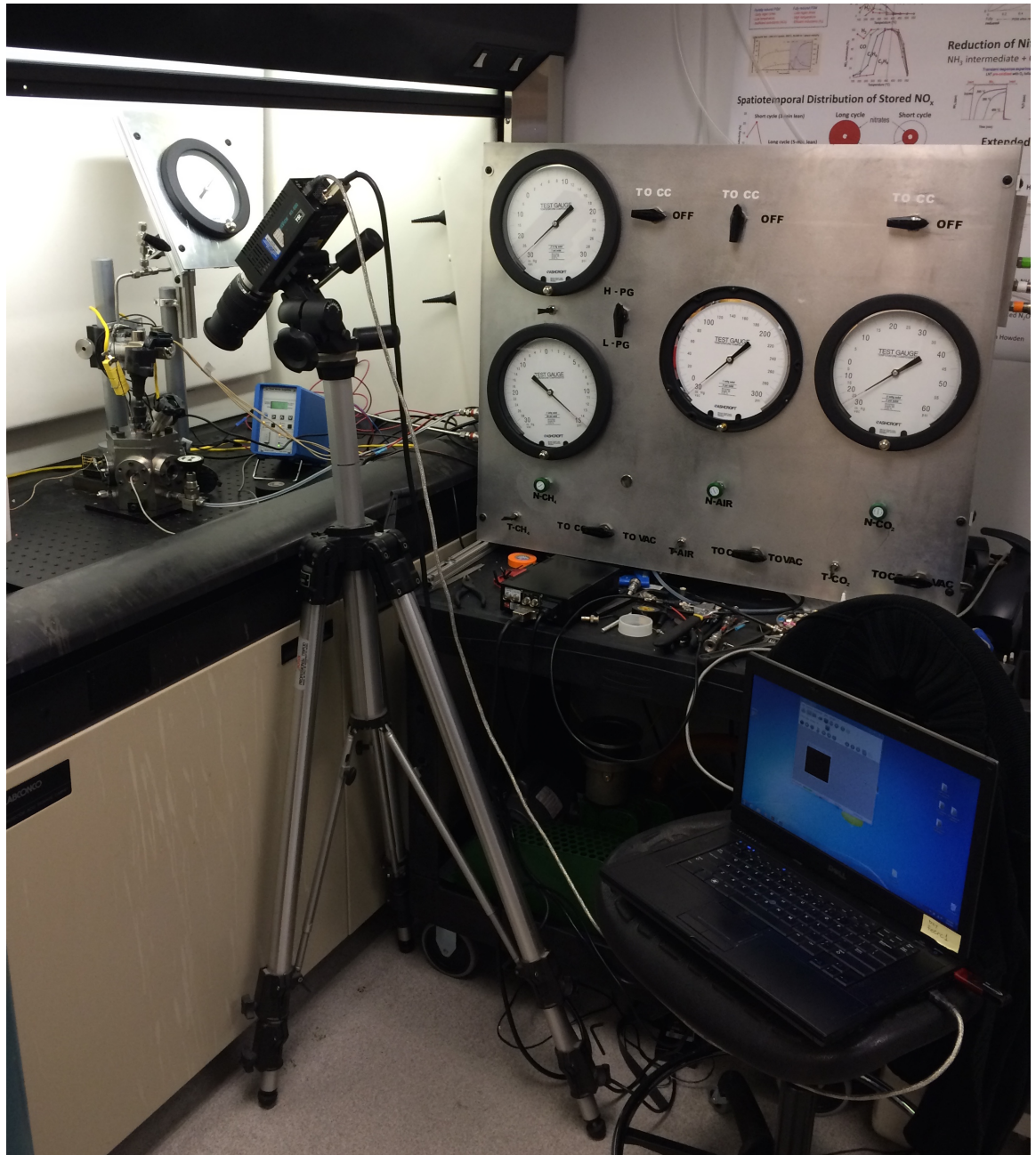


Figure 3.6 Photograph of high-speed camera used for experiments.

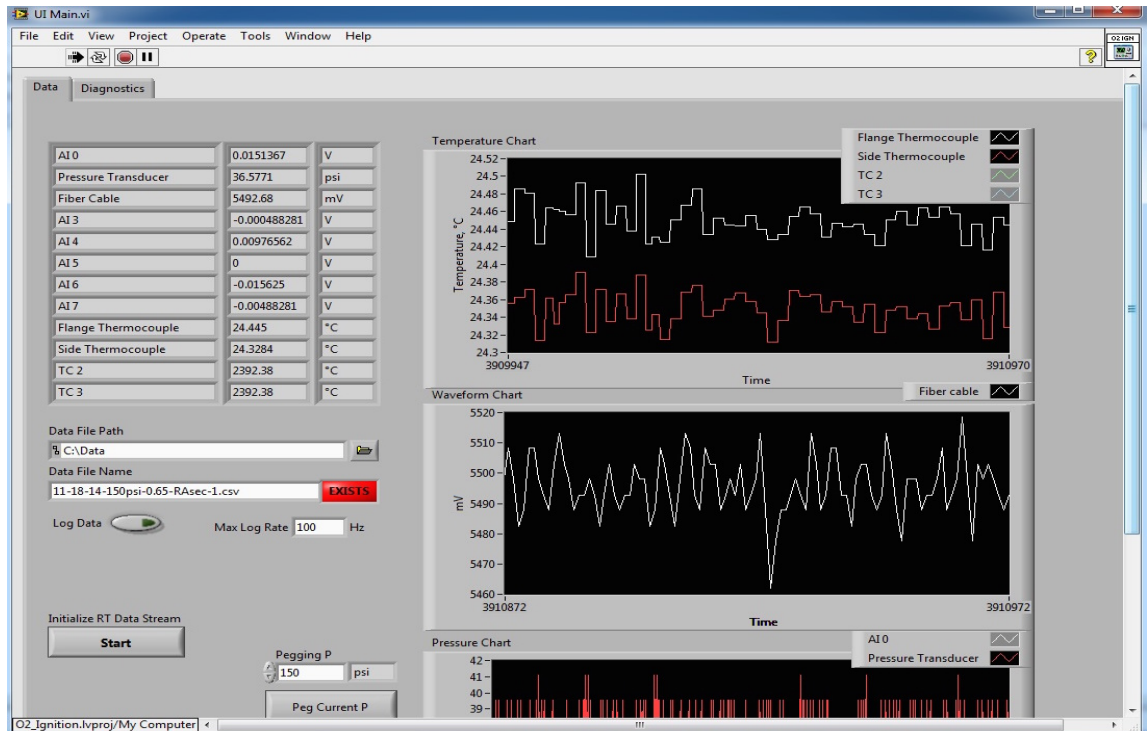
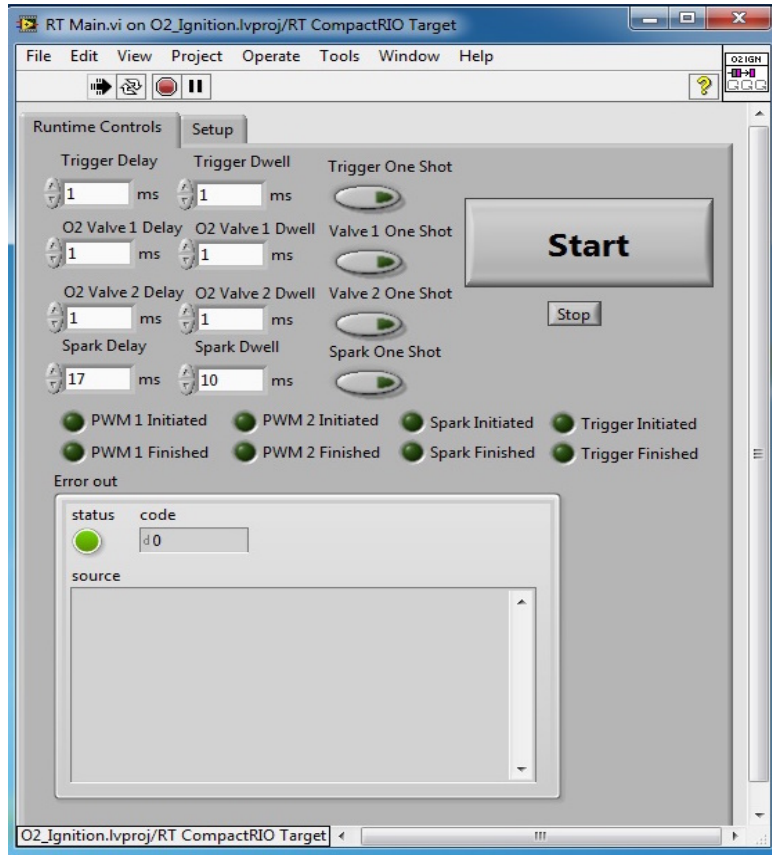


Figure 3.7 Lab View virtual interface.

given equivalence ratio and chamber pressure, the partial pressures of methane, air and carbon dioxide are determined. For the range of pressures between 0.34 and 1.03 MPa investigated in the present study the partial pressure of methane is between 0.0062 and 0.1317 MPa, carbon dioxide between 0.01 and 0.27 MPa and air between 0.32 and 0.97 MPa. Once the chamber is evacuated, the desired equivalence ratio at a given chamber pressure is obtained by pressurizing the chamber to the prescribed partial pressure of each gas. Since the partial pressure of methane is always lowest at any given equivalence ratio and chamber pressure, methane is introduced first into the combustion chamber, followed by the gas of the next higher partial pressure. In the experiments with EGR the gas of the next highest pressure is CO₂, followed by air. Depending on the equivalence ratio and the chamber pressure, methane is introduced into the chamber using either low-pressure or high-pressure gauge. A pressure relief valve is installed at the bottom of the combustion chamber and is set to activate when the pressure inside the chamber reaches above 13.78 MPa.

The methane, air, carbon dioxide and oxygen are introduced into the combustion chamber from the pressurized cylinders using the piping system shown schematically in Figure 3.8. At the end of each experiment the combustion chamber is depressurized by venting the product gases into the atmosphere. In general it takes approximately 10 minutes to evacuate completely all the product gases as well as the removal of the water condensate from the wall of the combustion chamber and the inside surface of the observation quartz window.

Before the effects of the oxygen injection on the ignition and combustion of

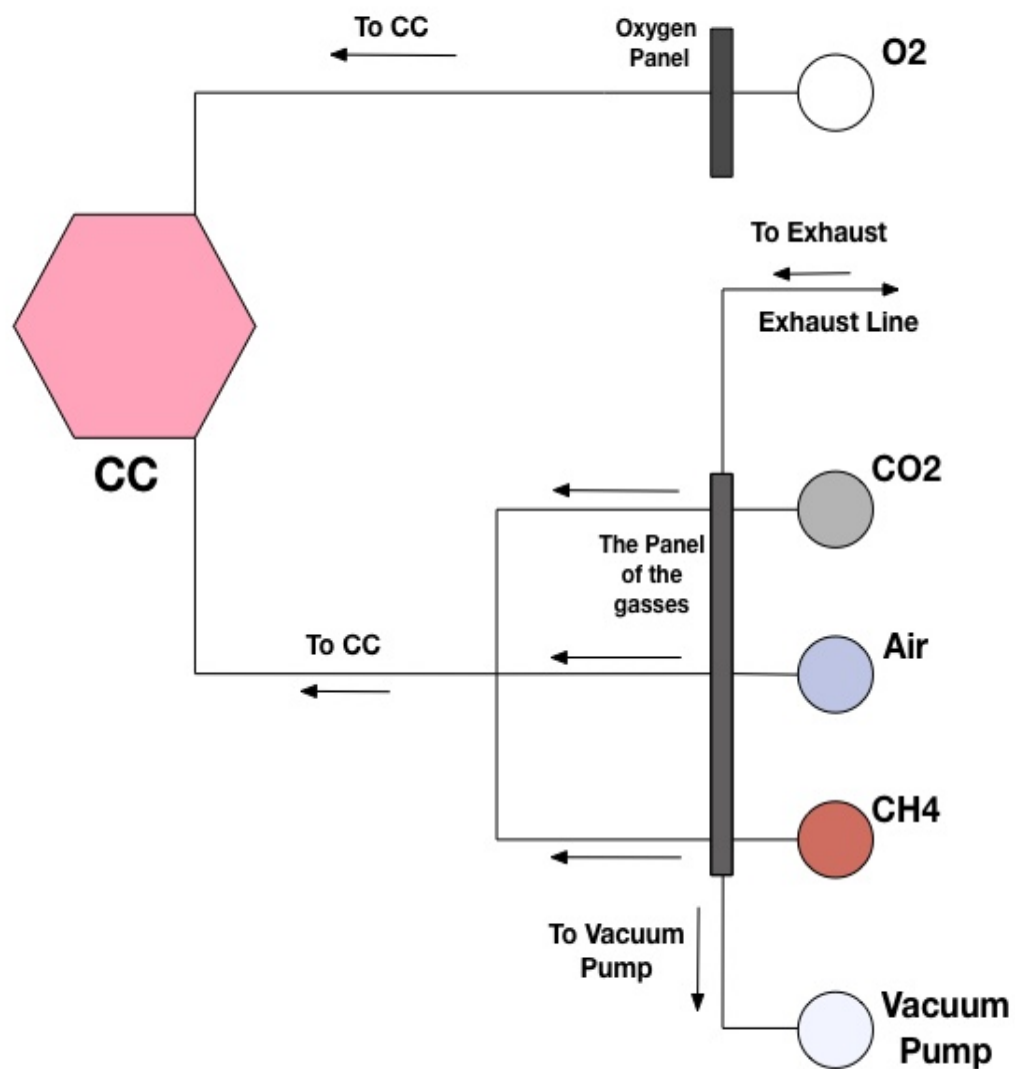


Figure 3.8 Schematic of experimental apparatus.

methane-air mixtures are investigated, it is desired to determine the time required for the charge to be stratified at a given pressure. This time is estimated by varying the time delay between the end of the charging and the introduction of the spark. A total of four time delays are considered: 5 s, 30 s, 5 min and 10 min. As will be shown in details in Chapter 4 at any equivalence ratio and chamber pressure the 5 second-delay time appears to minimize the effects of stratification since the obtained pressure and temperature are highest in comparison to other time delays.

To determine the lean limit for methane-air mixture at a given chamber pressure, the mixture is reduced from stoichiometric to the equivalence ratio at which ignition of the mixture is no longer possible, as evidenced by the temperature and the pressure curves. At least five experiments are performed at any given equivalence ratio and chamber pressure.

In the region of the lean limit without injection the mixture does not always ignite with the first discharge of the spark plug. In this case the spark plug is discharged repeatedly until ignition of the mixture is achieved. If the ignition of the mixture still does not take place after numerous discharges of the spark plug, then it is concluded that the mixture does not ignite at this equivalence ratio.

The effect of oxygen injection on the lean limit is investigated by injecting oxygen into the spark plug gap at the lean limits where ignition and combustion of the mixture are impossible to sustain.

In addition to oxygen, nitrogen and carbon dioxide are injected using the same procedure in order to determine whether the extension of the lean limit is

simply due to the charge motion or the formation of oxygen radicals or highly-energetic oxygen molecules.

3.6 INJECTION SOLENOID VALVE TIME RESPONSE

Knowledge of the time response of the injection solenoid valve is necessary in order to ensure the presence of oxygen in the gap of the spark plug prior to the energizing of the spark. This can be accomplished only when the time response of the solenoid valve is precisely known.

The time response of the solenoid valve is determined using the setup depicted in Figure 3.9. The gas flow through the capillary nozzle is directed to impinge onto a flexible metal strip. Prior to the gas flow the metal strip is in contact with the tip of the capillary tube, thus forming a close circuit; an electrical circuit is created using the LPD-422A-FM power supply. An electrical current of approximately 1 A runs through the circuit when there is no gas flow in the capillary nozzle. Once the solenoid valve is triggered, the gas flow in the capillary nozzle impinges onto the flexible metal strip, bending the strip backward, and thus disrupting the circuit. The signals from the trigger and the close circuit are recorded by a Tektronix TDS 220 oscilloscope. The time elapsed between the trigger and the disruption of the circuit recorded by the oscilloscope is the response time of the solenoid valve. With the present circuit setup the response time of the solenoid valve is determined to be 17 ms. Once the time response of the solenoid valve is known, the trigger of the solenoid valve and the energizing of the spark plug can be

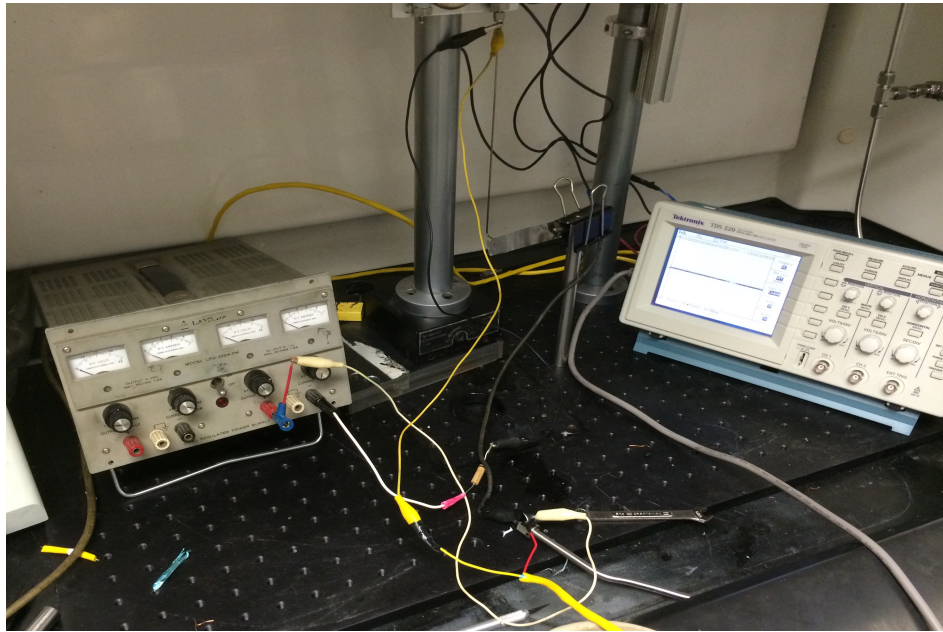


Figure 3.9 The set up for determining response time of solenoid valve.

adjusted to ensure the presence of oxygen in the space between the electrodes of the spark plug prior to the spark discharge.

3.7 MASS OF INJECTED GASES

It is important to estimate the amount of gas injected into the combustion chamber via an injection system consisted of a solenoid valve and a capillary injection nozzle prior to the ignition of the mixture. The amount of injected gas is estimated based on the injection pressure change. Since a small amount of the injected gas is trapped in the solenoid valve and capillary injection nozzle, it is necessary to determine this amount. The amount of a gas trapped in the capillary nozzle is calculated based on the volume of the nozzle. The volume of the gas trapped in the solenoid valve is determined by filling up the valve with water and measuring its weight. After the water-filled valve is weighed, it is connected to a low-pressure air outlet to blow off the trapped water from the system. Once the mass of the water trapped in the solenoid valve and capillary nozzle is determined, the volume can be estimated, from which the actual amount of the gas injected into the gap of the spark plug can be determined. The mass of the injected gas is then used to estimate the change in the equivalence ratio of the mixture inside the chamber as a result of injection.

CHAPTER 4

RESULTS AND DISCUSSION

The results obtained from the present investigation are presented in this chapter. Section 4.1 describes all procedure and calculations have been done prior experiments. The analysis of the time elapsed between the end of combustion chamber charging and the beginning of the spark plug ignition is presented in Subsection 4.1.1. Subsection 4.1.2 discusses the lean limits of the air-methane mixture at different pressures. Solenoid valve injection analysis discusses in Subsection 4.1.3. The effects of O₂, N₂ and CO₂ injections on the extension of the lean limit are described in details in Section 4.2. EGR cases for with and without injection are described in the Section 4.3. All these cases are then compared using a high-speed video camera, a heat released and a product analysis data as well as a pressure and a temperature curves.

4.1 COMBUSTION ANALYSIS

This section describes all procedures and calculations that have been done prior experiments with O₂, N₂ and CO₂ injection. Firstly, the effects of stratification on the ignition and combustion of methane-air mixtures are investigated. It is desired to estimate the time between charging the combustion chamber with air-methane mixture and spark plug ignition that would result in homogeneous mixture to ignite. Secondly, the effects of chamber pressure on the lean limit for a methane-

air mixture are determined. In the present investigation the lean limit is defined as the equivalence ratio at which the maximum pressure rise in the combustion chamber after energizing the spark plug is less than 10% of the initial chamber pressure. And, finally, the optimum time delay between the triggering of the solenoid valve of the injection system and the energizing of the spark plug is determined in order to ensure the presence of oxygen in the space between the electrodes of the spark plug prior to the appearance of the spark discharge.

4.1.1 EFFECTS OF ELAPSED TIME BETWEEN END OF CHARGING AND ENERGIZING SPARK PLUG

It is of utmost important in the present investigation to ensure that the mixture is to remain homogeneous prior to the spark discharge; and that the mixture is not stratified after charging the chamber due to different molecular weight of various constituents in the mixture. Accordingly, experiments are carried out to determine the effect of time delay between charging the chamber and energizing the spark plug on the stratification of the methane-air mixture. At a given chamber pressure and an equivalence ratio individual gases are introduced into the chamber based on their partial pressures, the gas with the lowest partial pressure introduced first, followed by the gas with the higher partial pressure. Thus, in the present investigation methane is always introduced first into the chamber followed either by CO₂, depending on whether experiments are carried out with and without EGR, and then finally air. Generally, a minimum of 5 s is required between the end of

combustion chamber charging and the triggering of Labview data acquisition system or energizing the spark plug.

Figure 4.1 shows the effect of time delay on the pressure rise and for a methane-air mixture at a chamber pressure of 0.34 MPa and an equivalence ratio of 0.6 for four different time delays of 5 s, 30 s, 5 min and 10 min. The effect of stratification on the pressure rise, defined as the difference between the peak pressure during combustion and the initial pressure in the combustion chamber. A maximum pressure rise of 1.0 MPa is obtained when the time duration is 5 s. As a result the combustion is more complete and flame propagation is the highest if the time duration between the end of charging and energizing the spark plug is within 5 s. Based on these results, a time delay of 5 s between the end of combustion chamber charging and the triggering of the data acquisition system is used in all subsequent experiments in the present investigation.

Another important fact that led to make a decision to use the 5 s duration timing than the 30 s is that even though the temperature at the top of the chamber for the 30 s case is few degrees higher than the 5 s case; its peak pressure is noticeably lower and takes longer to reach than that in the 5 s case. Since methane has lower molecular weight than air, and consequently after some time the stratification of the mixture would result in a slightly rich region at the top of the chamber. As a result igniting such a mixture would produce a slightly high temperature rise at the top of the chamber but a lower temperature rise at the center of the chamber as can be seen in Figures 4.2 and 4.3.

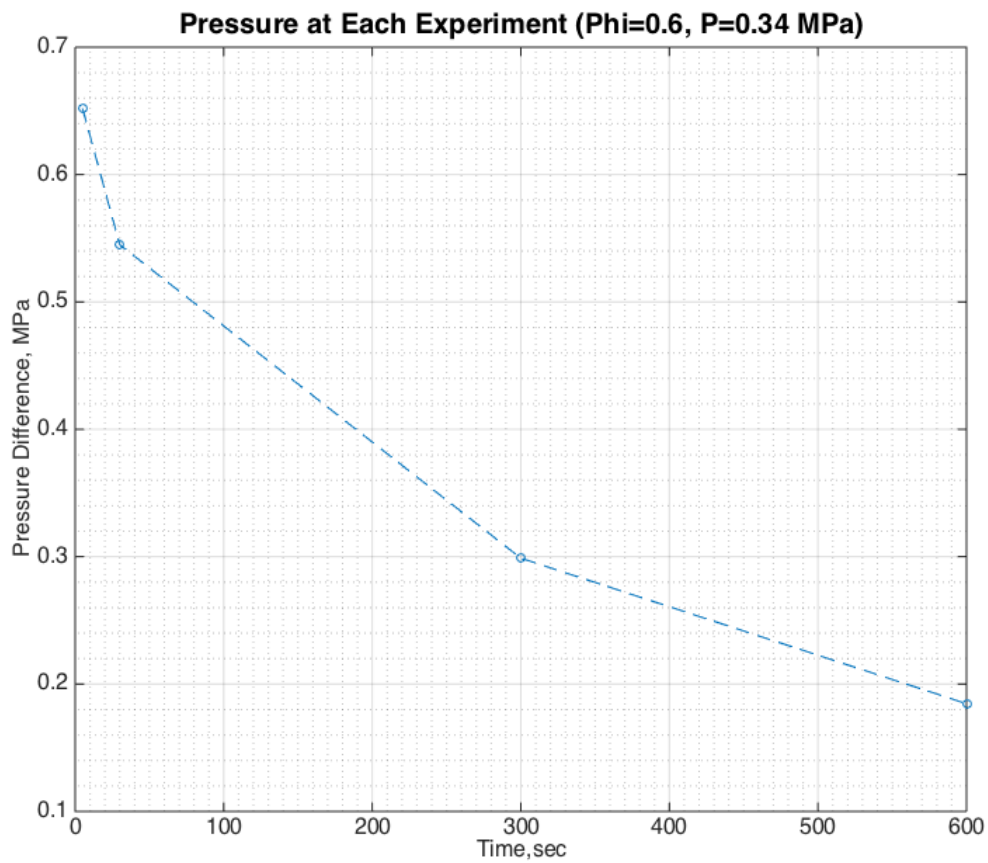


Figure 4.1 Effects of time delay between chamber charging and energizing spark plug on pressure rise of methane-air mixture at chamber pressure of 0.34 MPa and $\phi = 0.6$

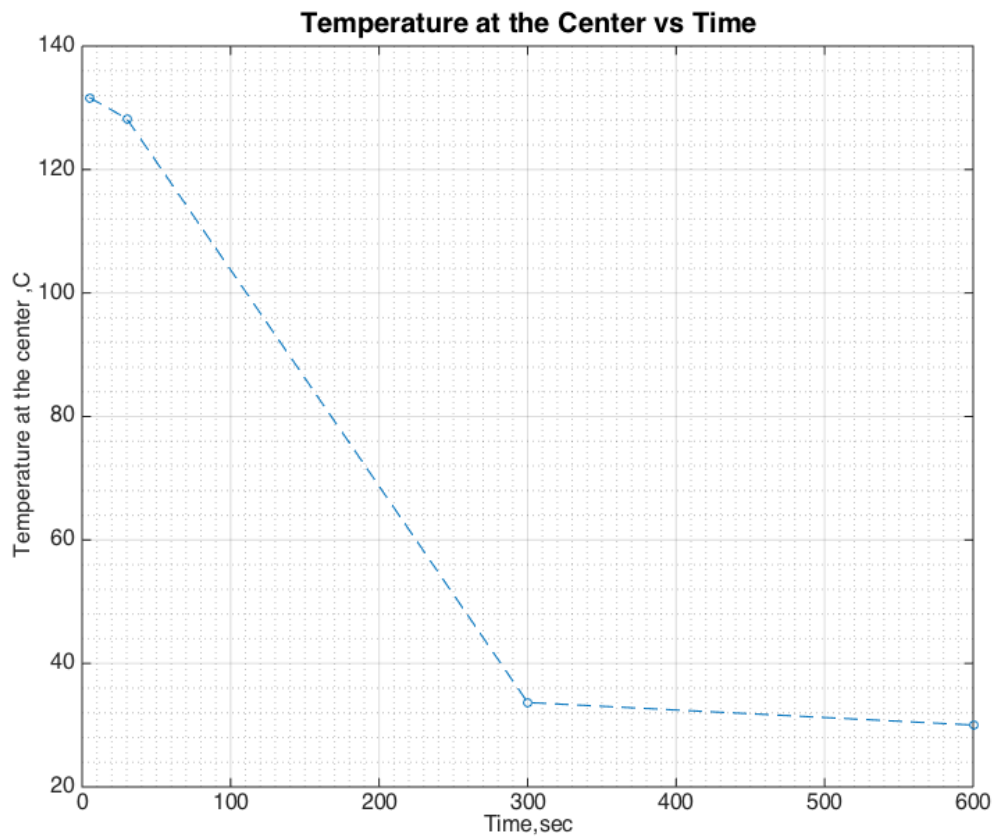


Figure 4.2 Effects of time delay between chamber charging and energizing spark plug on temperature rise near the center of chamber

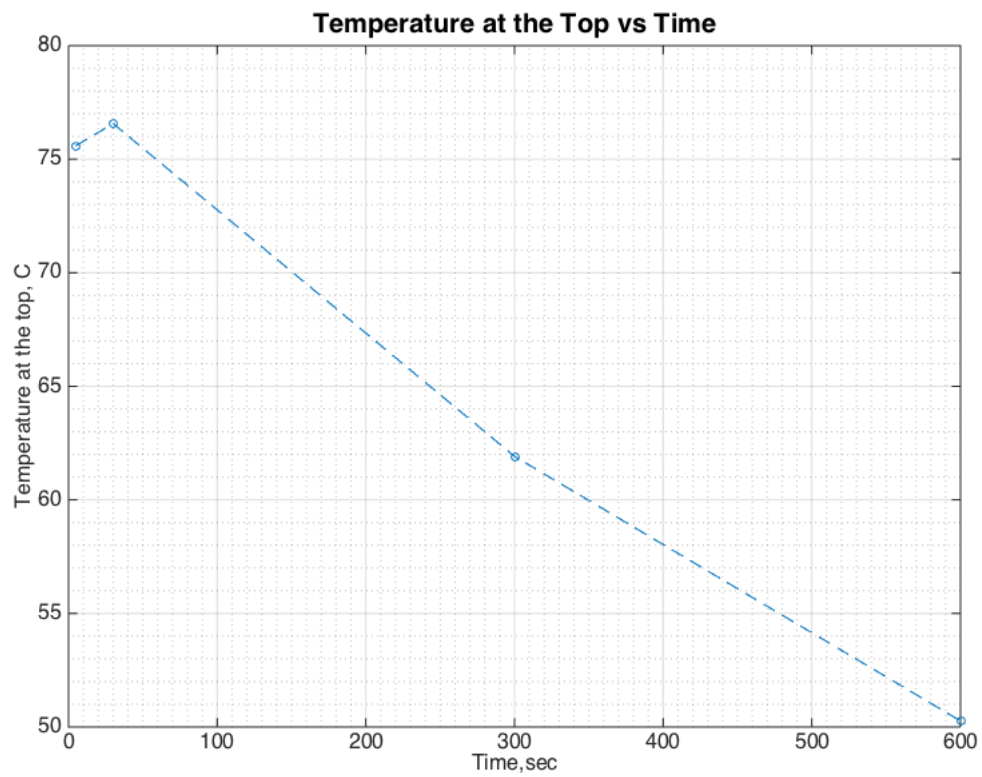


Figure 4.3 Effects of time delay between chamber charging and energizing spark plug on temperature rise near spark plug

4.1.2 DETERMINING LEAN LIMIT FOR AIR-METHANE MIXTURE AT DIFFERENT PRESSURES

To investigate the effect of chamber pressure on the lean limit, the equivalence ratio of the methane-air mixture at a given chamber pressure is reduced from stoichiometric to a lean mixture until ignition of the mixture is no longer possible. Minimum of five experiments is carried out at each equivalence ratio, from which the average peak pressure and the average temperatures at two different locations are obtained. Table 4.1 lists the effect of equivalence ratio on the peak pressure at a given chamber pressure. As seen in the table, the higher the equivalence ratio and the chamber pressure the higher the peak pressure.

For a chamber pressure of 1.03 MPa experiments are conducted only at equivalence ratios of 0.7 and below since at equivalence ratios higher than 0.7, large pressure rises would occur and might damage the quartz observation window.

The lean limit occurs at equivalence ratio $\phi = 0.54$ at initial chamber pressures of 0.34 and 0.48 MPa, where the maximum peak pressure inside the chamber is 38.8% and 14.5% higher than the initial chamber pressure, respectively. Similar trend is observed for the higher initial chamber pressures of 0.69 and 1.03 MPa where the lean limit is obtained at $\phi = 0.56$. Increasing the initial chamber pressure appears to shift the lean limit towards a higher equivalence ratio, i.e., richer mixture. This can be attributed to lower flame speed at high pressure as a result of quenching.

As seen from Figure 4.4 at equivalence ratios below 0.6 the effect of either chamber pressure or equivalence ratio on the average peak pressure is not as

Table 4.1 Effects of chamber pressure and equivalence ratio on average peak pressure of methane-air mixture without injection

Chamber Pressure, MPa	Equivalence Ratio, ϕ							
	1	0.9	0.8	0.7	0.6	0.58	0.56	0.54
Average Peak Pressure, MPa								
0.34	2.31	2.22	1.95	1.71	1.06	0.89	0.67	0.56
0.48	3.43	3.35	2.96	2.52	1.22	0.98	0.83	0.57
0.69	5.02	4.75	4.32	3.57	1.57	1.14	1.10	----
1.03	----	----	----	5.07	1.65	1.21	1.14	----

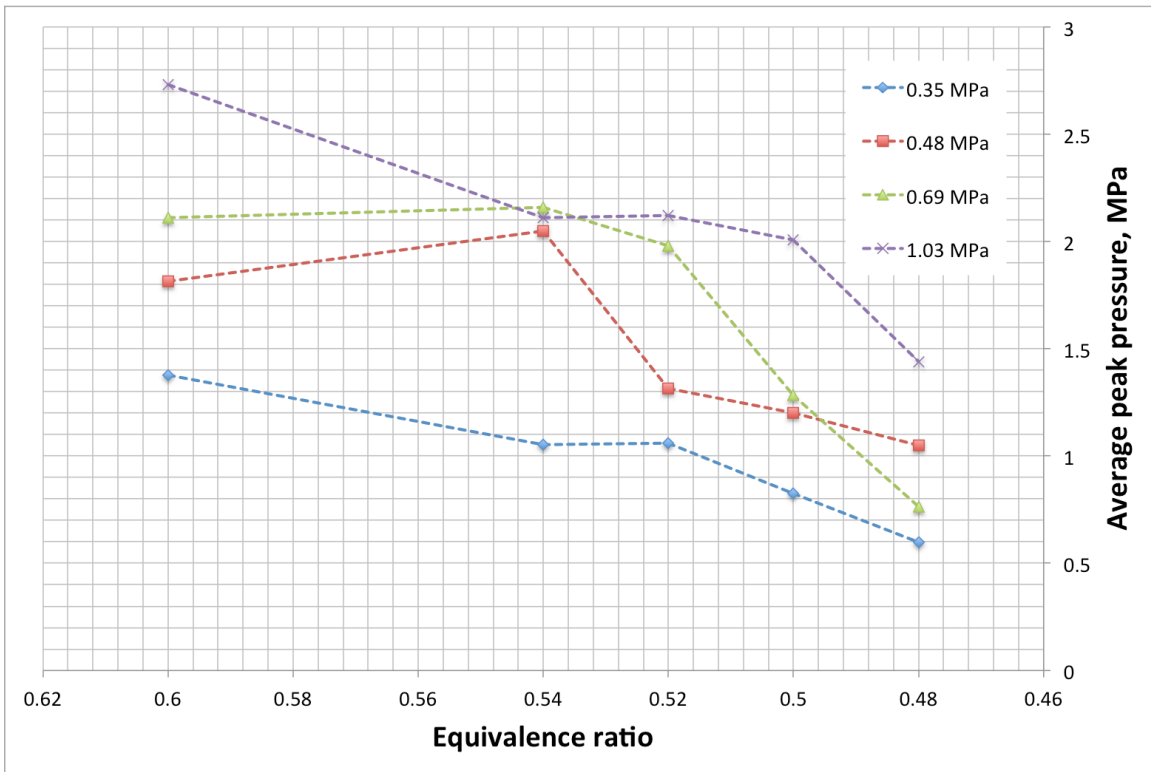


Figure 4.4 Effects of equivalence ratio and chamber pressure on average peak pressure for methane-air mixture

pronounced as at equivalence ratios above 0.7, because the mixture approaches the lean limit. Figure 4.5 shows the average peak temperatures obtained at two different locations: one nearly at the top of the chamber close to the spark plug gap; and the other at the center of the chamber. With the exception at a chamber pressure of 1.03 MPa the temperature at the top of the chamber is higher than that at the chamber center. The flame in this case does not propagate as well as for a lower pressure cases. This could be due to thermal quenching effects occurring at high pressures.

4.1.3 SOLENOID VALVE INJECTION ANALYSIS

As discussed earlier it is of utmost important to ensure that O_2 is present in the gap between the electrodes of the spark plug prior to the spark discharge. Since it takes some time for the solenoid valve to be fully-opened and for the oxygen or any other gases to travel along capillary tube to the spark plug gap, there must be a minimum delay time between the triggering of the solenoid valve and the energizing of the spark plug in order to ensure the presence of oxygen in the gap of the spark plug. This time delay is referred to as the spark timing.

The experiments described in Section 3.6 are performed to investigate the solenoid valve's response time. The system is triggered and the oscilloscope connected to the flexible metal strip current circuit is used to record the signal as a function of time. From the results it is estimated that it takes at least 13 ms for the solenoid valve to be fully-opened and 17 ms for the flow to travel to the end of

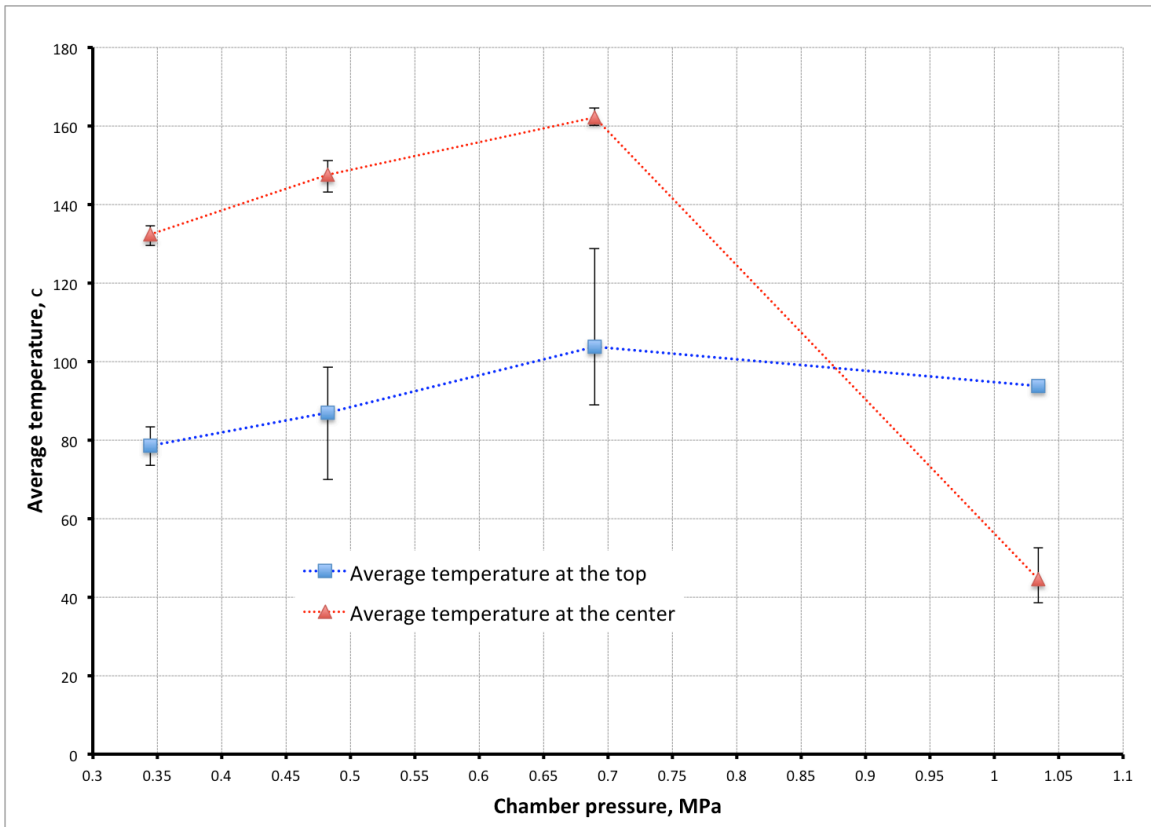


Figure 4.5 Effects of temperature at center and at top on chamber pressure at $\phi=0.6$

capillary tube.

Consequently, the presence of O_2 in the spark plug gap can be ensured only when a minimum delay time (or spark timing) of 17 ms is maintained between the activation of the solenoid valve and the energizing of the spark plug. The signal for closing the solenoid valve is sent approximately 4 ms after the flow appears at the tip of the capillary injection nozzle in order to ensure that the duration of O_2 lasts for 4 ms, which is typically the duration of the spark discharge.

The mass of the injected gas is estimated based on the change in pressure in the injection line, which in turn depends on the chamber pressure. The amount of oxygen injected is regulated by varying the injection pressure rather than by varying the opening duration of the solenoid valve due to the slow response time of the solenoid valve. The change in the equivalence ratio inside the combustion chamber as a result of injection can then be estimated based on the mass of the injected gas. The injected gas is assumed to be as a part of the air in air-fuel ratio. It turns out that oxygen injection does not significantly change the equivalence ratio at all chamber pressures investigated in the present study. It is estimated that the maximum equivalence ratio change is approximately 0.2%.

4.2 EFFECTS OF O_2 , N_2 AND CO_2 INJECTION ON IGNITION, COMBUSTION AND LEAN LIMIT OF METHANE-AIR MIXTURE

In this section the effects of O_2 , N_2 and CO_2 injection on the ignition, combustion and the lean limit of a methane-air mixture are presented. The lean limits for the range of chamber pressures are determined based on the results

presented in the Subsection 4.1.2. The experiments are performed mainly in the lean limit region where the mixture is either poorly ignited or not ignited at all. In addition several experiments are performed at an equivalence ratio of 0.6, from which the pressure and temperature curves are compared for cases with and without injection.

4.2.1 DETERMINING LEAN LIMIT FOR RANGE OF CHAMBER PRESSURES WITH O₂ INJECTION

In this subsection results obtained during experiments with oxygen injection are presented. The experiments are performed at 0.34, 0.48, 0.69 and 1.03 MPa. At a given chamber pressure and a given equivalence ratio, methane and air are introduced into combustion chamber until the desired partial pressures of the gases are reached.

Table 4.2 shows the effects of initial chamber pressure and equivalence ratio on the peak pressure in the case with O₂. The pressure in the injection line at a given chamber pressure and an equivalence ratio is varied until the peak pressure during the combustion in the chamber is maximum. Once the optimum injection pressure is obtained, five to eight experiments are performed under the same injection pressure. The oxygen injection pressures used in the present investigation are shown in Table 4.3. As seen in Table 4.2, the lean limit can be extended with oxygen injection at all chamber pressures investigated in the present study. There are two major factors that could significantly affect the resulting pressure rise in the combustion chamber after ignition. One factor is the pressure variation in the

Table 4. 2 Effects of chamber pressure and equivalence ratio on average peak pressure with oxygen injection

Chamber Pressure, MPa	Equivalence Ratio, ϕ					
	0.6	0.54	0.52	0.5	0.48	0.46
	Average Peak Pressure, MPa					
0.34	1.38	1.05	1.06	0.83	0.60	-----
0.48	1.81	2.05	1.31	1.20	1.05	0.54
0.69	2.11	2.16	1.98	1.28	0.76	1.07
1.03	2.73	2.11	2.12	2.00	1.44	1.08

Table 4.3 Oxygen injection pressure performed to obtain average peak pressure for each chamber pressure and equivalence ratio.

Chamber Pressure, MPa	Equivalence Ratio, ϕ					
	0.6	0.54	0.52	0.5	0.48	0.46
	Injection Pressure, MPa					
0.34	0.58	0.51	0.51	0.48	0.48	-----
0.48	0.72-0.86	0.79	0.584	0.58	0.65	0.58
0.69	0.86	0.86	0.76-0.86	0.86	0.76	0.76
1.03	1.14	1.09	1.17	1.27	1.20	1.27

injection line and the other is the duration of opening of the solenoid valve. The opening duration of the solenoid valve is more or less constant and described in details in the Chapter 3, thus the amount of O_2 injected is varied depending on the injection pressure. As seen in Tables 4.2 and 4.3 the injection of O_2 into the spark plug gap results in a dramatic increase in the peak pressure at an equivalence ratio of 0.5; the peak pressure at an equivalence ratio of 0.5 is almost the same as in the case of an equivalence ratio of 0.6 but without O_2 injection. For a chamber pressure of 1.03 MPa the peak pressures at equivalence ratios of 0.52 and 0.54 are slightly less than the peak pressure rise at an equivalence ratio of 0.5. This is mainly due to the variation in the injected pressure of the injection line shown in the Table 4.3. Slightly higher injection pressure at an equivalence ratio 0.5 resulted in the higher peak pressure compare to equivalence ratios of 0.52 and 0.54.

The effects of injection pressure on the peak pressure in the region of lean limit, where the equivalence ratio is between 0.46 and 0.6, could be a topic of further research. It is observed that the oxygen injection does not significantly affect the peak pressure after ignition for equivalence ratio above 0.6. For example the average peak pressures inside the chamber are almost the same at an equivalence ratio of 0.6 with and without oxygen injection. However, the pressure traces show that the burning rate is much higher and the flame propagation is much faster with the oxygen injection. Comparison plots are represented in Figures 4.6 to 4.11.

Figures 4.12 to 4.15 show the peak pressure inside the chamber for range of chamber pressures with oxygen injection. The error bars represent the maximum and minimum pressure rise inside the chamber at a given equivalence ratio. As seen

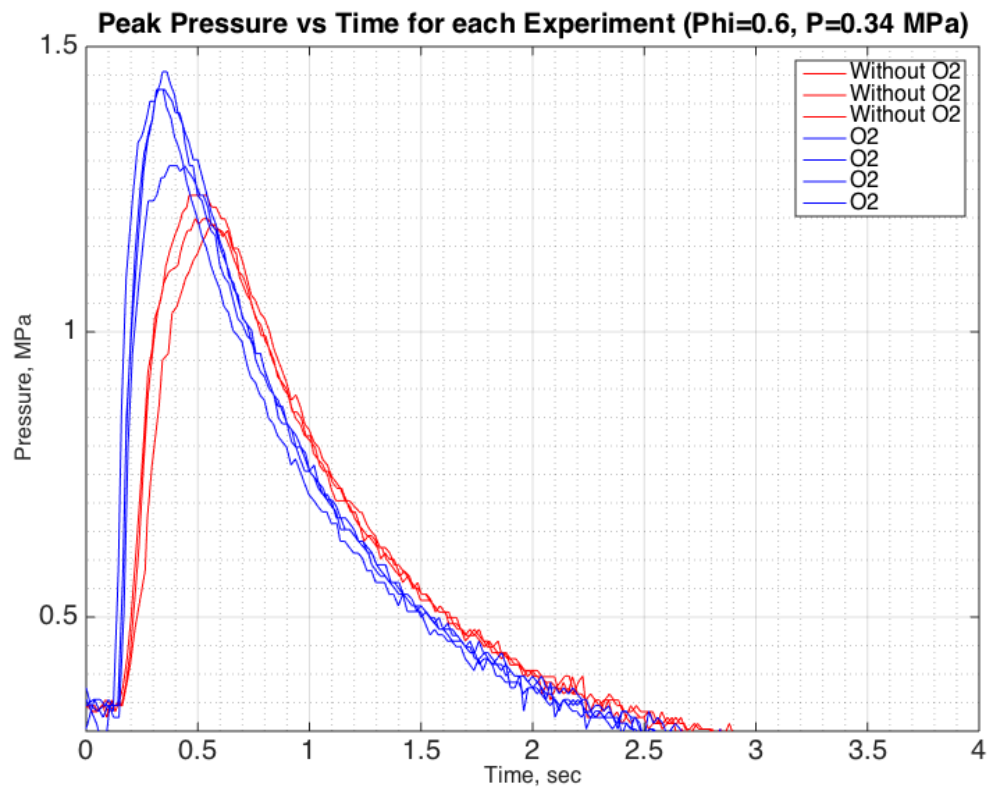


Figure 4.6 Effects of O₂ injection on pressure of methane-air mixture at $\phi = 0.6$ and chamber pressure of 0.34 MPa (--- without O₂ injection, --- with O₂ injection)

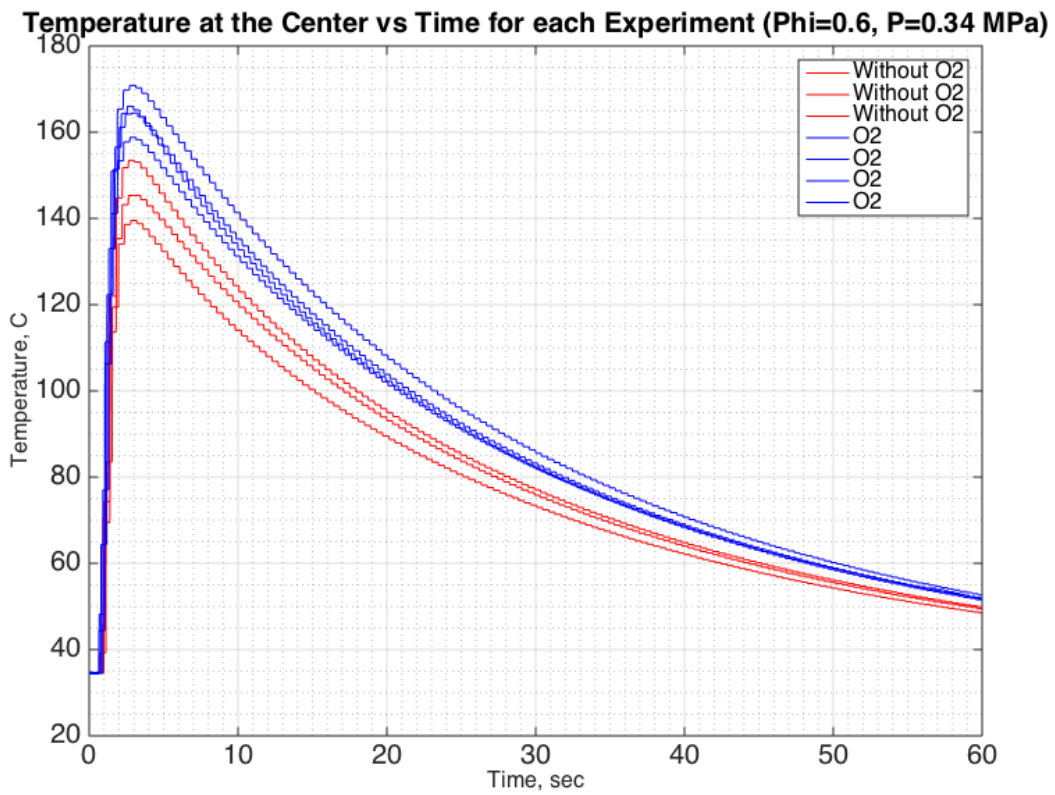


Figure 4.7 Effects of O₂ injection on temperature at center of combustion chamber of methane-air mixture at $\phi = 0.6$ and chamber pressure of 0.34 MPa (--- without O₂ injection, - - - with O₂ injection)

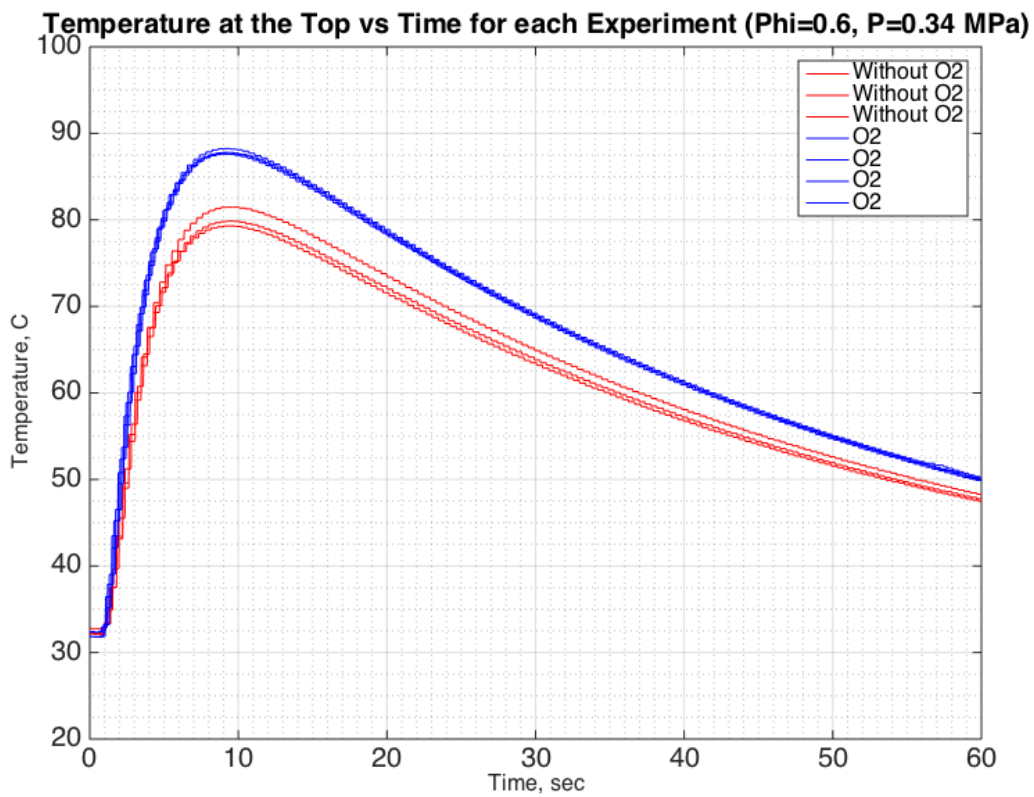


Figure 4.8 Effect of O₂ injection on temperature near the spark plug of methane-air mixture at $\phi = 0.6$ and chamber pressure of 0.34 MPa (--- without O₂ injection, --- with O₂ injection)

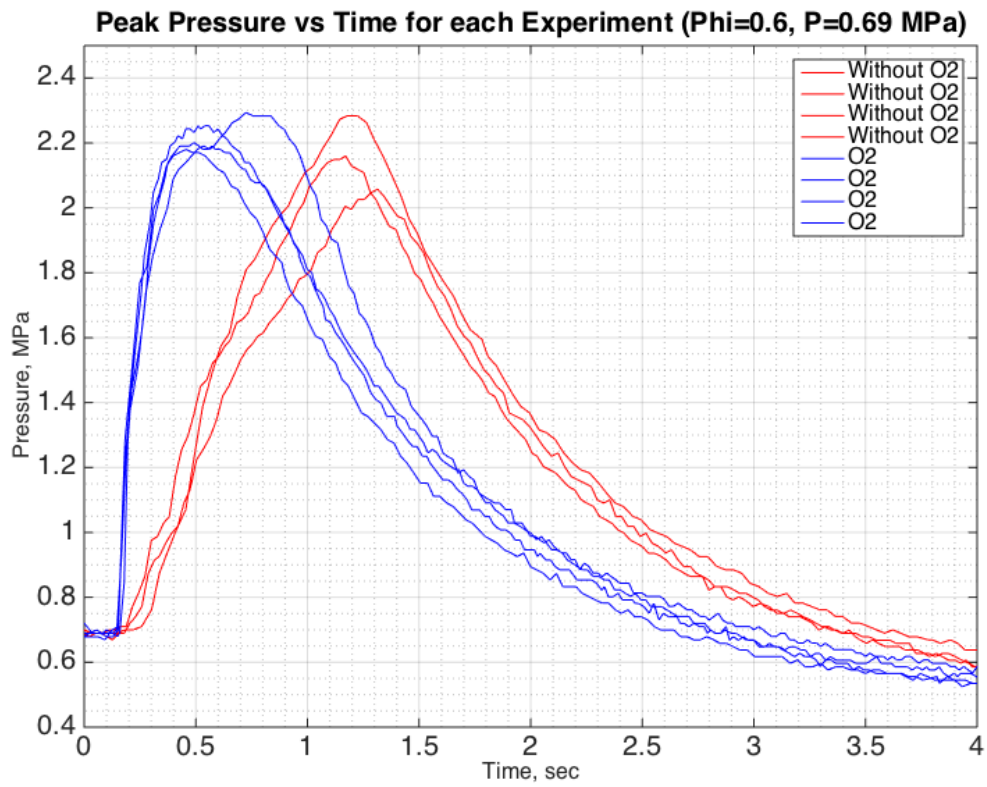


Figure 4.9 Effect of O₂ injection on pressure of methane-air mixture at $\phi = 0.6$ and chamber pressure of 0.69 MPa (--- without O₂ injection, --- with O₂ injection)

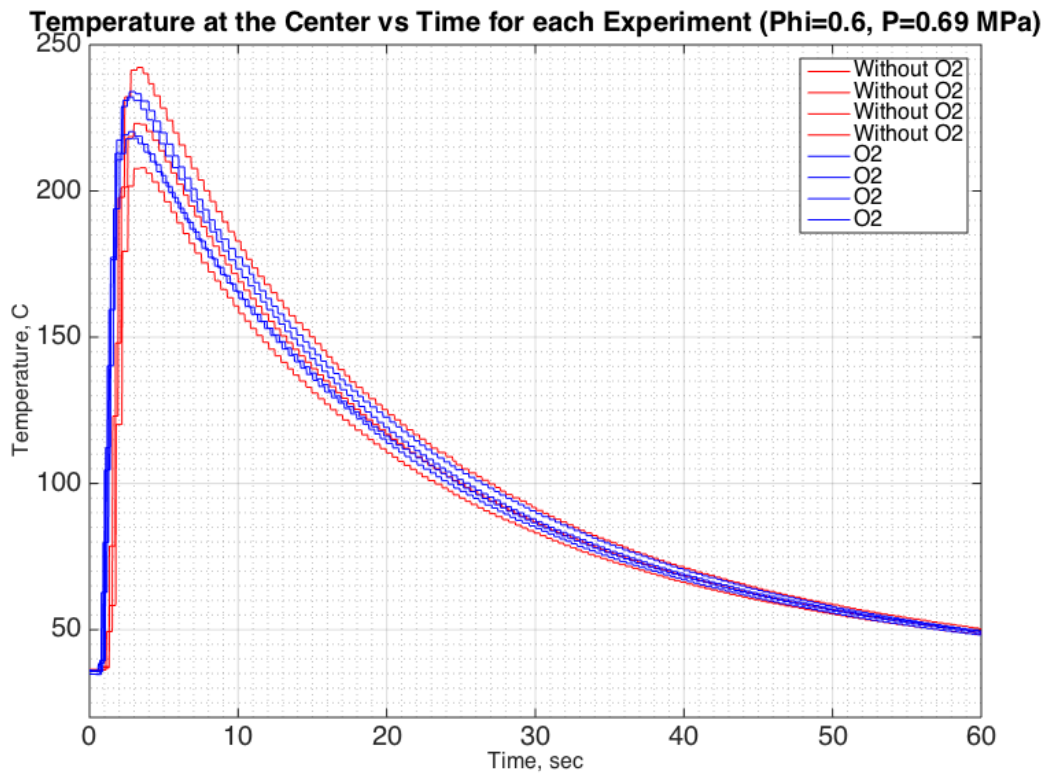


Figure 4.10 Effect of O_2 injection on temperature at center of combustion chamber of methane-air mixture at $\phi = 0.6$ and chamber pressure of 0.69 MPa (---without O_2 injection, --- with O_2 injection)

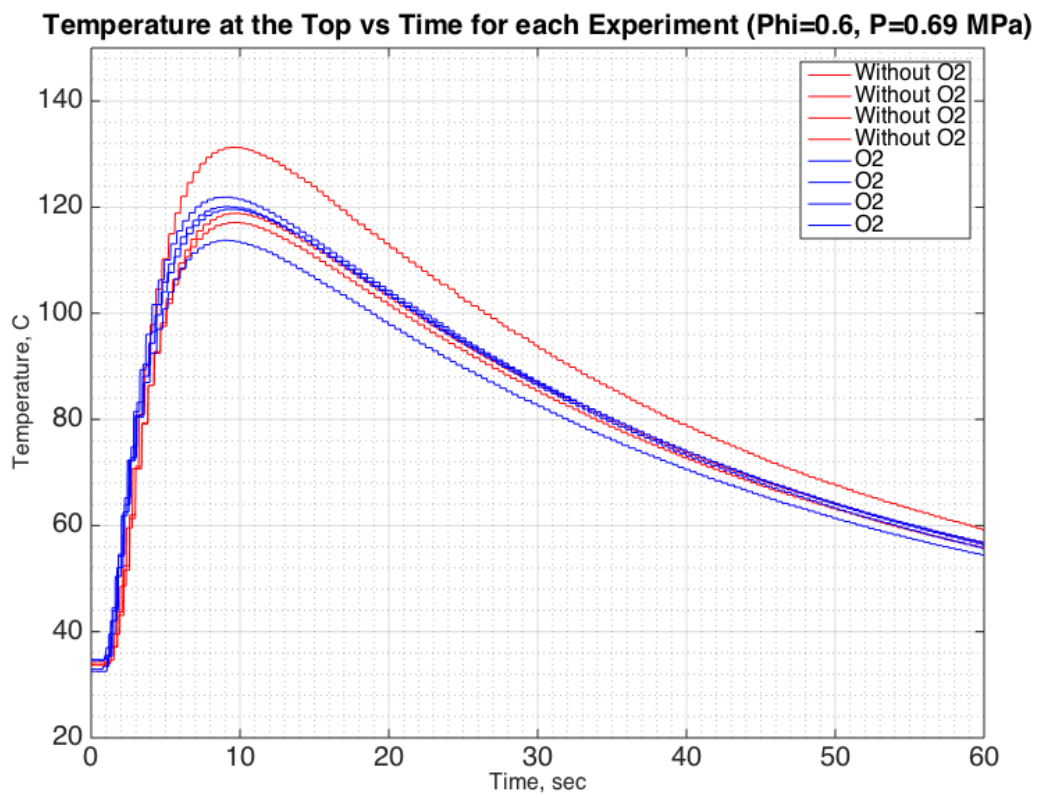


Figure 4.11 Effect of O₂ injection on temperature near the spark plug of methane-air mixture at $\phi = 0.6$ and a chamber pressure of 0.69 MPa (--- without O₂ injection, - - with O₂ injection)

as the chamber pressure increases the peak pressure also increases.

At each chamber pressure investigated in the present study, with O₂ injection the peak pressure at an equivalence ratio of 0.5 is almost the same or higher as at an equivalence ratio of 0.6 with no injection, and thus it is important to compare the results obtained with O₂ injection to those with N₂ and CO₂ injection. For this purpose the average peak pressures obtained with O₂ injection at equivalence ratios of 0.46, 0.48, and 0.5 and a chamber pressure of 1.03 MPa are listed in Table 4.4.

4.2.2 EXTENDING LEAN LIMIT AT CHAMBER PRESSURE OF 1.03 MPA WITH N₂ INJECTION

To determine whether the extension of the lean limit by oxygen injection is due to the formation of highly reactive oxygen radicals or induced charge motion, experiments are carried out with N₂ injection. In this subsection results obtained with nitrogen injection are presented. Nitrogen is injected into the gap of the spark plug under the same injection pressure and solenoid valve timing as oxygen. In addition, the injection pressure for equivalence ratios of 0.5, 0.48 and 0.46 is intentionally reduced in order to investigate the effect of injection pressure on the peak pressure. The experiments are performed only at a chamber pressure of 1.03 MPa since at such a high pressure the error due to the pressure gage resolution could be significantly minimized. The initial equivalence ratio for the experiments is chosen to be 0.5, and then is reduced in an increment of 0.02 until ignition of the mixture is no longer possible. The reason an initial equivalence ratio of 0.5 is that at a chamber pressure of 1.03 MPa without injection, no ignition of the mixture is

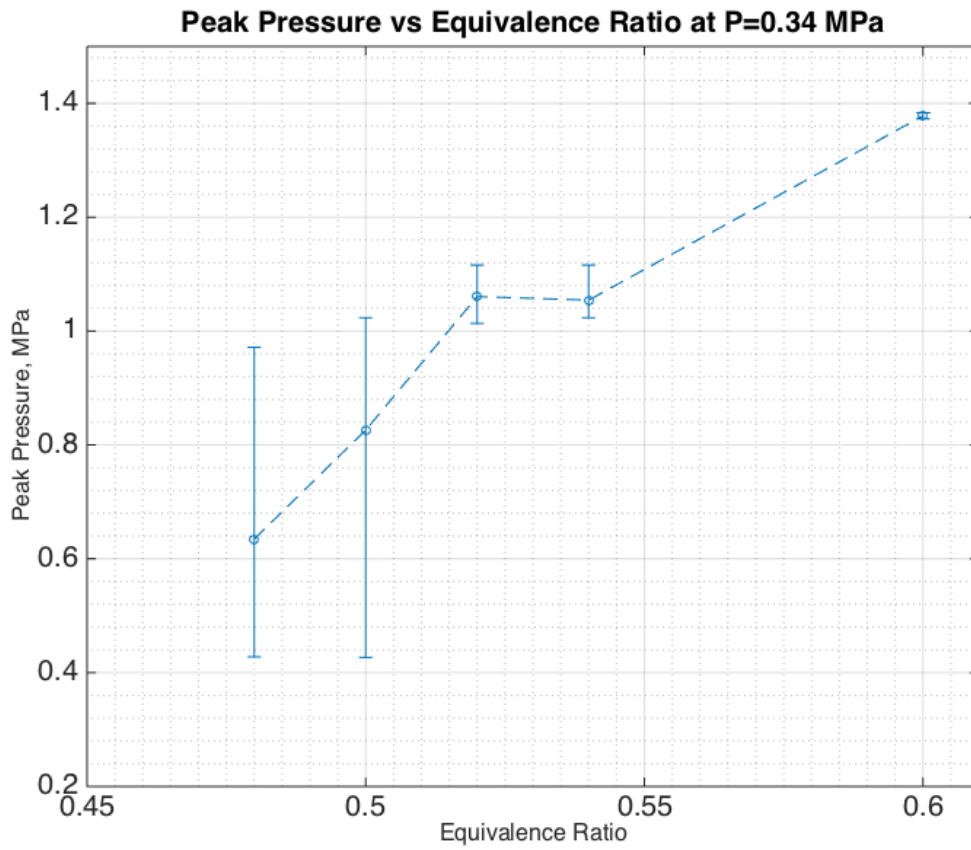


Figure 4.12 Effect of equivalence ratio on peak pressure of methane-air mixture at a chamber pressure of 0.34 MPa with O₂ injection

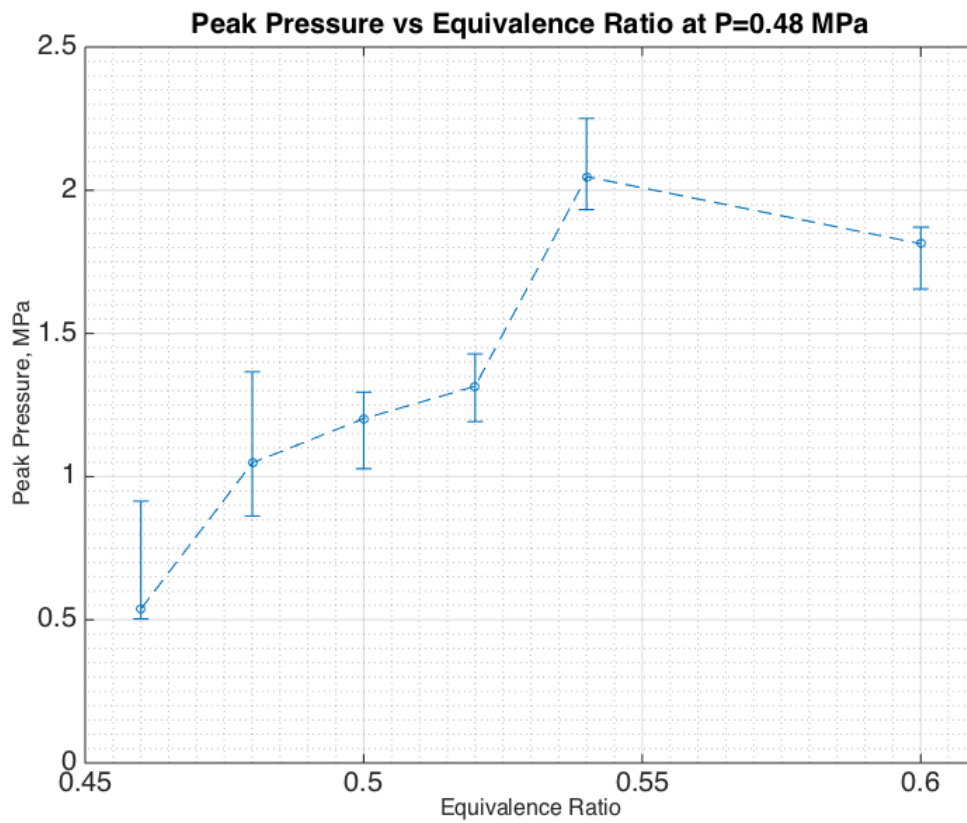


Figure 4.13 Effect of equivalence ratio on peak pressure of methane-air mixture at a chamber pressure of 0.48 MPa with O₂ injection

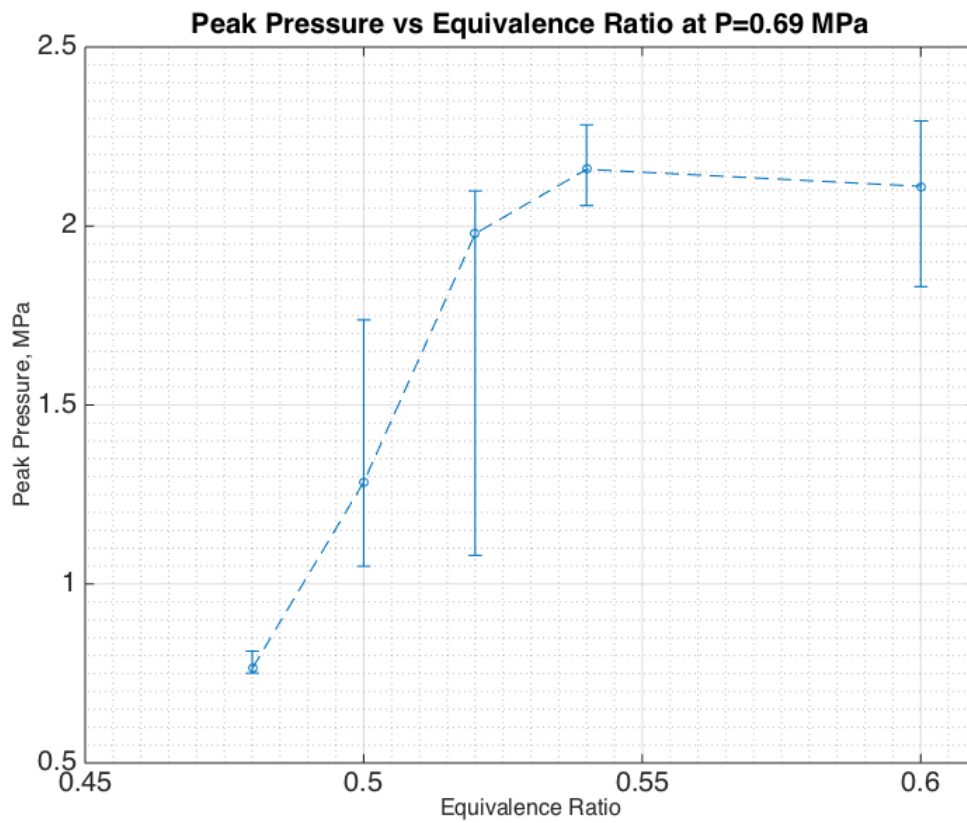


Figure 4.14 Effect of equivalence ratio on peak pressure of methane-air mixture at a chamber pressure of 0.69 MPa with O₂ injection

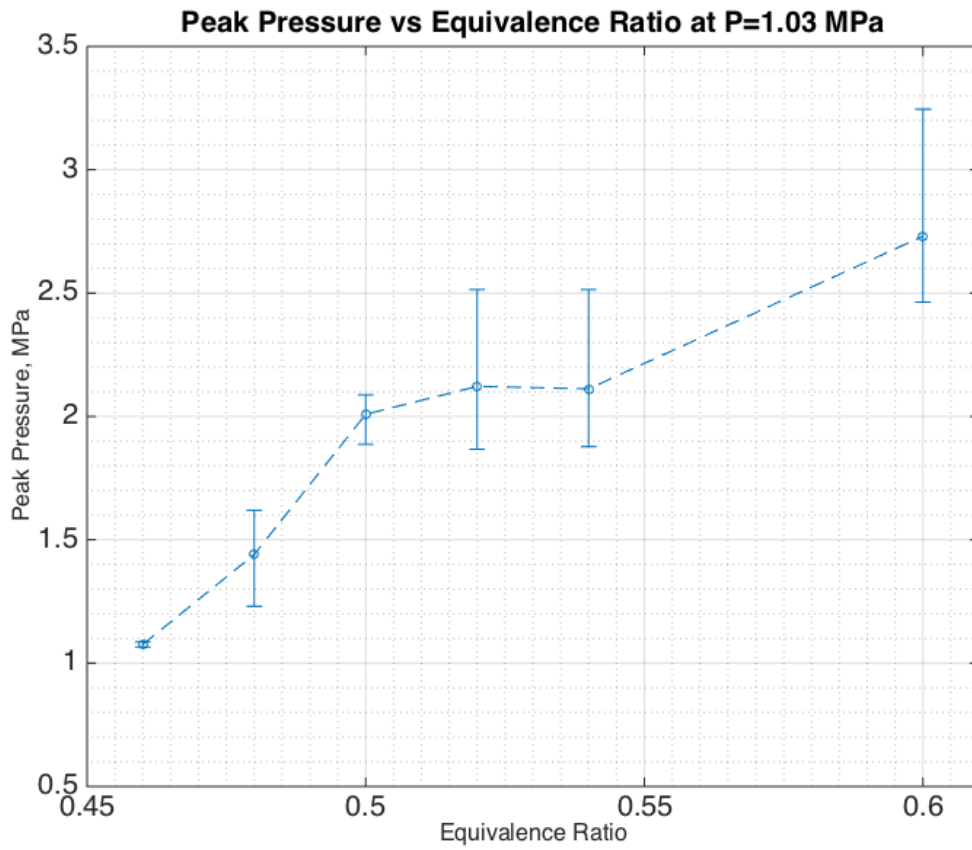


Figure 4.15 Effect of equivalence ratio on pressure of methane-air mixture at chamber pressure of 1.03 MPa with O₂ injection

Table 4.4 Average peak pressure with O₂ injection at chamber pressure of 1.03 MPa and equivalence ratios of 0.5, 0.48 and 0.46

Chamber Pressure, MPa	Equivalence Ratio, ϕ	Average Peak Pressure, MPa	Pressure of Injection, MPa
1.03	0.50	2.00	1.27
	0.48	1.44	1.20
	0.46	1.07	1.27

observed. Minimum of five experiments are performed at each equivalence ratio, and the results are listed in Table 4.5.

As seen in Table 4.5 the injection pressure has a strong effect on the peak pressure of the methane-air mixtures. For example, increasing the injection pressure lead to the higher peak pressure in the chamber. However, further increasing of the injection pressure leads to no ignition. Interestingly, the same behavior is observed in experiments with methane-rich injection in the spark plug gap carried out by Mezo (Mezo 2009).

Similar to oxygen injection at a chamber pressure of 1.03 MPa the lean limit can also be extended to $\phi = 0.46$ by injecting nitrogen into the spark plug's gap. The pressure and the temperature traces obtained at an equivalence ratio of 0.5 and a chamber pressure of 1.03 MPa for both oxygen and nitrogen injections are shown in Figure 4.16.

4.2.3 DETERMINING LEAN LIMIT AT INITIAL CHAMBER PRESSURE OF 1.03 MPA WITH CARBON DIOXIDE INJECTION

To confirm the extension of the lean limit of a methane-air mixture is mainly due to the induced charged motion, experiments are carried out with CO₂ injection. Results obtained with carbon dioxide injection are presented in this subsection. CO₂ is injected into the spark plug's gap under the same injection pressure and solenoid valve timing as nitrogen. As with oxygen and nitrogen injection, experiments are performed only at a chamber pressure of 1.03 MPa, and the equivalence ratio is reduced from an initial equivalence ratio of 0.5 in an increment of 0.02 until ignition

Table 4.5 Average peak pressure with N₂ injection at chamber pressure of 1.03 MPa and equivalence ratios of 0.5, 0.48 and 0.46

Chamber Pressure, MPa	Equivalence Ratio, ϕ	Average Peak Pressure, MPa	Injection Pressure, MPa
1.03	0.50	2.03	1.27
	0.50	1.40	1.14
	0.48	1.18	1.14
	0.46	1.12	1.14

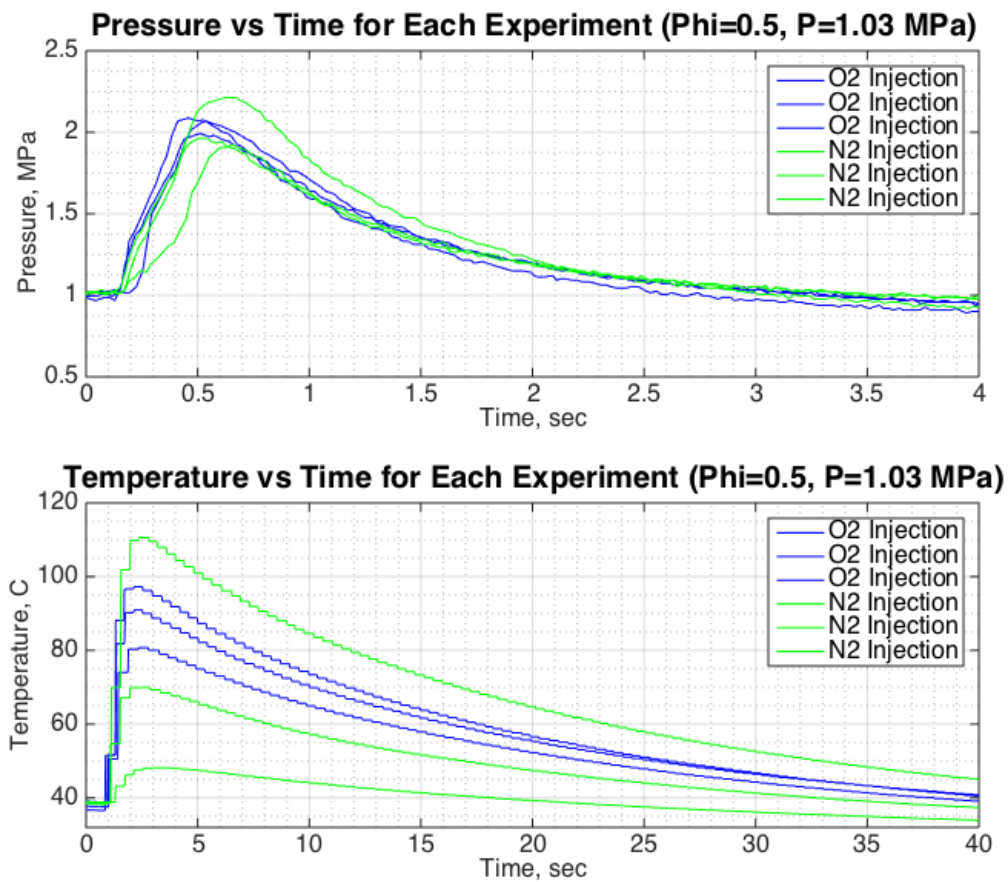


Figure 4.16 Effects of O₂ and N₂ injection on pressure and temperature at center of a methane-air mixture at $\phi = 0.5$ and a chamber pressure of 1.03 MPa (--- with N₂ injection, --- with O₂ injection)

of the mixture is no longer possible. A minimum of five experiments are performed at each equivalence ratio and the results are listed in Table 4.6.

As in the case of nitrogen and oxygen injections the lean limit can also be extended to $\phi = 0.46$ with carbon dioxide injection. Figure 4.17 shows the pressure and temperature traces at a chamber pressure of 1.03 MPa and an equivalence ratio of $\phi = 0.5$ for N_2 and CO_2 injections. Temperature curves start at different initial temperatures, because the experiments are performed on different day and the temperature in the lab where the gas tanks are stored is different. It is not expected that such a small difference in the initial temperatures of approximately $3^\circ C$ would affect the ignition and combustion behavior significantly. Due to different molecular weight and consequently induced charge motion behavior, the peak pressure and temperature obtained with N_2 injection are higher than with CO_2 injection.

4.2.4 EFFECTS OF O_2 , N_2 AND CO_2 INJECTIONS ON COMBUSTION OF FUEL/AIR MIXTURE WITH IMAGES FROM HIGH-SPEED VIDEO CAMERA

The injection of O_2 , N_2 and CO_2 into the gap between the electrodes of a spark plug has extended the lean limit of methane-air mixtures from $\phi = 0.54$ to $\phi = 0.46$ at a chamber pressure of 1.03 MPa. This subsection presented images of the development of the flame kernel from a methane-air mixture at a chamber pressure of 0.69 MPa and an equivalence ratio of 0.6 captured by the high-speed video camera. At an equivalence ratio of 0.6 a methane-air mixture is always ignites even without injection, thus the resulting average peak pressure and an images from the

Table 4.6 Average peak pressures with CO₂ injection at chamber pressure of 1.03 MPa and equivalence ratios 0.5, 0.48 and 0.46

Chamber Pressure, MPa	Equivalence Ratio, ϕ	Average Peak Pressure, MPa	Injection Pressure, MPa
1.03	0.5	1.22	1.14
	0.48	1.17	1.14
	0.46	1.12	1.14

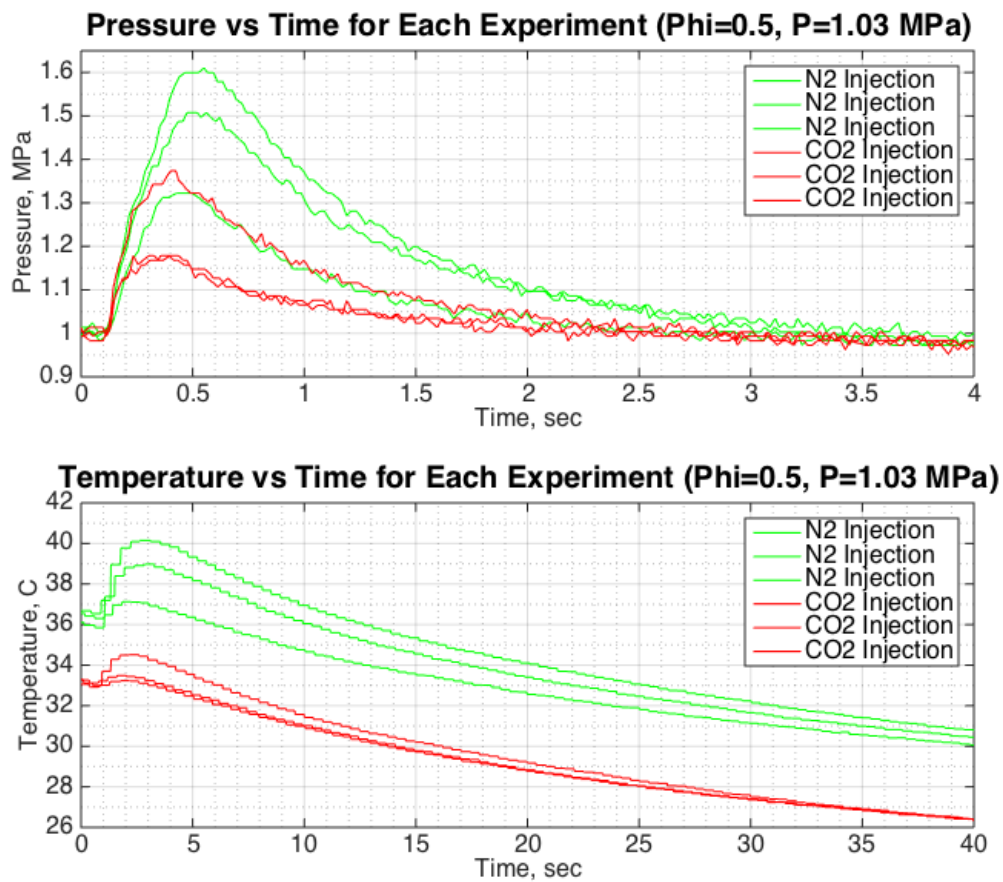


Figure 4.17 Effects of CO₂ and N₂ injection on pressure and temperature at center of a methane-air mixture at $\phi = 0.5$ and chamber pressure of 1.03 MPa (--- with N₂ injection, --- with CO₂ injection)

high-speed video camera can be recorded and then compared to those at an equivalence ratio of 0.54 and a combustion chamber pressure of 0.69 MPa with and without injection. Without injection ignition of the methane-air mixture at an equivalence ratio of 0.54 is impossible regardless the chamber pressure. By performing the experiments at an equivalence ratio of 0.54 with injection the difference in the development of the flame kernel, as recorded by the high-speed camera for the cases of injection and without injection can be delineated. The injection of O_2 , N_2 and CO_2 into the methane-air mixture at an equivalence ratio of 0.54 and a combustion chamber pressure of 0.69 MPa is carried out under the same injection pressure of 0.86 MPa.

The high-speed video camera is capable to record a maximum of 40,000 frames per second. However, increasing the number of frames per second would sacrifice the resolution of the images. Furthermore, the maximum speed can be accomplished only with a perfectly bright light background, which is nearly impossible to accomplish with the present set up of the combustion chamber. Since the duration of the spark discharge is about 3 ms, a frame speed of 3000 frames per second is selected, which results in one frame for every 0.3 ms. It is expected that at a speed of 3000 frames per second, the high-speed video camera is more than adequate to capture major events such as initiation of spark plug's arc, and the formation and growth of the flame kernel.

In addition the heat release analysis is carried out to determine whether complete combustion does take place with injections. Relative efficiency in the calculations simply shows the ratio between calculated heat released and fuel

energy. The fuel energy is obtained based on the lower heating value of methane and dependent on the equivalence ratio.

Results obtained from heat release analysis, plots of pressure, and temperature at the center of the combustion chamber at $\phi = 0.6$ and a chamber pressure of 0.69 MPa are shown in Table 4.7 and Figure 4.18, respectively. The heat-released calculations are shown in the Appendix.

The initial experiments without injection are carried out at a chamber pressure of 0.69 MPa and an equivalence ratio of 0.6. The images captured by the high-speed video camera are shown in sequence in Figure 4.19. The flame kernel appears at the time of a spark discharge. It is biggest at the beginning and progressively gets smaller. The duration of the flame kernel lasts for about 3 ms, which is also the typical duration of spark plug's discharge (see Figure 4.19-a). Due to the limited field of view of the high-speed video camera, the resulting flame kernel is not visible as it propagates out of the region of the spark plug; and subsequent images shown as a dark background similar to those captured before spark discharge for about 197 ms. (see Figures 4.19 (b,c,d)). It is then followed by the appearance of a faintly luminous region in the field of view of the high-speed camera, with an intensity that slowly increases and then decreases until the brightness fades back to the level of the pre-spark discharge state (see Figure 4.19 (e)); this stage lasts for about 153 ms. The total time between energizing of the spark plug and the end of this stage lasts for about 354 ms without injection.

The second set of experiments is carried out with O₂ injection at a chamber pressure of 0.69 MPa and an equivalence ratio of 0.6. The images are shown in

Table 4.7 Effects of O₂, N₂ and CO₂ injection on pressure and temperature traces of methane-air mixture at $\phi = 0.6$ and chamber pressure of 0.69 MPa

Initial pressure in the Chamber, MPa	Type of Injection	Heat Released, kJ	Fuel Energy, kJ	Relative Efficiency $\eta_c, \%$
0.69	O ₂	0.85	4.37	19.36
	N ₂	0.80	4.38	18.16
	CO ₂	0.81	4.39	18.52
	No injection	0.60	4.37	13.67

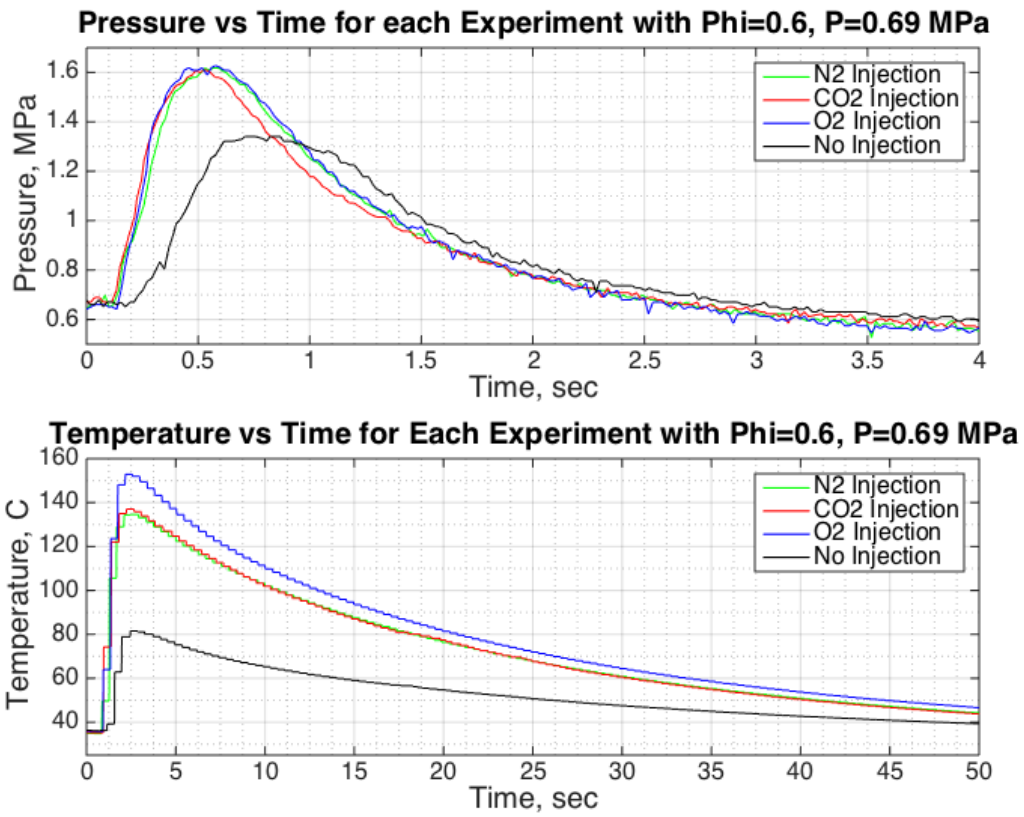
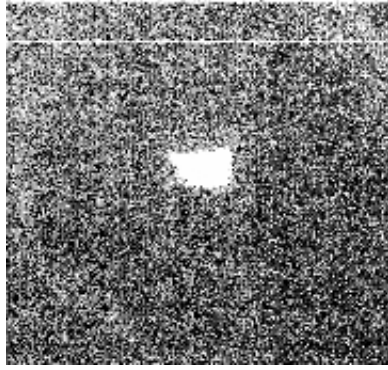
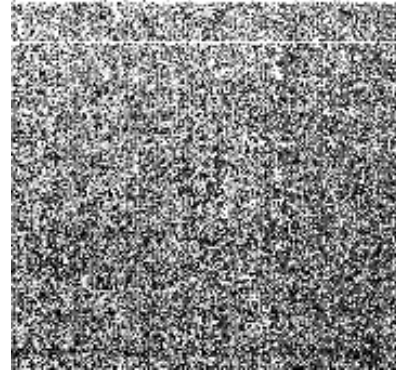


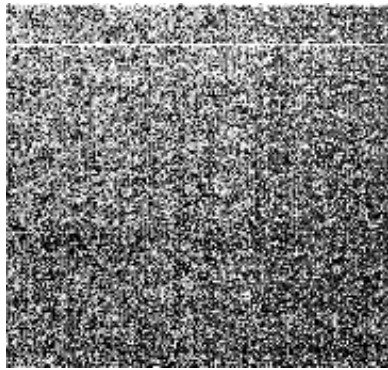
Figure 4.18 Effects of O₂, N₂ and CO₂ injection on pressure and temperature traces of methane-air mixture at $\phi = 0.6$ and chamber pressure of 0.69 MPa (--- with N₂ injection, --- with CO₂ injection, --- with O₂ injection, --- with no injection)



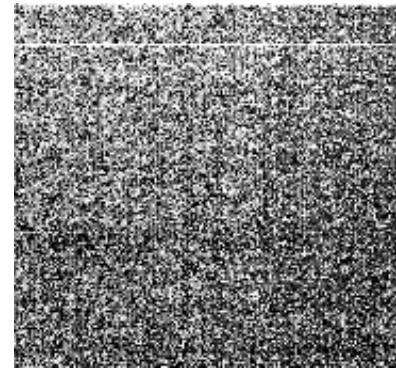
a) Event duration: 3.3 ms



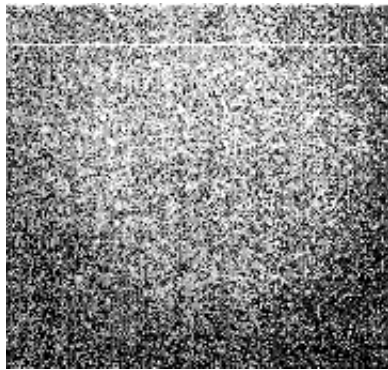
b) Event duration: 19.2 ms



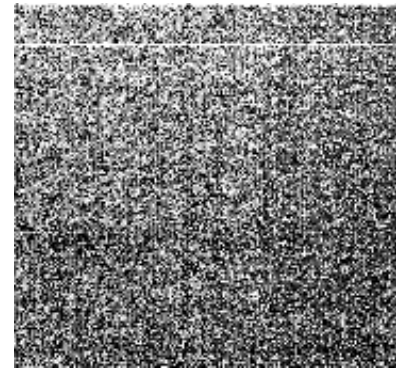
c) Event duration: 7.8 ms



d) Event duration: 170.4ms

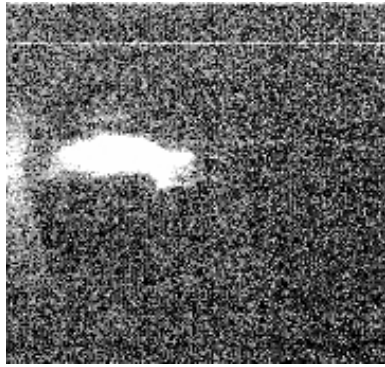


e) Event duration: 153.3 ms

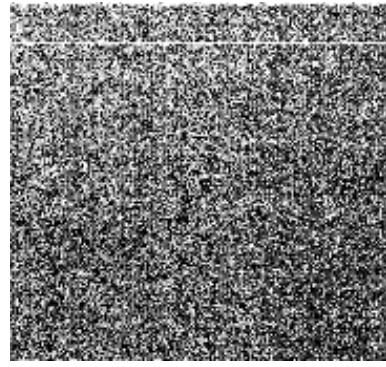


f) Frame number 1180

Figure 4.19 Images taken via high-speed video camera with no injection and duration of each event. Initial pressure in chamber is 0.69 MPa and $\phi = 0.6$



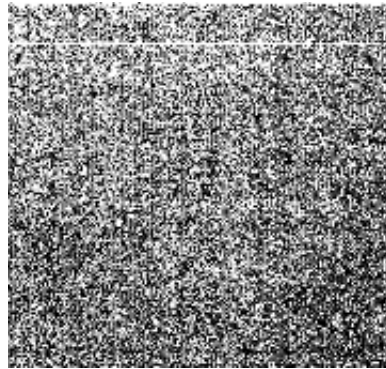
a) Event duration: 1.5 ms



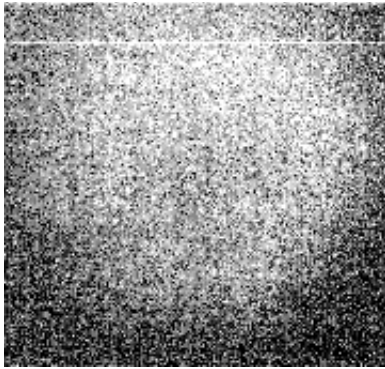
b) Event duration: 19.2 ms



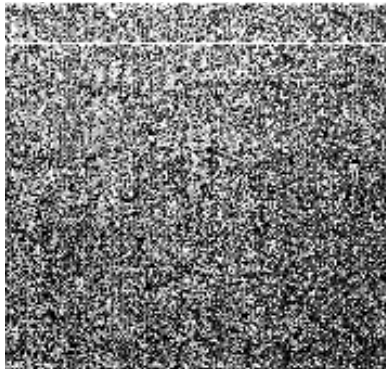
c) Event duration: 7.8 ms



d) Event duration: 82.2 ms



e) Event duration: 136.2 ms

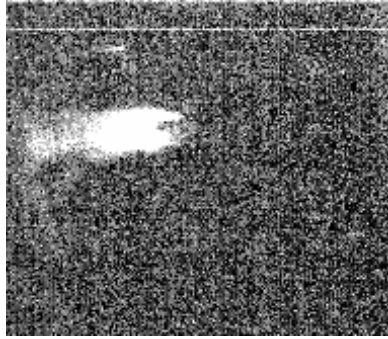


f) Frame number 823

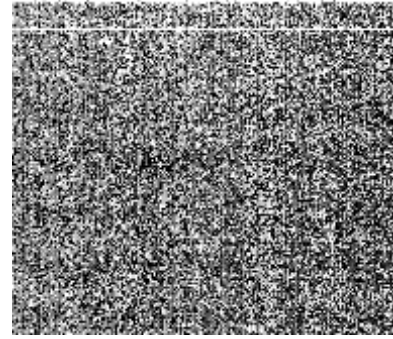
Figure 4.20 Images taken via high-speed video camera with O_2 injection and duration of each event. Initial pressure in chamber is 0.69 MPa, $\phi = 0.6$

Figure 4.20. The flame kernel is largest at the beginning of the spark plug's discharge and much larger than without injection. In addition, the flame kernel is stretched in the direction of injection, and the duration is 1.5 ms – almost half of that without injection (see Figure 4.20 (a)). The flame kernel then propagates out of the high-speed video camera's field of view, and no luminosity is evidenced in subsequent images for about 19 ms (see Figure 4.20 (b)). In contrast to without injection, a second appearance of the flame kernel is observed. The flame kernel travels back to the tip of the capillary injection nozzle and then extinguishes. This has been observed only with oxygen injection, and the duration of the second appearance of the flame kernel lasts about 8 ms. The images taken after this event are similar to those before the spark plug's discharge and last for approximately 82 ms. A luminous region is then observed with increasing and subsequent decreasing of its intensity until it begins to fade out (see Figure 4.20 (e)). This event lasts for about 136 ms, and the peak intensity of the luminous region is much higher with O₂ injection compared to without injection. The total time between energizing of the spark plug and the disappearance of the luminous region is about 247 ms with O₂ injection.

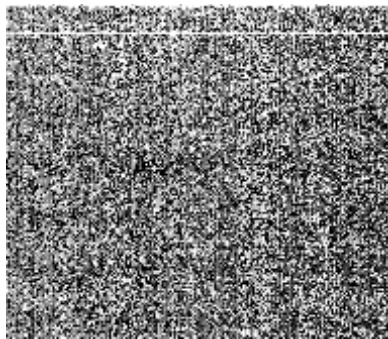
The third set of experiments is carried out with N₂ and CO₂ injections. The duration of the flame kernel is also half of that without injection and lasts for about 0.9 and 1.2 ms with N₂ and CO₂ injections, respectively (see Figures 4.21 (a) and 4.22 (a)) The flame kernel, similar to O₂ injection, is largest at the beginning of the spark discharge and is stretched in a direction of an injection flow for both N₂ and CO₂ injections. As in previous experiments, the flame kernel after the spark



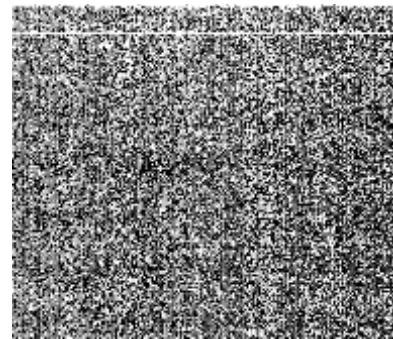
a) Event duration: 0.9 ms



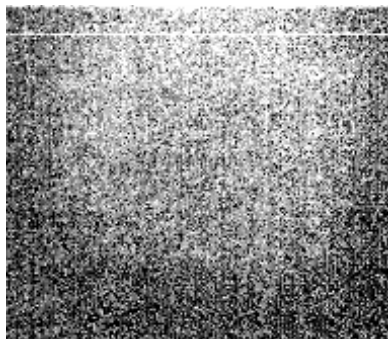
b) Event duration: 19.2 ms



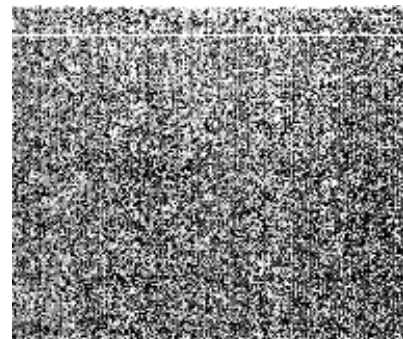
c) Event duration: 7.8 ms



d) Event duration: 97.5 ms

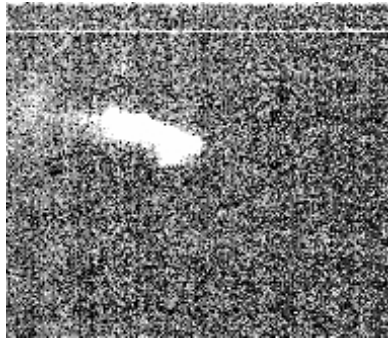


e) Event duration: 125.7 ms

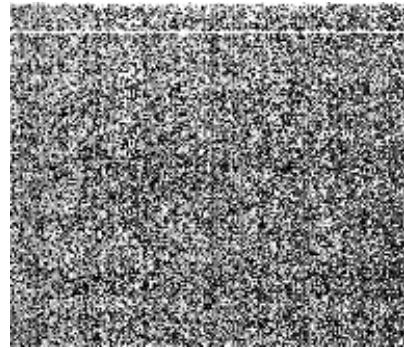


f) Frame number 837

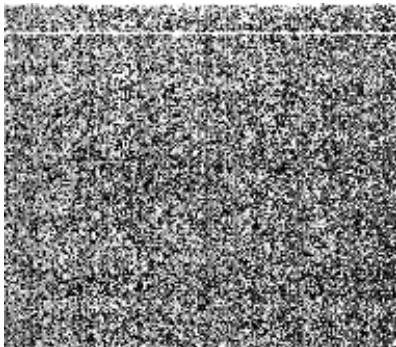
Figure 4.21 Images taken via high-speed video camera with N_2 injection and duration of each event. Initial pressure in chamber is 0.69 MPa, $\phi = 0.6$



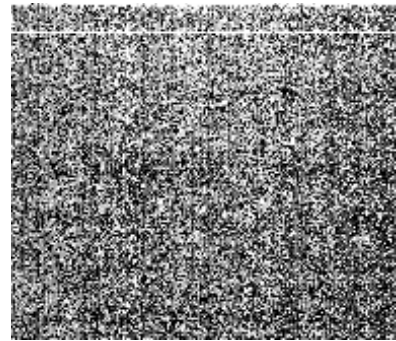
a) Event duration: 1.2 ms



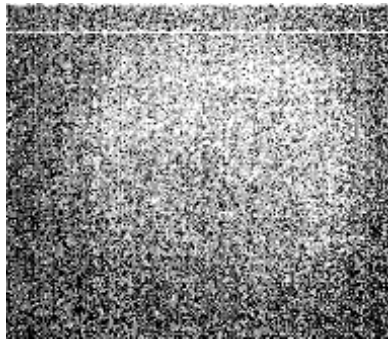
b) Event duration: 19.2 ms



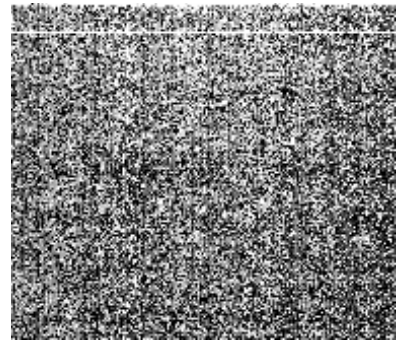
c) Event duration: 7.8 ms



d) Event duration: 96.6 ms



e) Event duration: 118.5 ms



f) Frame number 811

Figure 4.22 Images taken via high-speed video camera with CO₂ injection and duration of each event. Initial pressure in chamber is 0.69 MPa, $\phi = 0.6$

discharge propagates out of the high-speed camera's field of view, and no flame kernel is observed in subsequent images for approximately 125 and 124 ms with N₂ and CO₂ injections, respectively (see Figures 4.21 (b,c,d) and Figure 4.22 (b,c,d)). It is followed by the appearance of a luminous region, with an intensity that slowly increases and then decreases until the brightness fades out. The duration of the luminous region is about 126 and 119 ms with N₂ and CO₂ injections, respectively (Figure 4.21 (e) and Figure 4.22 (e)). The luminous regions observed with N₂ and CO₂ injections are similar to the intensity seen with O₂ injection. However, unlike O₂ injection, the second appearance of the flame kernel does not occur. The total time between energizing of the spark plug and the end of the luminous region is about 251 ms with N₂ and 243 ms with CO₂ injections.

At a chamber pressure of 0.69 MPa and an equivalence ratio of 0.6 with O₂, N₂ and CO₂ injections, the duration of luminous region is much shorter than without injection (by ~100 ms), indicating much higher reaction rates. Figure 4.18 also shows that the peak pressures are nearly the same for O₂, N₂ and CO₂ injections and are much higher than without injection.

Experiments at a chamber pressure of 0.69 MPa and an equivalence ratio of 0.54 are carried out to investigate the appearance of a second flame kernel. Gases are injected with the same injection pressure, and images are taken with frequency of 3000 frames/s. The results of the peak pressure, the temperature and the pressure traces are shown in Table 4.8 and in Figure 4.23, respectively. The images show that the behavior of the flame kernel formation during the spark plug's discharge for O₂, N₂ and CO₂ is similar to those captured at an equivalence ratio of

Table 4.8 Effects of O₂, N₂ and CO₂ injection on pressure and temperature traces of methane-air mixture at $\phi = 0.54$ and chamber pressure of 0.69 MPa

Initial pressure in the Chamber, MPa	Type of Injection	Heat Released, kJ	Fuel Energy, kJ	Relative Efficiency $\eta_c, \%$
0.69	O ₂	0.82	4.36	18.84
	N ₂	0.58	4.39	13.24
	CO ₂	0.57	4.38	13.06

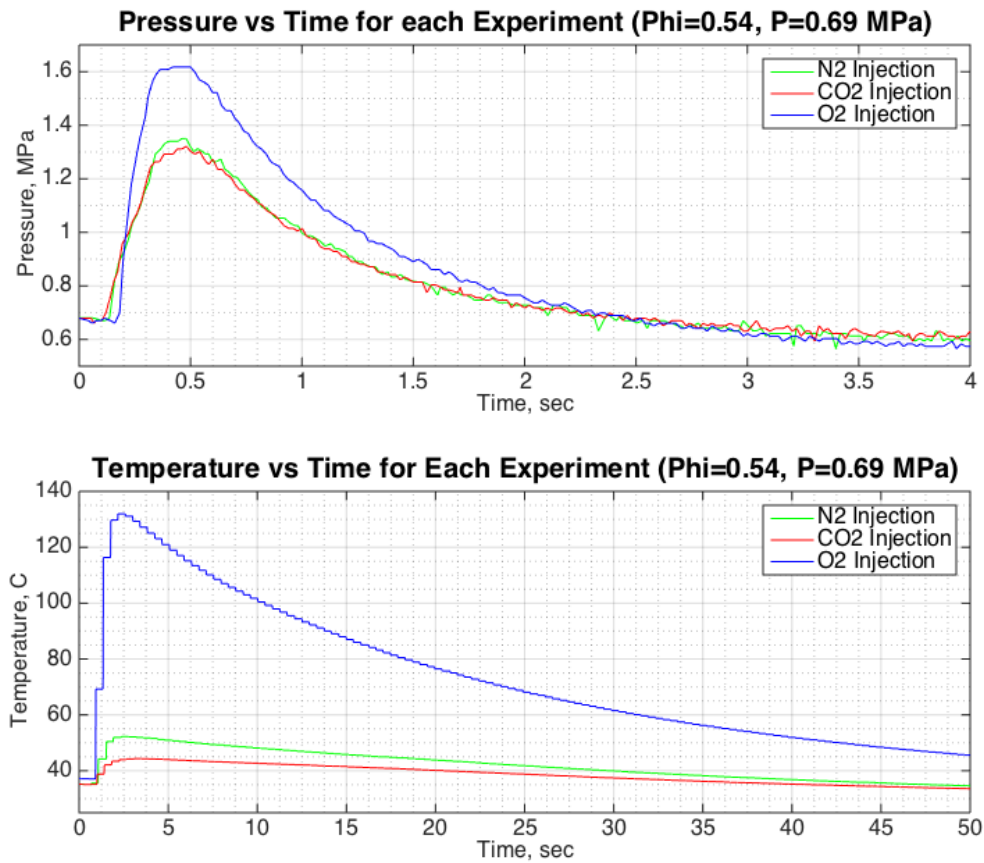


Figure 4.23 Effects of O₂, N₂ and CO₂ injection on pressure and temperature traces of methane-air mixture at $\phi = 0.54$ and chamber pressure of 0.69 MPa (--- with N₂ injection, --- with CO₂ injection, --- with O₂ injection)

0.6. The major difference between O_2 , N_2 and CO_2 injections at an equivalence ratio of 0.54 is the appearance of a second flame formation, which is only observed with O_2 injection.

4.3 EFFECTS OF O_2 , N_2 AND CO_2 INJECTION ON FLAMMABILITY LIMIT OF AIR–METHANE–CARBON DIOXIDE MIXTURE AT 0.69 MPA PRESSURE AND NEAR STOICHIOMETRIC EQUIVALENCE RATIO

In this section results obtained for a mixture of methane-air-carbon dioxide are presented. As discussed in Chapter 1, EGR is commonly used to increase engine efficiency, fuel economy and reduce NO_x emissions. In actual natural gas engines EGR is accomplished by introducing burned gases into the combustion chamber. In the present investigation CO_2 is used to simulate the actual exhaust gas recirculation (EGR) process in the natural gas engines. Experiments are performed only at a chamber pressure of 0.69 MPa with the partial pressure of CH_4 always maintained at near stoichiometric condition. Then the flammability limit of the mixture is determined by increasing the amount of EGR in the mixture; or in the present investigation the concentration of CO_2 in the mixture. Once the flammability limit is determined the effects of O_2 , N_2 and CO_2 injection and injection pressure on the extension of the flammability limit are investigated.

4.3.1 DETERMINATION OF FLAMMABILITY LIMIT OF METHANE-AIR MIXTURE WITH EXHAUST GAS RECIRCULATION (EGR)

This subsection presents results obtained during the experiments with EGR. The experiments begin with 10% CO_2 in the methane-air mixture. Then the

concentration of CO_2 is increased until ignition of the mixture is no longer achieved. Since CO_2 is assumed to be a part of the total chamber pressure, the partial pressure of methane in the mixture is held constant at stoichiometric regardless the percentage EGR in the mixture. On the other hand the partial pressures of air and CO_2 are varied depending on the percentage of the EGR.

Since the peak pressure during the combustion can be exceedingly high, i.e., ~ 5.0 MPa, for safety reason all experiments are performed at an initial chamber pressure of 0.69 MPa. Furthermore, a small change in the amount of the methane can alter the equivalence ratio considerably, and, thus it is preferably to perform the experiments at a higher chamber pressure in order to increase the pressure gauge resolution. At each percentage of EGR a total of five experiments are performed. As seen from Table 4.9, ignition and combustion of the mixture can be achieved only when the EGR is 18 % or below, as evidenced by a small increase in either the pressure or the temperature of the mixture measured at the center of the chamber. Further increase in the concentration of CO_2 in the mixture beyond 18% results in no ignition of the air–methane–carbon dioxide mixture. The pressure and temperature traces are shown in Figure 4.24 to 4.26. In Figure 4.26 the initial temperature of the mixture is different for different experiments for the case of 18% EGR. This is due to the fact that the experiments are performed at different days with different room temperatures. However, it could be clearly seen all temperature traces obtained in the five experiments exhibit the same trend and the same magnitude.

Table 4.9 Effects of percent EGR on average peak pressure

Chamber, MPa	EGR, %	Average Peak Pressure, MPa
0.69	10	3.87
	15	2.91
	18	0.93

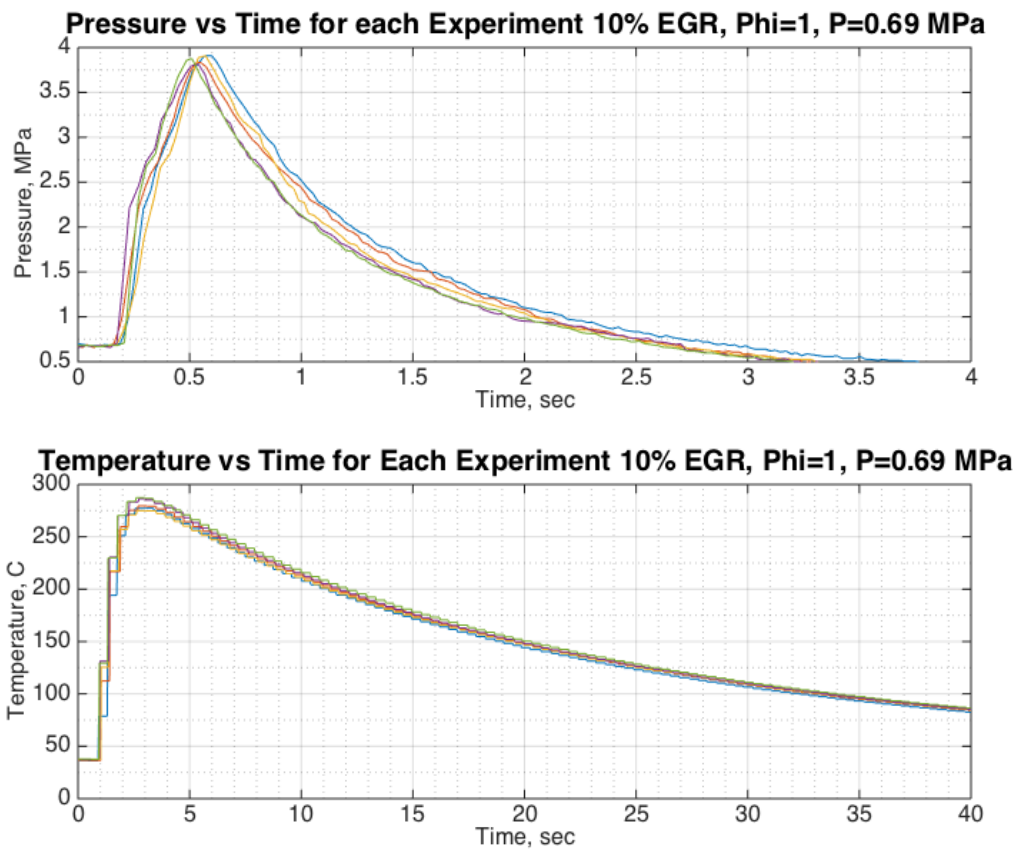


Figure 4.24 Pressure and temperature at chamber center in case of 10% EGR and chamber pressure of 0.69 MPa as function of time for five different experiments

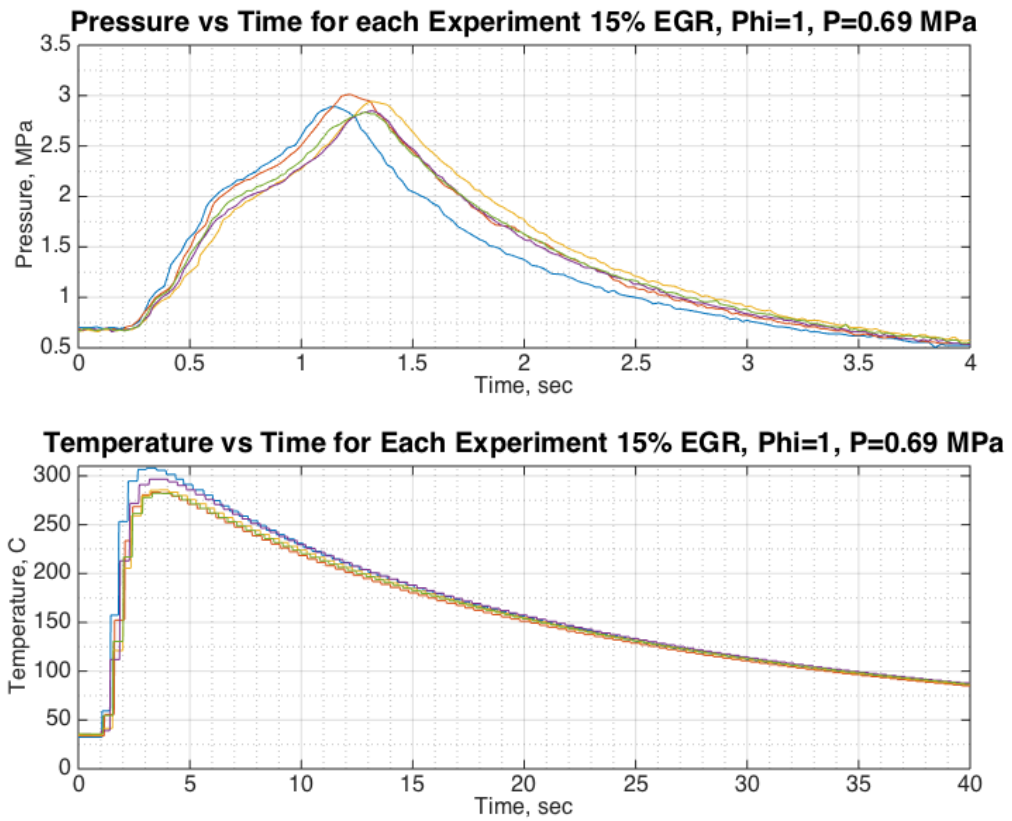


Figure 4. 25 Pressure and temperature at chamber center in case of 15% EGR and chamber pressure of 0.69 MPa as function of time for five different experiments

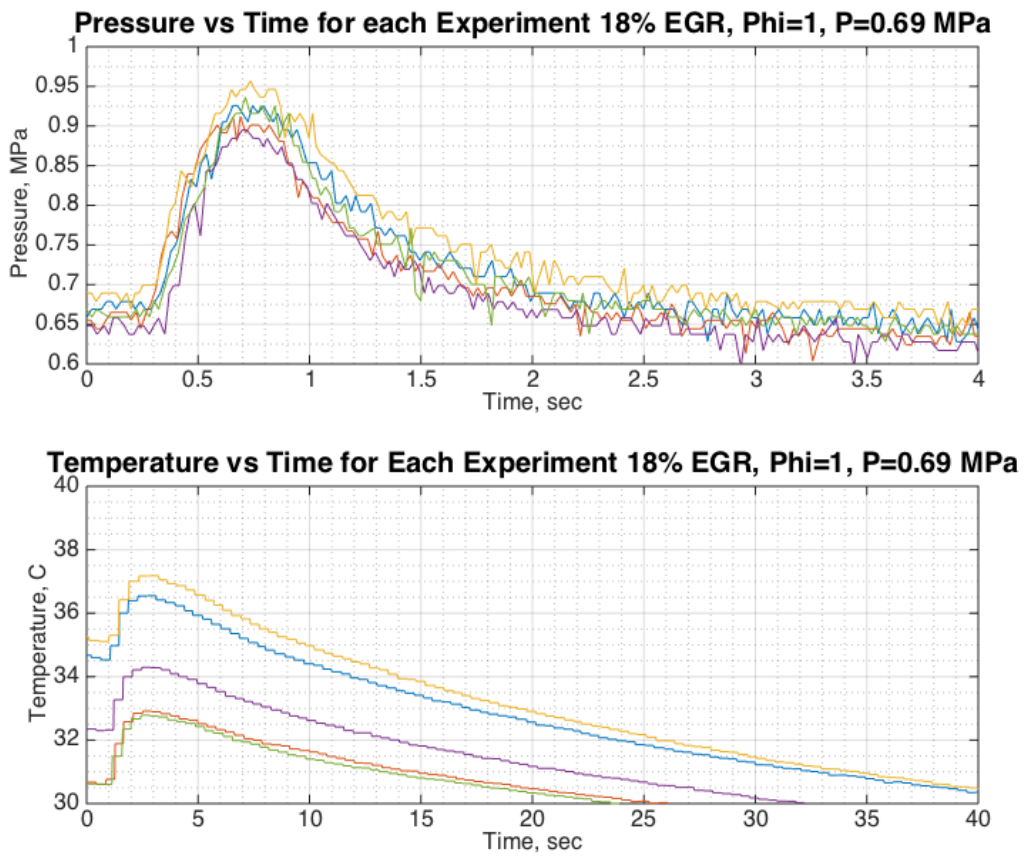


Figure 4.26 Pressure and temperature at chamber center in the case of 18% EGR and chamber pressure of 0.69 MPa as function of time for five different experiments

4.3.2 DETERMINATION OF THE HIGHEST PERCENT EGR WITH O₂, N₂ AND CO₂ INJECTION

This subsection presents results obtained from the experiments in which the effects of O₂, N₂ and CO₂ injection on the extension of percentage of EGR in methane air mixture is maintained at 10%, then it is gradually increased until ignition of the mixture is no longer achieved.

Experiments are first performed with O₂ injection, followed by N₂ and CO₂ injection. As in the case of methane-air mixtures, the injection pressure is varied until the peak pressure in the chamber is maximum. Once the optimum injection pressure is determined, two to eight experiments are performed at each EGR concentration, i.e., CO₂ concentration.

The solenoid valve of the injection system is rated at about 3.1 MPa. And, thus to prevent the solenoid valve from damages caused by high pressures produced by the methane-air-carbon dioxide near stoichiometric condition, only few experiments are conducted at 10% and 18% EGR, whereas five to eight at 20% EGR and above. The effect of percent EGR on the average peak pressure with O₂ injection at injection pressure of 1.14 MPa is shown in Table 4.10. With O₂ injection the flammability limit is extended to 22 % EGR and the average peak pressure is almost the same as that at 18% EGR. Further increasing of % EGR results in no successful ignition. As a result of O₂ injection in the area between the electrodes of the spark plug, the peak pressure at 22% EGR is almost the same as that at 15% EGR without O₂ injection (see Tables 4.9 and 4.10). Figure 4.27 shows the effect of the O₂ injection at 10% EGR and a chamber pressure of 0.69 MPa. As seen in Figure 4.27

Table 4.10 Effects of percent EGR on average peak pressure with O₂ injection

Chamber Pressure, MPa	EGR, %	Average Peak Pressure, MPa	Injection Pressure, MPa
0.69	10	3.82	1.14
	18	2.90	1.14
	20	2.90	1.14
	22	3.01	1.14

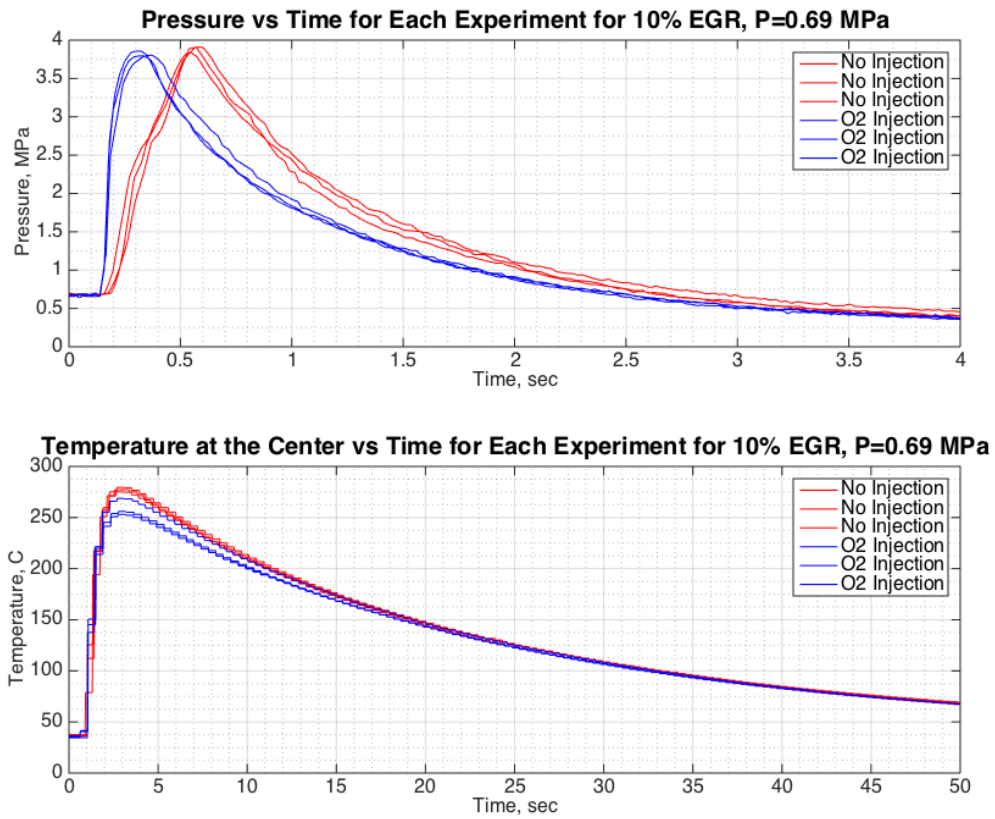


Figure 4.27 Effects of O₂ injection on pressure and temperature traces of methane-air mixture diluted with 10% CO₂ and chamber pressure of 0.69 MPa (--- without injection, --- with O₂ injection)

the peak pressure reaches its maximum value about 300 ms earlier with O₂ injection than without O₂ injection, indicating a faster reaction rate. The results obtained with O₂ injection for EGR cases are similar to those obtained with O₂ injection for methane-air mixtures without EGR. In contrast to O₂ injection, it is impossible to ignite the methane-air mixture with N₂ and CO₂ injection, even at a low percent dilution of 10 % EGR at all injection pressures. Further investigations are needed in order to ascertain the exact reason for such a behavior.

CHAPTER 5

CONCLUSIONS

In the present investigation experiments are performed in a combustion chamber of a volume of 400 cc. O₂, N₂ and CO₂ are injected to the area between spark plug's gap via a 0.16-cm OD stainless steel capillary injection nozzle. The formation and growth of the flame kernel between the spark plug electrodes are recorded using a high-speed video camera.

The objectives of the present study are three-fold: first, to investigate the feasibility of extending the lean limit of methane-air mixtures by injecting oxygen into the gap between the electrodes of spark plug; and second, to ascertain whether the extension of the lean limit is due to the induced charged motion or the formation of oxygen radicals and electronically-excited O₂ molecules. And, finally, the effect of the oxygen injection on the flammability limit of a stoichiometric methane-air mixture with EGR represented by carbon dioxide dilution is also investigated.

At chamber pressures of 0.34 and 0.48 MPa the lean limit occurs at $\phi = 0.54$ and slightly higher at $\phi = 0.56$ at chamber pressures of 0.69 and 1.03 MPa. The lean limit for the higher chamber pressures is slightly higher, possibly due to lower flame speeds at high pressures.

The injection of O₂ can extend the lean limit to an equivalence ratio of 0.46 for chamber pressures between 0.34 and 1.03 MPa. Injection of N₂ and CO₂ at chamber pressure of 1.03 MPa exhibits similar trend towards extension of a lean limit to an equivalence ratio of 0.46. This seems to indicate that the extension of the

lean limit is mainly due to induced charge motion, more so than the formation of oxygen radicals and electronically-excited O_2 molecules. Images taken from the high-speed video camera show that the duration of the spark is much shorter and flame kernel is much larger in the cases with O_2 , N_2 and CO_2 injection as compared to the case with no injection. Heat released analysis is much higher with O_2 , N_2 and CO_2 injection compared to without injection.

The injection pressure has a strong effect on the peak pressure of the methane-air mixtures; the higher the injection pressure the higher the peak pressure. For example, for N_2 injection with a chamber pressure of 1.03 MPa and an equivalence ratio of 0.5, an injection pressure of 1.14 MPa results in a peak pressure of 1.40 MPa, whereas a peak pressure of 2.03MPa is obtained at an injection pressure of 1.27 MPa.

With O_2 injection the flammability limit of a stoichiometric mixture of methane-air is extended from 18 % EGR to 22 % EGR at a chamber pressure of 0.69 MPa. On the other hand it is impossible to ignite the methane-air mixture with N_2 and CO_2 injection, even at a low percent dilution of 10 % EGR at all injection pressures. The injection of inert gases such as N_2 and CO_2 dilute the mixture further in the region between the spark plug gap, preventing the growth of the flame kernel, and the ignition of the mixture becomes impossible.

REFERENCES

1. DOE and EPA: see U.S. Department of Energy, Office of Energy Efficiency and Renewable Energy, and U.S. Environmental Protection Agency.
2. Rood M, Santini D, Werpy, Burnham A., and Mintz M.,(2010), "*Natural Gas Vehicles: Status, Barriers, and Opportunities*". DE-AC02-06CH11357. Available at: http://www.afdc.energy.gov/pdfs/anl_esd_10-4.pdf (last access May 2015).
3. Tunestal P., Christensen M., Einewall P., Anderson T., Johanson B. (2002), "*Hydrogen Addition For Improved Lean Burn Capability of Slow and Fast Burning Natural Gas Combustion Chamber*". SAE paper 2002 - 01 - 2686. Powertrain & Fluid systems Conference & Exhibition, San Diego, California USA.
4. Bauer C.G, Forest T.W., (2001), "*Effect of hydrogen addition on the performance of methane-fueled vehicles. Part I: effect on S.I. engine performance.*" Pergamon paper. International Journal of Hydrogen Energy 26(2001) 55-70.
5. Bell S.R., Gupta M., (1996), "*Extension of the Lean Operating Limit for Natural Gas Fueling of a Spark Ignited Engine Using Hydrogen Blending*". Combustion Science and Technology, 123:1-6,23-48. Link to the article: <http://dx.doi.org/10.1080/00102209708935620>
6. Ma F., Wang Y., (2007), "*Study on the Extension of Lean Operation Limit Through Hydrogen Enrichment in a Natural Gas Spark-Ignition Engine*". International Journal of Hydrogen Energy 33 (2008) 1416-1424.
7. Gold M.R., Whitelaw J.H., Xu H.M., (1997), "*Local Mixture Injection to Extend the Lean Limit of Spark-Ignition Engines*". Experiments in Fluids 26(1999) 126 - 135.
8. Reynolds B. O., Evans R.L., (2003), "*Improving Emissions and Performance Characteristics of Lean Burn Natural Gas Engines Through Partial Stratification*". International Journal of Engine Research, February 1, 2004 5:105-114.
9. Wang T., Peng Z., Liu S-L., Xiao H-D., Zhao H., (2007) "*Optimization of Stratification in a Spark Ignition Engine by Double-Pulse Port Fuel Injection*". Department of Engineering and Design, University of Sussex, Brighton, UK, DOI: 10.1243/09544070JAUTO376.
10. Evans R.L., (2009), "*Extending the Lean Limit of Natural-Gas Engines*". Journal of Engineering For Gas Turbines and Power - Transaction of the ASME, May 2009, DOI 10.1115/1.3043814.

11. Cheolwoong P., Sungdae K., Hongsuk K., Yasuo M., (2012), "*Stratified Lean Combustion Characteristics of a Spray – Guided Combustion System in a Gasoline Direct Injection Engine*". 23rd International Conference on Efficiency, Cost, Optimization, Simulation and Environmental Impact of Energy Systems. DOI: 10.1016/j.energy.2012.02.060.
12. Arcoumanis C., Hull D.R., Whitelaw J.H., (1997), "*Optimizing Local Charge Stratification in a Lean–Burn Spark Ignition Engine*". Journal: Proceedings of the Institution of Mechanical Engineers. Part D, Journal of Automobile Engineering. Ill Number: -8610744.
13. Harrington J., Shishu R., Asik J., (1974), "*A Study of Ignition System Effects on Power, Emissions, Lean Misfire Limit, and EGR Tolerance of a Single–Cylinder Engine–Multiple Spark versus Conventional Single Spark Ignition*". Journal: Technical paper series, February 1974, Pages 740188. New York. N.Y. : SAE.
14. Rado W., Amey J., Bates B., Turner A., (1976), "*The Performance of a Multi-Gap Spark Plug Designed for Automotive Applications*". SAE paper 760264, DOI: 10.4271/760264
15. Durbin E., Tsai K., (1983), "*Extending the Lean Limit Operation of an SI Engine with a Multiple Electrode Spark Plug*". SAE paper 830476, DOI: 10.4271/830476.
16. Nakamura N., Baika T., Shibata Y., (1985), "*Multipoint Spark Ignition for Lean Combustion*". SAE paper 852092. DOI: 10.4271/852092
17. Kupe J., Wilhelmi H., (1987), "*Operational Characteristics of a Lean Burn SI–Engine: Comparison Between Plasma–Jet and Conventional Ignition System*". SAE paper 870608.
18. Hanada K., Murase E., Ono S., (1994), "*Pulsed Combustion Jet Ignition in Lean Mixtures*". SAE paper 942048.
19. Checkel M., Dale J., Smy P., (1997), "*Application of High Energy Systems to Engines*". Pergamon paper 0360 – 1285/97. PII: S0360-1285(97)00011-7.
20. Hotta E., Tanoue K., Kuboyama T., Moriyoshi Y., Imanishi Y., Shimizu N., Iida K., (2010), "*Extension of Lean and Diluted Combustion Stability Limits by Using Repetitive Pulse Discharges*". SAE paper. DOI: 10.4271/2010-01-0173.
21. DeFilippo A., Saxena S., Rapp V., Dibble R., Chen J., (2011), "*Extending the Lean Stability Limits of Gasoline Using a Microwave-Assisted Spark Plug*". SAE paper. DOI: 10.4271/2011-01-0663.

22. Rapp V., DeFilippo A., Saxena S., Chen J., Dibble R., Nishiyama A., Moon A., Ikeda Y., (2012), "*Extending Lean Operating Limit and Reducing Emissions of Methane Spark-Ignited Engines Using a Microwave-Assisted Spark Plug*". Journal of Combustion, Volume 2012, Article ID 927081, 8 pages. DOI: 10.1155/2012/927081.
23. Mohamed T., (2010), "*Compressed Natural Gas Direct Injection (Spark Plug Fuel Injector), Natural Gas*", ISBN: 978-953-307-112-1, In-Tech
24. Suplee C., (2008). "*What You Need to Know About Energy*". National Academy of Science, 2008
25. Keck J., Eisazabeh-Far K., Metghalchi H., (2010). "*On Flame Kernel Formation And Propagation In Premixed Gases*". Combustion And Flames. DOI:10.1016/j.combustflame.2010.07.016.
26. Mezo A., Davy M., Evans R.,(2009). "*The Ultra Lean Burn Partially Stratified Charge Gas Engine*". SAE paper 2009-24-0115.
27. Dale J., Checkel M., Smy P., (1997). "*Application Of High Energy Ignition Systems To Engines*". Pergamon paper. PII: S0360-1285(97)00011-7.
28. Smirnov V., Stelmakh O., Fabelinsky V., Kozlov D., Starik A.,(2008). "*On The Influence Of Electronically Excited Oxygen Molecules On Combustion Of Hydrogen-Oxygen Mixture*". Journal Of Physics DOI: 1088/0022-3727/41/192001

APPENDIX

CALCULATIONS OF THE HEAT RELEASED

Quantity of heat released:

$$Q = \Delta P \frac{\gamma}{\gamma - 1} V$$

where

P – pressure (determined by integration of the pressure curve from beginning of the combustion to the peak pressure)

V – volume of the chamber (~344cc)

γ - heat capacity ratio (it is calculated based on equivalence ratio)

```
% Postprocessor to calculate apparent heat release from O2 enrichment.  
Gamma should be manually set to the appropriate value for the mixture  
and it is calculated via second law of thermo and equivalence ratio  
initial temperature and pressure of the chamber.
```

```
gamma = 1.3970;
```

```
t = Time;
```

```
nsamples = size(t,1);
```

```
hr = 0;
```

```
hrr = zeros(nsamples,1);
```

```
hrr_s = zeros(nsamples,1);
```

```
V = 0.000344; % m^3
```

```
PConv = 6.89475729317; % psi to kPa
```

```
P = PConv*PressureTransducer;
```

```
TAvg = (FlangeThermocouple(1)+SideThermocouple(1))/2;
```

```
% Pmax = peak pressure; nmax = index of peak pressure
```

```
[Pmax,nmax] = max(P);
```

```
% Determine start of combustion (i.e., spark timing) from Status
```

```
SOC = 0;
```

```
for i = 2:nsamples
```

```
    if (SOC == 0)
```

```
        if (Status(i) >= 8)
```

```
            SOC = i;
```

```
        end
```

```
    end
```

```
end
```

```
% hrr_s is actually in units of kJ/s rather than kJ/data point, but a  
small number of the data sets have reduced-resolution timestamps (as if  
the files have been edited and re-saved with fewer digits of  
precision), and thus the time is identical for several consecutive  
points and makes step changes, resulting in div/0 errors that prevent  
calculation of a cumulative heat release. Therefore, hrr is used for  
integrating cumulative heat release.
```

```
for i=2:nsamples
```

```
    hrr(i) = (1/(gamma-1))*V*(P(i)-P(i-1));
```

```
    hrr_s(i) = (1/(gamma-1))*V*(P(i)-P(i-1))/(t(i)-t(i-1));
```

```
end

% Heat release is integrated from spark to peak pressure (the decay
after that has a negative heat release rate due to heat transfer, and
would result in a net-zero value for the cycle if included in the
integration)

for i=SOC:nmax
    hr = hr + hrr(i);
end

figure
subplot(2,1,1)
plot(t,P)
xlabel('Time, s')
ylabel('Pressure, kPa a')
subplot(2,1,2)
plot(t,hrr_s)
xlabel('Time, s')
ylabel('Heat Release Rate, kJ/s')
```

VITA

Artem Alexandrovich Temerev was born in Tura, Krasnoyarsk region, Russia on October 16th, 1984. At the age of 17 he moved to Krasnoyarsk to pursue his degree in Aerospace Engineering at the Siberian Aerospace University, Krasnoyarsk, where he studied for five years. In 2011 he entered the University of Tennessee, Knoxville where he earned a degree of Bachelor of Engineering in Aerospace Engineering in May 2013. He then continues his education pursuing a degree of Master of Science in Mechanical Engineering in August 2013.